Polo-like kinase 1 mediated phosphorylation regulates PAX3/FOXO1 in alveolar rhabdomyosarcoma

Master Thesis in Human Biology
University of Zurich

Presented by
Dominik Laubscher

Zurich, January 2014

Polo-like kinase 1 mediated phosphorylation regulates PAX3/FOXO1 in alveolar rhabdomyosarcoma

Zurich, January 2014

Department of Oncology,
University Children's Hospital of Zurich

First Referee:	Prof. Dr. Beat W. Schäfer
Second Referee:	Prof. Dr. Thierry Hennet
Supervisor:	Verena Thalhammer

I affirm that the work presented in this thesis is my own work.

Dominik Laubscher

Table of contents

List of abbreviations

AC	adenylyl cyclase
AML	acute myelogenous leukemia
AP2beta	activating enhancer binding protein 2 beta
BCA	bicinchoninic acid
bp	base pairs
BSA	bovine serum albumin
aRMS	alveolar rhabdomyosarcoma
AKT (or PKB)	Protein kinase B
CBP	CREB binding protein
CDK1/2	cyclin dependen kinase 1/2
CHX	cycloheximide
CIP	calf intestinal phosphatase
CK1/2	casein kinase 1/2
CREB	cAMP response element-binding protein
cAMP	cyclic adenosine monophosphate
cDNA	complementary deoxyribonucleic acid
DMEM	Dulbecco's modified eagles medium
DMSO	dimethylsulfoxide
DTT	dithiothreitol
E.coli	Escherichia coli
EDTA	ethylenediaminetetraacetic acid
EGTA	ethyleneglycoltetraacetic acid
eRMS	embryonal rhabdomyosarcoma
FACS	fluorescence activated cell sorting
FBS	fetal bovine serum
FBXW7	F-box/WD repeat-containing protein 7
Fig.	Figure
FOXO1 (or FKHR)	forkhead box O gene 1
GFP	green fluorescent protein
GSK3	glycogen synthase kinase 3
HeBS	HEPES buffered saline
HEPES	4-(2-hydroxyethyl)-1-piperazineethanesulfonic acid
IGF2	insulin-like growth factor 2
IPTG	isopropyl-β-D-1-thiogalactopyranoside
IRES	internal ribosomal entry site
IRF3	interferon regulating transcription factor 3
INK4A/ARF	INK4A locus alternative reading frame
LB	Luria Bertani
LDS	lithium duodecyl sulfate
LOH	loss of heterozygosity
MoMLV	moloney murine leukemia virus

(m/h)MSC	(mouse/human) mesenchymal stem cell
NCOA1/2	nuclear receptor coactivator 1/2
NF1	neurofibromin 1
OD	optical density
PAX3/7	paired box gene 3/7
PBS	phosphate buffered saline
PCR	polymerase chain reaction
PI	propidium iodide
PI3K	phosphatidylinositide 3 kinase
PKA	protein kinase A
PLK1	Polo-like kinase 1
PMSF	phenylmethylsulfonylfluorid
P3F	PAX3/FOXO1
qRT-PCR	quantitative reverse transcription PCR
RMS	rhabdomyosarcoma
rpm	rounds per minute
RT	reverse transcription
SDS	sodium duodecyl sulfate
SV40-LT	simian virus large T antigen
TBS(T)	tris buffered saline (tween)
TNM	tumor, (lymph) nodes, metastases
TRP53 (or p53)	tumor protein p53
VSV-G	vesicular stomatitis virus glycoprotein
Wt	wild type
3'UTR	3' untranslated region

Summary

Rhabdomyosarcoma (RMS) is a highly malignant soft tissue sarcoma which commonly occurs in childhood and is associated with the skeletal muscle lineage. Two major subtypes can be determined according to histological features; alveolar RMS (aRMS) and embryonal RMS (eRMS). Patients with aRMS in general have a poorer prognosis than patients with eRMS. Molecular characteristics of aRMS tumors are chromosomal translocations. The most common translocation found in aRMS results in expression of the oncogenic PAX3/FOXO1 fusion transcription factor. This fusion protein seems to be the underlying aberration leading to disease development. Further, aRMS cells depend on PAX3/FOXO1 expression for survival. Therefore, this fusion protein represents an interesting target for therapy. Since it is not possible to inhibit PAX3/FOXO1 directly with small molecules, other strategies for targeted therapy are needed. Previous studies revealed that transcriptional activity of PAX3/FOXO1 is regulated by phosphorylation and identified PLK1 as potential upstream kinase. In this work I show that downregulation of PLK1 leads to reduced transcriptional activity of PAX3/FOXO1. This effect most probably involves a mechanism, by which PAX3/FOXO1 is stabilized through PLK1 mediated phosphorylation. Further I identified possible PLK1 phosphorylation sites within PAX3/FOXO1 in vitro. Site directed mutagenesis of these sites was performed. Alanine phosphomutants were tested in regard to their stability compared to PAX3/FOXO1 wild type using cycloheximide treatment of transfected RD cells (an eRMS cell line). I identified that inhibition of phosphorylation at S503 results in decreased protein stability of PAX3/FOXO1. These findings provide a mechanism, by which PLK1 regulates the transcriptional activity of PAX3/FOXO1. Additionally I found that retroviral transduction of RD or hMSC cells with the fusion transcription factor resulted in PAX3/FOXO1 target gene expression, suggesting that this might be a useful tool to test transcriptional activity of PAX3/FOXO1 phosphomutants.

1 INTRODUCTION

1.1 Cancer

Cancer is one of the leading causes of death and its incidence has significantly increased during the last century because of aging, growth of the world population, and an increase of cancer causing behavior [1]. Cancers can occur anywhere in the body [2]. In men, the most common cancer is prostate cancer followed by lung and colon cancer. In women, breast cancer is the most diagnosed type. Lung cancer has the highest mortality rate in general [3] (Fig. 1). Cancer is a heterogeneous group of diseases characterized by uncontrolled cell growth of abnormal cells, which in most cases form a tumor. Additionally, these cells possess the ability to invade other tissues.

Males				Females		
Lung & bronchus	86,220	29%		Lung & bronchus	71,080	26%
Prostate	32,050	11%		Breast	39,840	15%
Colon & rectum	26,580	9%		Colon & rectum	24,790	9%
Pancreas	18,770	6%		Pancreas	18,030	7%
Liver & intrahepatic bile duct	12,720	4%		Ovary	13,850	5%
Leukemia	12,660	4%		Non-Hodgkin lymphoma	9,500	4%
Esophagus	11,650	4%		Leukemia	9,180	3%
Non-Hodgkin lymphoma	10,710	4%		Uterine Corpus	7,950	3%
Urinary bladder	10,410	3%		Liver & intrahepatic bile duct	6,190	2%
Kidney & renal pelvis	8,210	3%		Brain & other nervous system	5,720	2%
All Sites	**299,200**	**100%**		**All Sites**	**270,290**	**100%**

Figure 1: Estimated cancer-caused deaths by Sex, 2010 in the Uited states [3]

1.1.1 Hallmarks

Cancer cells arise because of alterations in their DNA. These range from point mutations, insertions and deletions to chromosomal translocations and amplifications. These alterations exert a pathologic effect by causing loss of function of tumor suppressor genes or gain of function of oncogenes. Under normal circumstances, these damages can either be repaired or the cell undergoes apoptosis. Most DNA damages are generated by mistake during normal cell division or by environmental factors (age, carcinogens, viruses). In fewer cases, DNA damage can also be inherited [2]. Carcinogenesis is a multistep process during which normal cells are transformed into malignant and invasive phenotypes. Because of genetic instability over several rounds of cell divisions, cancer cells can accumulate properties allowing them to resist cell death, sustain proliferative signaling, resist growth suppression, activate invasion and metastasis, aquire replicative immortality and induce angiogenesis. These are the so called hallmarks of cancer, which are

responsible for the transformation of normal cells into cancer cells. Recently, new hallmarks were defined including the deregulation of cellular energetics, escaping from immune response and tumor promoting inflammation (Fig. 2). Altogether, they help us to develop a deeper understanding of how cancers arise [4].

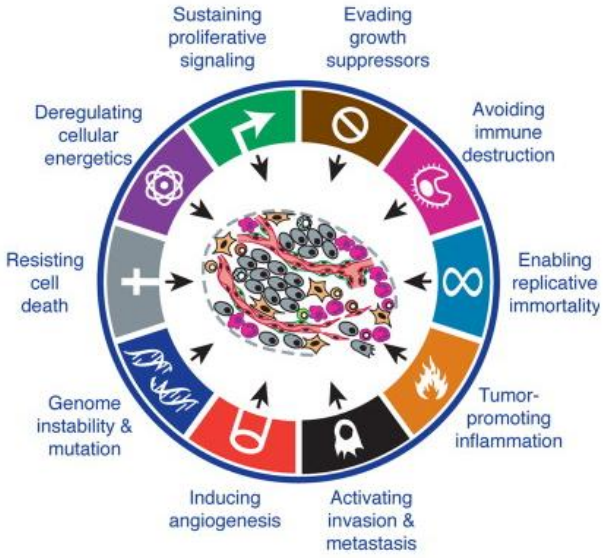

Figure 2: Hallmarks of cancer [4]

1.1.2 Subtypes

There exist many different types of cancers and they all behave differently. They can grow at different rates and respond to different treatments. Also they display a huge genetic heterogeneity. According to their cells of origin, cancer types can be classified into different subtypes. Carcinomas arise from cells within epithelial structures, myelomas are derived from cells of the bone marrow, leukemias originate from cells of the hematopoietic lineage, lymphomas are coming from malignant cells belonging to the immune system, neuroectodermal tumors originate from the outer cell layer of the early embryo and sarcomas derive from mesenchymal cells [2]. Mesenchymal cells comprise bone, cartilage and connective tissues. This is why sarcomas can present almost anywhere in the body. We recognize more than 50 subtypes of sarcomas.

1.1.3 Childhood cancers

Cancer is the second leading cause of death in children between the ages of 10 to 14 years. Only a small minority of 1% of all cancer cases are childhood cancers. Cancers appearing in children are rarer and also very different from those developing in adults. Childhood cancers arise because of DNA changes, which happen very early in life and sometimes even before birth. Unlike adult cancers, there is no strong link to lifestyle or risk factors. With a few exceptions, children tend to tolerate and respond better to chemotherapy [5]. In general, only very few mutations are found in

childhood cancers [6, 7]. As a consequence of this, childhood cancers are dependent on fewer oncogenes. Also, childhood cancers differ from adult cancers in regard of their distribution and prognosis [8].

Carcinomas are the most frequent cancer type in adults, whereas children are more affected by leukemias, cancers of the central nervous system, lymphomas and soft tissue sarcomas (mainly Neuroblastoma and Rhabdomyosarcoma) [9]. Soft tissue sarcomas are far more common among children than in adults (Fig. 3).

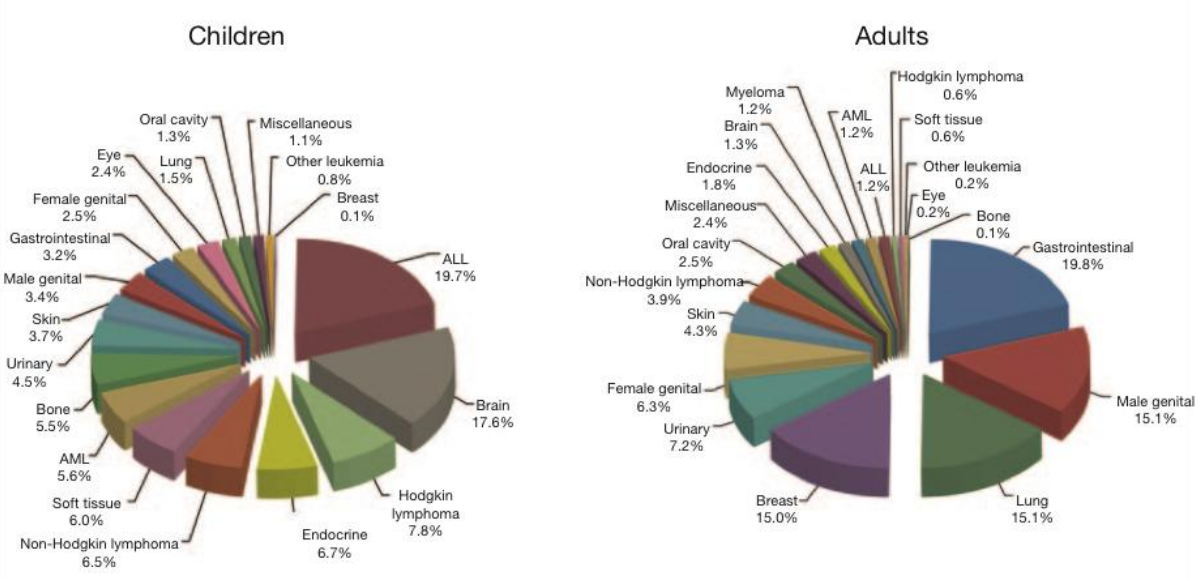

Figure 3: Frequency of cancner types in children and adults [7]

1.2 Rhabdomyosarcoma

The most common soft tissue sarcoma of childhood (≈50%) is Rhabdomyosarcoma (RMS) [10], a heterogeneous family associated with the skeletal muscle lineage [10-13]. Typically, RMS presents at an age before 10 years and slightly affects more males than females. It approximately accounts for 3-4% of all pediatric cancers with an estimated frequency of 350 new cases per year for the United States [11-13].

1.2.1 Origin of RMS

Almost all RMS cases occur sporadically. However, the disease is known to be linked to familial syndromes like Li-Fraumeni and neurofibromatosis, both of which are autosomal dominant disorders. This association most likely involves the inactivation of the p53 tumor suppressor gene by a germ line mutation (Li-Fraumeni) and hyperactivation of the RAS oncogene due to the loss of its negative regulator NF1 also by mutation (neurofibromatiosis) [10, 13]. These rare conditions indicate that a key to understanding RMS is to investigate genes responsible for growth and development in early life. Because one third of all children with RMS carry congenital

anomalies, it is believed that prenatal events contribute to tumor development [14]. A complete family history is therefore important to have. Up until now, no carcinogens have been identified but marijuana or cocaine may be teratogenous during pregnancy and support the development of RMS [15].

Mutations in embryonic signaling pathways, which regulate muscle development and regeneration, can act as potential RMS oncogenes. They may be primary events or act as secondary cooperating mutations. Therefore they play a critical role in RMS tumorigenesis in addition to other genetic changes. Notch, WNT and Hedgehog signaling pathways play an important role in skeletal muscle differentiation by controlling the balance of proliferation versus differentiation [16].

Although the exact cell of origin for RMS is not known yet, skeletal muscle precursors are the main suspects. The current opinion is that RMS arises from mesenchymal stem cells (MSCs) [13, 17]. This is supported by the fact that they possess stem cell characteristics like self-renewal, high proliferation rates, senescence resistance and reversion of quiescence, which are shared with cancer cells [16]. Additionally, RMS tumors express multiple “stemness” and skeletal muscle markers. For this reason, RMS is believed to arise from stem-like cells of the myogenic lineage, which fail to undergo correct differentiation. As these cells are of embryonic origin, it supports the fact that it mainly occurs in children [12, 13, 16]. An alternative hypothesis states that differentiated muscle cells undergo mutations that stimulate dedifferentiation and self-renewal [16].

1.2.2 Subtypes of Rhabdomyosarcoma: eRMS and aRMS

Histologically, rhabdomyosarcoma is classified as a small round blue cell tumor and can be divided into two subtypes (Fig. 4).

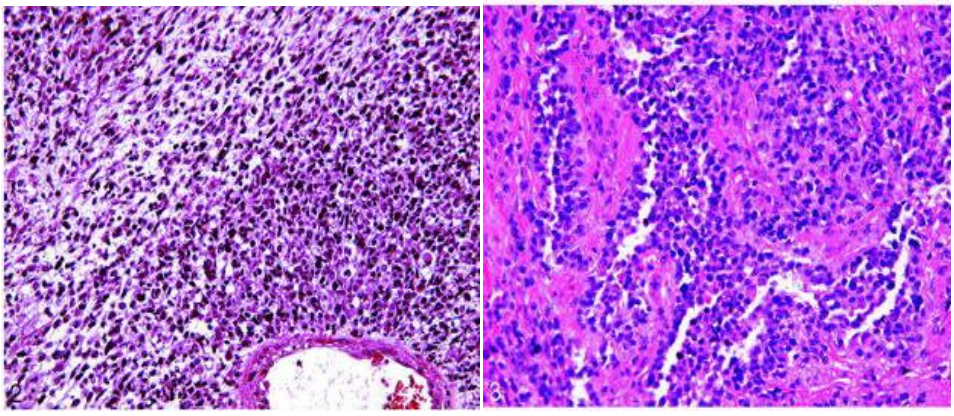

Figure 4: Histological differences between embryonal RMS (left) and alveolar RMS (right) (hematoxylin-eosin, 200x magnification) [18]

The embryonal subtype (eRMS) shows similarities to embryonic developing muscles and accounts for about 70-80% of all RMS cases. The other subtype is called alveolar (aRMS) because it typically contains alveolar structures similar to those seen in the lungs and it constitutes another 20-30% of RMS cases [11-13, 16]. There is also a third and rather uncommon type of RMS, which is called anaplastic rhabdomyosarcoma and appears in adults. It grows quickly and requires intensive therapy [10, 13, 18].

These variants also display clinically distinct phenotypes. Whereas eRMS mainly occurs in patients younger than 10 years, aRMS affects children as well as adolescents and young adults. The head and neck region, genitourinary tract and retroperitoneum are sites to which eRMS is often localized. aRMS instead tends to occur in the extremities and trunk region [13, 18]. Generally, aRMS is more aggressive than eRMS and is associated with an unfavorable prognosis because of its tendency to form metastases, poor response to therapy and high frequency of relapse [10-12, 19].

The differences between the subtypes are further reflected by the unique genetic features of eRMS and aRMS. A loss of heterozygosity at 11p15.5 in 80% and point mutations are often observed in eRMS [13]. This LOH seems to cause overactivation of the IGF2 gene, which could explain the growth of a tumor. In contrast, a characteristic feature of aRMS are chromosomal translocations occurring in 70-80% of all aRMS cases [16]. It is not exactly known what causes these genomic anomalities. Translocation positive aRMS displays an unfavourable prognosis (Fig. 5). The remaining 20% of aRMS cases are fusion negative and have comparable genetic characteristics and clinical outcomes of eRMS tumors (Fig. 5) [12, 13].

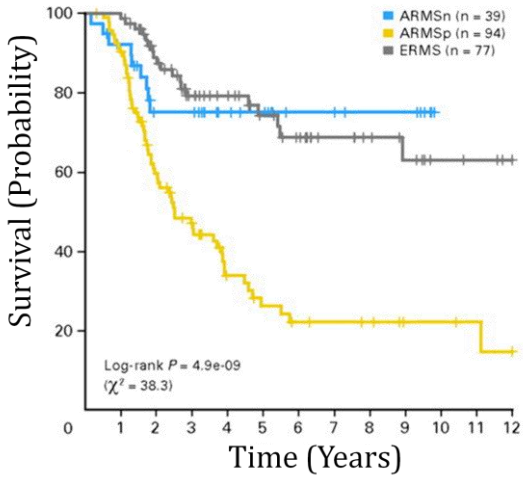

Figure 5: Kaplan Meyer overall survival curves for eRMS (grey), fusion negative aRMS (blue) and fusion positive aRMS (yellow) [20]

1.2.3 The PAX3/FOXO1 fusion protein

The most common translocation found in fusion positive aRMS is t(2;13)(q35;q14), which can be detected in 60% of cases. This event results in the formation of the oncogenic fusion protein PAX3/FOXO1. By this event, the DNA binding domain of PAX3 on chromosome 2 is fused to the transactivation domain of FOXO1 on chromosome 13 in an in-frame fashion (Fig. 6). In a similar way, the second most frequent fusion protein PAX7/FOXO1 is generated by a t(1;13)(p36;q14) translocation and is found in another 20% of aRMS [12]. These two translocations are specific to aRMS. In rare cases, a fusion between PAX3 and nuclear receptor coactivator genes NCOA1 and NCOA2 is found [21].

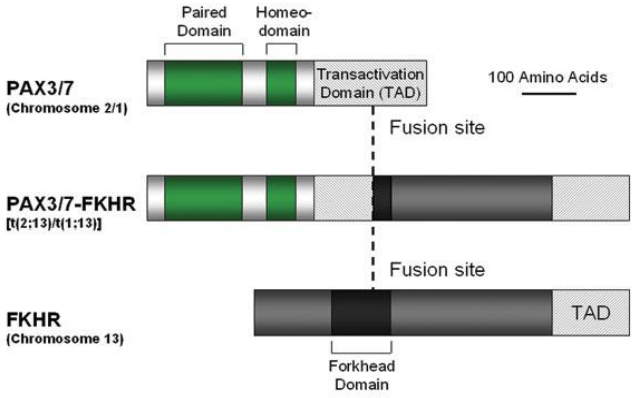

Figure 6: Schematic representation of the PAX3/7-FOXO1 fusion protein [22]

PAX3 and PAX7 belong to the family of paired box transcription factors. PAX3 plays a critical role in formation of various lineages during early embryonic development. Most importantly, it is necessary for the formation of skeletal muscle tissue [23]. In particular it is required for trunk muscle formation and delamination and migration of myogenic progenitor cells from the dermamyotome to the limb buds [24, 25]. Particularly, PAX3 controls cell survival, proliferation, and entry into myogenic program in these myogenic progenitor cells [26]. More than that, it regulates genes responsible for differentiation of neural crest cells, where it is also expressed during embryonic development, into more specialized cell types like nerve cells, craniofacial bones and melanocytes [24, 26-28]. PAX3 mutations are associated with Waardenburg-syndrome [25], which is characterized by deafness, pigmentation errors and facial dysplasia.

FOXO1 is also a transcription factor belonging to the Forkhead box O subfamily. FOXO proteins are key regulators within a conserved pathway downstream of insulin and insulin-like growth factor receptors [29, 30]. The first forkhead gene was identified in Drosophila embryos and named after the changes of the head structure, which are seen upon mutation of this gene. They are involved in many cellular processes like proliferation, apoptosis, response to reactive oxygen species,

longevity, cell cycle regulation and metabolism [29, 31]. These transcription factors are regulated by posttranslational modifications and protein-protein interactions in response to conditional changes and cues [31, 32].

The PAX3/FOXO1 fusion protein is a functionally hyperactive transcriptional regulator compared to PAX3 [33-35]. Gene expression and genome-wide binding studies showed that PAX3/FOXO1 transcriptional targets involve PAX3 target genes and others [36, 37], responsible for the inhibition of differentiation, promotion of cell survival and proliferation of myogenic cells [38]. Despite its oncogenic potential, PAX3/FOXO1 is generally not sufficient for complete transformation [12]. Additionally, it must cooperate with other genetic changes like INK4a/ARF and Trp53 loss of function to finally lead to the formation of aRMS [39]. Important to mention is that the fusion status of aRMS tumors has prognostic value. Within the aRMS subgroup, the PAX3/FOXO1 fusion status is associated with the worst overall survival (Fig. 7) [12, 13, 19].

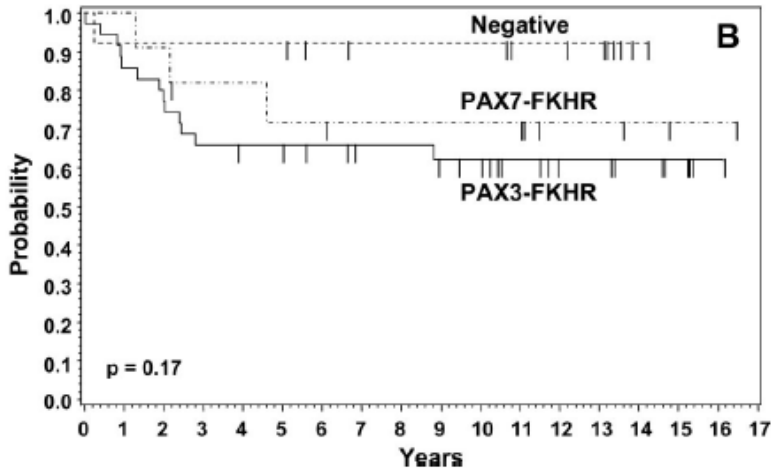

Figure 7: Kaplan Meyer plots of failure free survival for aRMS cases according to fusion status [40]

1.2.4 Diagnostics and Therapy

In parts of the body where the tumor can be recognized easily, RMS can often be found very early. As far as diagnostics are concerned, complete evaluation of a patient prior to treatment is necessary. This includes standard laboratory work as well as imaging techniques [10, 13]. However, the only way to confirm the diagnosis is to obtain a biopsy of the malignant mass for laboratory testing [10, 13]. All patients suffering from RMS require multimodal therapy. If possible, tumor resection is recommended followed by chemotherapy [10].

Depending on factors like subtype categorization, extent of distant disease, TNM classification and postsurgical residual disease, risk stratification is performed [10, 13]. Radiation therapy is used to improve local control of postoperative residual

disease and outcome. But this application has limitations in young children due to late side effects by coradiation of surrounding structures [13].

All patients suffering from RMS receive chemotherapy. Usually, therapeutic regimens consist of a combination of vincristine, actinomycin-D, and cyclophosphamide [13]. This multimodal drug therapy in combination with risk stratification and cooperative clinical trials has led to immense advances in improving outcomes of patients with low and intermediate risk disease [41]. But only little progress in the field of advanced RMS has been made [13, 16]. Patients with high-risk disease still have a very poor five year overall survival rate of 20-30%. Especially for the aRMS subgroup of patients, almost no improvement was achieved [42]. This is mainly due to the lack of new agents and protocols, highlighting the importance to find new therapeutic approaches. So far, no targeted drug therapy is available for this tumor.

1.3 Targeted therapy

Targeted therapy has shown to effectively inhibit specific signal transduction pathways and therefore prevent tumor growth and even induce regression. Unlike classical chemotherapeutics, which affect all rapidly dividing cells, targeted therapy interferes with cancer specific molecules directly associated with carcinogenesis and tumor growth [43, 44]. Very often, cancer cells are dependent on the continuous activity of altered proteins or pathways (oncogene addiction) [45]. Therefore, targeted therapy is supposed to be more effective and have fewer side effects. The two main categories of substances in use are small molecules and monoclonal antibodies. Small molecules are able to penetrate the cells and act on intracellular targets, whereas monoclonal antibodies target antigens on the cell surface. Small molecules are designed to block the enzymatic activity of the target protein [44]. Tumors especially suitable for such a treatment have aberrations in upstream signaling cascade components, cell surface receptors or cytoplasmic kinases [46]. One of the first successfully applied small-molecule inhibitors was Gleevec, a tyrosine kinase inhibitor, targeting the BCR/ABL fusion protein in chronic myelogenous leukemia [47].

1.3.1 Targeting transcription factors

A key role of oncogenic transformation can be attributed to transcription factors in a variety of cancers. In fact, transcription factors are the second most frequently mutated class of proteins found in human cancers [48]. In other cases, activity of transcription factors is altered by mutations in upstream signaling pathway components. Further, most oncogenic signaling pathways converge at sets of transcription factors as terminal effectors. Because many cancers are associated with aberrant gene expression patterns, transcription factors are promising targets for

therapeutic strategies [44, 49-51]. However, it is difficult to directly target transcription factors with small molecules because of their predominant nuclear localization, which makes them less accessible, the lack of enzymatic activity and large surface areas of their functional domains, which are more difficult to target than deep binding pockets of kinases. Strategies for the indirect inhibition of transcription factor activity with small molecules include interfering with activation, subcellular translocation, interaction with other proteins, or DNA binding [44, 49-51].

1.3.2 Targeting PAX3/FOXO1 in aRMS

The major cancer specific aberrant target in aRMS is PAX3/FOXO1. Because the PAX3/FOXO1 chimeric transcription factor (no targetable enzymatic activity) lies at the end of intracellular signaling and is constantly located in the nucleus (resistant to Akt mediated regulation) [11], no direct inhibitors are available. Nevertheless, it has been shown that translocation positive RMS cells depend on the expression of PAX3/FOXO1. Downregulation of PAX3/FOXO1 by siRNA or antisense oligonucleotides reduced proliferation and motility, decreased invasion, induced differentiation and even led to induction of apoptosis [52-54]. These findings suggest that interfering with PAX3/FOXO1 expression is a possible therapeutic strategy. As it is, for reasons of technical complexity, rather difficult to transfer this method in vivo, clinical implementations are out of reach at the moment. Other mechanisms by which PAX3/FOXO1 could be indirectly inhibited are therefore interesting to investigate [46].

Strategies to indirectly target PAX3/FOXO1 involve the recognition of PAX3/FOXO1 as a tumor antigen by immunotherapy [11]. Interfering with PAX3/FOXO1 interaction partners necessary for transcriptional activity might also be an interesting approach as well as restricting DNA binding at the epigenetic level by modulation of chromatin accessibility. Previous studies have shown that interfering with posttranslational modifications of PAX3/FOXO1 may be a useful strategy for the establishment of novel therapies. For example camptothecin, a topoisomerase I inhibitor, enhanced degradation of the fusion protein in aRMS cell lines probably by modulating its ubiquitination status [11]. Most importantly for this thesis, altering the phosphorylation status of either the C-terminal FOXO1 part, responsible for transactivation, or the N-terminal PAX3 part, responsible for DNA binding, is a promising possibility [11].

1.4 Regulation of transcription factors by phosphorylation

One way by which the activity of transcription factors can be regulated is by phosphorylation. Phosphorylation can induce changes in properties like subcellular localization, protein stability, DNA-binding activity and protein-protein interactions

[55]. The following is meant to illustrate these changes based on a few examples. Afterwards, I want to shortly summarize what is known about phosphorylation in FOXO1 and PAX3. After all, this should clarify why interfering with phosphorylation of transcription factors could be a useful strategy for targeted cancer therapy.

1.4.1 Examples

Stability of the oncogenic transcription factor MYC is controlled by a series of events including phosphorylation. Phosphorylation at Ser 62, which is linked to Polo-like kinase 1 (PLK1), interferes with phosphodegron-mediated ubiquitinylation by FBW7 ubiquitin ligase and subsequent proteasomal degradation of the protein. Therefore, MYC is stabilized. This event is triggered by activation of upstream PI3K signaling pathway [56, 57]. On the other hand, phosphorylation at Thr 58 promotes ubiquitylation and degradation of MYC [56].

The transcription factor CREB contains a transactivation domain, which is unstructured and inactive under normal conditions. Upon induction of adenyly cyclase (AC), in response to G protein coupled receptor activation, levels of the second messenger cAMP rise. This promotes the dissociation of protein kinase A (PKA) subunits. The caltalytic C subunits of PKA passively diffuse into the cell nucleus, where it phosphorylates the cAMP response element-binding protein (CREB) at Ser 133. Following this phosphorylation event, the transactivation domain undergoes a structural change allowing the interaction with CREB binding protein (CBP), which acts as a coaactivator [55, 58].

The interferon-regulated transcription factor IRF3, which plays an important role in innate immune systems response to viral infections, is modulated by multiple phosphorylation events within an autoinhibitory domain of the protein. If phosphorylated at these sites, the autoinhibitory domain unfolds and unmasks a region which is responsible for DNA binding, oligomerization and transactivation [55]. It activates the transcription of interferon alpha and beta as well as some other interferon induced genes.

1.4.2 FOXO1

Wild type FOXO1 activity is regulated by the canonical PI3K/AKT signaling pathway. This pathway is activated upon binding of growth factors to transmembrane receptor tyrosine kinases. Phosphorylation (Thr 24 / Ser 319, 256) of FOXO1 by AKT kinase (Fig. 8) promotes 14-3-3 protein binding and a subsequent sequestration in the cytoplasm [11, 30]. Therefore, FOXO1 is transcriptionally inactivated. Additionally, AKT-mediated phosphorylation at Ser 256 induces polyubiquitination and degradation of FOXO1 [59]. Of those three phosphorylation consensus sites found in wild type FOXO1, PAX3/FOXO1 retains two (Ser 319, 256). However, PAX3/FOXO1 is resistant to this AKT mediated regulation and is consistently localized in the

nucleus. This is probably because nuclear localization in PAX3/FOXO1 is controlled by N-terminal PAX3 domains [11].

The phosphorylation of FOXO1 at Ser 319 by AKT has been described to prime for subsequent phosphorylation of Ser 322 and Ser 325 by casein kinase 1 (CK1) (Fig. 8) [60]. Together with Ser 329 phosphorylation, mediated by dual-specific YAK1-related kinase 1 (DYRK1) (Fig. 8), this cluster was claimed to accelerate nuclear export by stimulating association with a protein complex containting the GTPase Ran [60].

Phosphorylation of FOXO1 by cyclin-dependent kinase 1 (Cdk1) at Ser 249 (Fig. 8) was described to block the interaction with 14-3-3 proteins, driving FOXO1 into the nucleus. Interestingly, Cdk2 can also phosphorylate FOXO1 at the same site but leads to an opposite output meaning cytoplasmatic localization and thereby inhibition [30, 31].

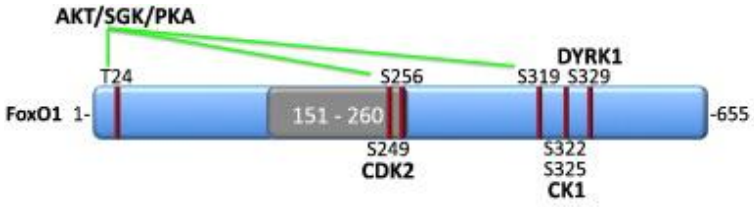

Figure 8: Overview of described phosphorylation sites in FOXO1 and the corresponding kinases with the forkhead domain depicted in grey [30]

1.4.3 PAX3

In contrast to FOXO1, phosphorylation of PAX3 is only poorly understood. Because wild type PAX3 is exclusively nuclear, it does not seem that subcellular localization is regulated by phosphorylation. Three phosphorylation sites (Ser 201, 205, 209) have been reported and the corresponding kinases have been identified. All three residues are retained in PAX3/FOXO1 [11].

It was shown that in proliferating primary myoblasts, casein kinase 2 (CK2) phosphorylates PAX3 as well as PAX3/FOXO1 at serine 205. Whereas this phosphorylation is lost on PAX3 upon induction of differentiation, it persists on PAX3/FOXO1 [24, 26, 28]. This first phosphorylation promotes a subsequent phosphorylation at Ser 201 by GSK3β. A third phosphorylation event is observed only in PAX3 after induction of differentiation. This phosphorylation at Ser209 could recently be linked to CK2 [28]. These findings suggest a distinct pattern of phosphorylation of PAX3 and PAX3/FOXO1 during early myogenic differentiation.

1.5 Previous Work

1.5.1 Regulation of PAX3/FOXO1 by phosphorylation

Through the analysis of gene expression data from therapeutic RMS biopsies, kinases with known tumorigenic capacity could be identified as possible targets. A series of kinase inhibitors against three of those kinases (EGFR, HGFR and FGFR) were then tested for their ability to reduce growth of different RMS cell lines. One compound with specific antigrowth and proapoptotic effect for the aRMS subgroup was PKC412, which induced apoptosis at submicromolar concentrations [46]. PKC412 inhibits several kinases like PKC, Akt, c-Kit, FLT3 and FGFR. PKC412 is currently evaluated as FLT3 inhibitor for the treatment of AML in a phase II clinical study.

It could be shown that PKC412 has an inhibitory effect on the transcriptional activity of PAX3/FOXO1. Further, mass spectrometry data revealed that this effect is based on modulation of phosphorylation sites in the PAX3 part of the fusion protein. These sites lie within the linker region between the two DNA-binding domains (Fig. 9A). Interestingly, simultaneous mutation of all six serine residues into alanine (P3F 6xA) led to strongest reduction of transactivation potency (Fig. 9B). This was measured using a reporter cell line containing a plasmid, on which the luciferase gene was downstream of paired domain or homeodomain DNA binding sites [46].

A

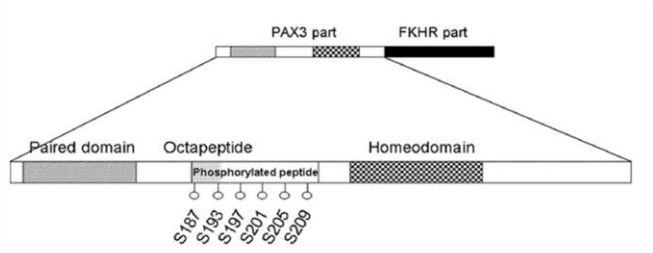

B

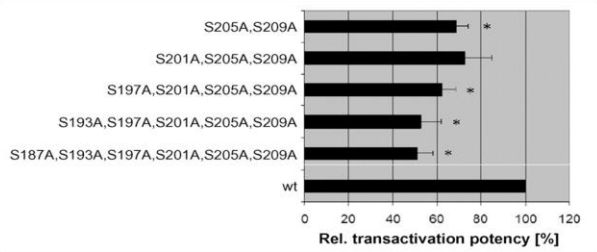

Figure 9: PAX3/FOXO1 DNA binding activity is regulated by phosphorylation
A) Schematic representation of the PAX3 domain structure with identified phosphorylation sites [46] **B)** Relative transactivation potencies of wt PAX3/FOXO1 and serine-alanine mutant PAX3/FOXO1 isoforms measured by luciferase reporter assay [46]

This suggests that a combination of phosphorylated sites is necessary for full transcriptional activity of PAX3/FOXO1. Because neither subcellular localization nor stability of PAX3/FOXO1 was affected, it was reasoned that DNA binding is decreased via the paired and the homeodomain.

An independent study identified that Glycogen synthase kinase 3 (GSK3) inhibitors preferentially reduce cell growth of the aRMS subtype by screening 160 kinase inhibitors in RD (eRMS) and Rh30 (aRMS) cells. Induction of apoptosis after treatment was more effective in aRMS cells. Also reduced transcriptional activity of PAX3/FOXO1 upon GSK3 inhibition was demonstrated. It was further shown that GSK3 is able to phosphorylate PAX3/FOXO1 in vitro [61].

Another study, which screened small molecule libraries, found that thapsigargin, an inhibitor of sarco/endoplasmic reticulum Ca^{2+} ATPase (SERCA), inhibited PAX3/FOXO1 transcriptional activity in reporter cells. It was revealed that this effect is mediated by AKT activation through thapsigargin. It was already published that AKT activation results in PAX3/FOXO1 phosphorylation in aRMS cells, which reduces its transcriptional activity [62]. They validated these findings and showed that this phoshphorylation event triggers PAX3/FOXO degradation by the proteasome pathway. An additional effect of thapsigargin treatment was reduced binding of PAX3/FOXO1 to regulatory elements of target genes. Further, thapsigargin blocked cell growth, survival and metastatic potential and was able to induce apoptosis in aRMS cells. Finally, thapsigargin treatment of human aRMS xenografts inhibited tumor growth in vivo [63].

Altogether, these findings suggest that small-molecule inhibition of kinases, which can influence the transcriptional activity of PAX3/FOXO1 by phosphorylation, is an alternative therapeutic approach in aRMS.

1.5.2 Kinome Screening

A functional RNAi screen of the human kinome was performed to identify upstream kinases with the ability to alter the transcriptional activity of PAX3/FOXO1. For this, Rh4 cells (aRMS cell line expressing PAX3/FOXO1) were transfected with a luciferase reporter plasmid containing the luciferase gene downstream of the AP2beta promoter (a known target of PAX3/FOXO1 [53]). A siRNA library containing 3 unique siRNAs per gene against 719 kinases was used to produce knockdowns of the targets (Fig. 10). Almost one third of kinases that showed reduced luciferase activity after silencing (15 of 47 hits) had a previously described role in cancer. The remaining candidates could all be linked to either muscular and skeletal system disorders or genetic malignancies [64].

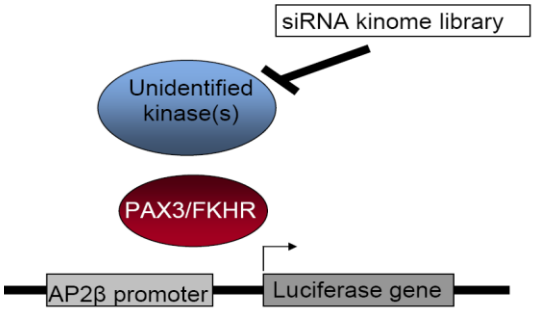

Figure 10: siRNA kinome screening with PAX3/FOXO1 activity read-out [65]

In a similar approach, the same reporter cell line (Fig. 10) was used to measure the effect of 125 different kinase inhibitors on PAX3/FOXO1 activity. From these two screening approaches, Polo-like kinase 1 (PLK1) was one of the top candidates for further investigations [65].

A different siRNA screening performed against 897 human phosphatases and kinases identified 16 phosphatases and 50 kinases with significant roles in growth control and survival in RMS cell lines. They found PLK1 to be one of the most important kinases supporting the survival of RMS. Silencing of PLK1 caused significant growth inhibition and apoptosis in RMS cells, whereas there was no effect observed in normal muscle cells. They additionally showed that other pediatric tumor cell lines were also highly sensitive to PLK1 inhibition [66].

Taken together, these studies indicate that PLK1 is a promising candidate to target for the treatment of aRMS, since it is most probably involved in regulating the transcriptional activity of PAX3/FOXO1 and also because it is responsible for the survival of RMS cells.

1.5.3 PLK1 as a novel therapeutic target

PLKs are Ser/Thr kinases containing a conserved Polo-box domain, which mediates protein interactions. This module recognizes phosphopeptides with the consensus core consensus motif Ser-pThr/pSer-Pro/X. There are four different PLKs in mammals. PLK1 expression and protein levels are low through G1, 0 and S phase and rise in G2 with a peak during M phase [67, 68]. PLK1 has several mitotic roles involving entry into M phase, centriole and centrosome maturation, mitotic chromosome segregation with involvement in the spindle assembly checkpoint and cytokinesis. It is also involved in the DNA damage checkpoint [69, 70]. More than that, PLKs seem to timely coordinate cell division during embryonal development [67, 68]. PLK1 is overexpressed in a variety of human tumors suggesting a role in carcinogenesis and has already been proposed as a therapeutic target [71-74]. Besides promoting proliferation, PLK1 overexpression contributes to carcinogenesis

by promoting chromosomal instability and aneuploidy [75]. Also, determination of PLK1 expression levels has prognostic value for different cancers. Elevated PLK1 protein levels have been correlated with poor prognosis in non-small cell lung cancer, squamous cell carcinoma, esophageal carcinoma, melanoma, oropharyngeal carcinoma, breast cancer, colorectal cancer, and endometrial carcinoma [72]. In addition, it serves as a marker for high risk of metastasis. It was already shown that inhibition of PLK1 led to mitotic catastrophe that induced apoptosis in tumor cell lines. Several inhibitors targeting PLK1 are currently being developed and investigated in clinical trials [68, 76, 77].

1.5.4 In vitro and in vivo studies of PLK1

Co-Immunoprecipitation experiments in aRMS cells revealed that PLK1 indeed interacts with PAX3/FOXO1 (Fig. 11A). Inhibition of PLK1 with siRNA or drug treatment reduced the expression of PAX3/FOXO1 target genes in aRMS cells (Fig. 11B). Additionally, drug treatment reduced PAX3/FOXO1 protein levels in those cells (Fig. 11C). This effect could be rescued by the proteasomal inhibitor bortezomib. It was also shown that in xenograft mouse models, PLK1 inhibition by BI2536 caused remarkable tumor regression [65]. It is worth to mention that PLK1 is overexpressed in human aRMS tumors compared to normal muscle tissue samples [65, 66].

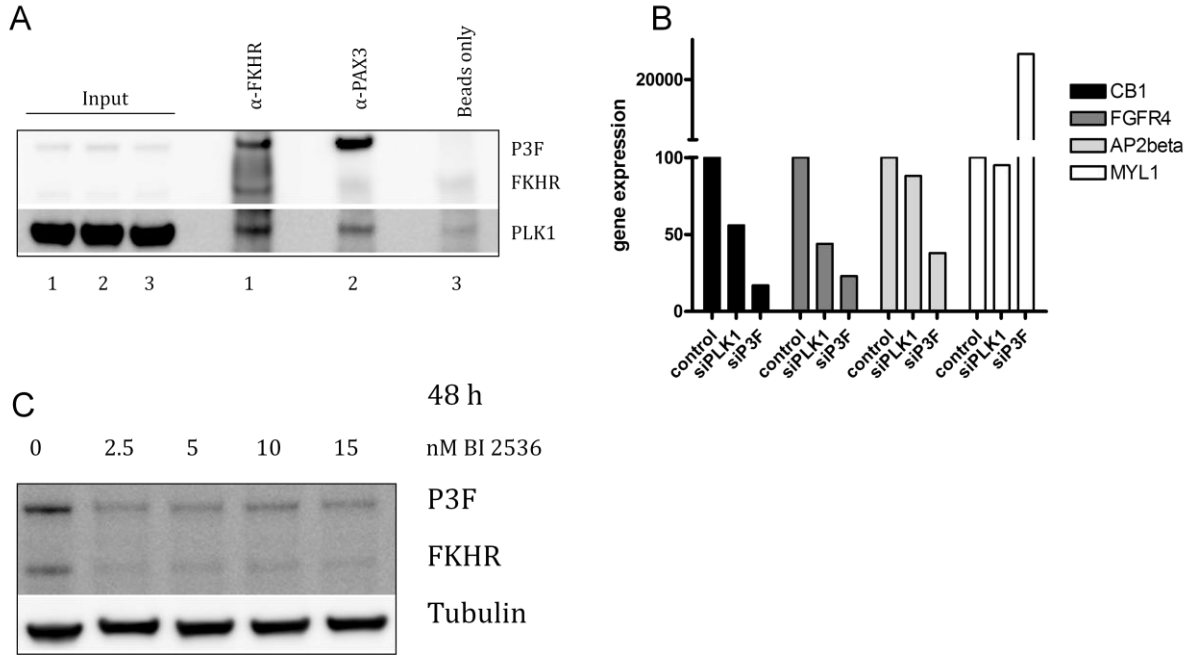

Figure 11: Preliminary data of in vitro studies of PLK1 [65]
A) endogenous co-IP from Rh4 cell lysates with anti-FKHR(1) and anti-PAX3 antibody(2) showing interaction of PAX3/FOXO1 with PLK1 **B)** PAX3/FOXO1 target gene expression levels after siRNA knockdowns of PLK1 and PAX3/FOXO1 in Rh4 cells compared to scrambled siRNA treatment; CB1: cannabinoid receptor 1, FGFR4: fibroblast growt factor receptor 4, AP2beta; activating enhancer binding protein 2 beta, MYL1: myosin light chain 1 **C)** PAX3/FOXO protein levels after treatment of Rh4 cells with different concentrations of PLK1 inhibitor after 48 hours

These experiments consolidate PLK1 as a possible regulator of PAX3/FOXO1 transcriptional activity. Further, these data show that PLK1 might have an influence on the stability of PAX3/FOXO1. Therefore, PLK1 is a potential therapeutic target in aRMS and required further investigation.

1.6 Aim of thesis

A first aim was to validate that PLK1 was regulating the transcriptional activity of PAX3/FOXO1.

Another goal of my master thesis was to investigate whether PLK1 is indeed able to phosphorylate PAX3/FOXO1 as previous findings suggested. Further I wanted to identify the sites of phosphorylation within PAX3/FOXO1, because these sites are considered to play a role in the regulation of its transcriptional activity.

The main part of my work was to test if any of these found phosphosites indeed have an influence on the transcriptional activity of PAX3/FOXO1. I also wanted to find out if any of the found phosphosites has an influence on the stability of PAX3/FOXO.

2 MATERIAL

2.1 Media and Buffers

2.1.1 Bacterial Media

Table 1: Bacterial Media

Media	Components	Amount
Luria Bertani medium	Bacto tryptone	10 g
	Yeast extract	5 g
	NaCl	10 g
	pH was adjusted to 7.5 with NaOH/HCl Water was added to a final volume of 1 l Sterilization was performed by autoclaving	
Luria Bertani medium with Agar for plates	Bacto tryptone	10 g
	Yeast extract	5 g
	NaCl	10 g
	Bacto agar	15 g
	pH was adjusted to 7.5 with NaOH/HCl Water was added to a final volume of 1 l Sterilization was performed by autoclaving	
SOC medium	Producer	
	Invitrogen, Basel, Switzerland	

2.1.2 Cell culture Media

Table 2: Cell culture Media

Media	Component	Amount
Complete Medium	Dulbeccos modified Eagles Medium (DMEM)	
	Fetal bovine serum (FBS)	10 %
	Penicilin	100 units/ml
	Streptomycin	100 units/ml
	L-glutamine	2 mM
Mesenchymal Stem Cell Medium	Producer	
	Pelo Biotech Gmbh, Planegg, Germany	

2.1.3 General Buffers

Table 3: General buffers

Buffer	Component	Amount
RIPA buffer	Tris-Cl (pH=7.5)	50 mM
	NaCl	150 mM
	NP 40	1%
	Na-Deoxycholate	0.5%
	SDS	0.1%
	EGTA	1 mM
	NaF	50 mM
	β-Glycerolphosphat	10 mM

	Natrium Pyrophosphat	5 mM
	Na_3VO_4	1 mM
	Complete protease inhibitor	1x
Lysis buffer	Tris-Cl (pH=7.5)	50 mM
	NaCl	125 mM
	NP 40	1%
	$MgCl_2$	1.5 mM
	NaF	25 mM
	β-Glycerolphosphat	10 mM
	Natrium Pyrophosphat	5 mM
	Na_3VO_4	2 mM
	Complete protease inhibitor	1x
Wash buffer	Tris-Cl (pH=7.5)	50 mM
	NaCl	150 mM
CIP 1x reaction buffer	Tris-Cl (pH= 7.5)	50 mM
	$MgCl_2$	1 mM
	$ZnCl_2$	0.1 mM
PLK1 5x reaction buffer	HEPES (pH=7.5)	250 mM
	$MgCl_2$	50 mM
	DTT	12.5 mM
	Triton X-100	0.05%
	ATP	200 µM
CH buffer	Tris-Cl (pH=8.0)	20 mM
	NaCl	500 mM
	Triton X-100	0.1%
	EDTA	1 mM
	Glycerol	10%
10x TBS-Tween	Tris-Cl (pH=7.5)	60.5 g
	NaCl	87.6 g
	H_2O	800 ml
	pH was adjusted to 7.5 with HCl Water was added to a final volume of 1 l	
	Tween 20	10 ml
Mixing solution	H_2O	50 ml
	1M HEPES	125 µl
2xHeBS	NaCl	0.28 M
	HEPES	0.05 M
	Na_2HPO_4	1.5 mM
	H_2O	800 ml
	pH was adjusted to 7.0 with NaOH, H_2O was added to a final volume of 1 l	

2.2 Cell lines

Table 4: Cell lines

Cell line	Source
Rh3	Susan Ragsdale, St.Jude Children`s Research Hospital, Memphis TN, USA
Rh4	Peter Houghton, The Research Institute at Nationwide Children's Hospital, Columbus, OH, USA
RMS13	Roland Kappler, Ludwig-Maximilians-Universität München, Germany
RMS	Janet Shipley, Institute of Cancer Research, London, GB
RD	American Type Culture Collection (ATCC)
mMSC	Life Technologies, Oslo, Sweden
HS5	American Type Culture Collection (ATCC)
Primary hMSC	Pelo Biotech Gmbh, Planegg, Germany
C2C12	American Type Culture Collection (ATCC)
Phoenix ampho	American Type Culture Collection (ATCC)
293 GPG	Richard C. Mulligan, Children's Hospital, Boston, MA, USA

2.3 Kits

Table 5: Kits

Product	Producer
QIAGEN Plasmid Mini Kit	Qiagen, Basel, Switzerland
In-Fusion HD cloning Kit	Clonetech, Saint-Germain-en-Laye, France
jetPRIME	Polyplus transfections, Basel, Switzerland
Pierce BCA protein assay Kit	Thermo Scientific, Reinach, Switzerland
RNeasy Mini Kit	Qiagen, Basel, Switzerland
QIAquick Gel Extraction Kit	Qiagen, Basel, Switzerland
High capacity cDNA reverse transcription Kit	Applied Biosystem, Zug, Switzerland

2.4 Antibodies

Table 6: primary antibodies

Antibody	Host organism	Producer
Anti-FOXO1 H-128	Rabbit	Santa Cruz Biotech, USA
Anti-Actin	Rabbit	Cell signaling, Danvers, USA
Anti-GAPDH	Rabbit	Cell signaling, Danvers, USA
Anti-Cyclin B1	Rabbit	Cell signaling, Danvers, USA
Anti-Flag	Mouse	Sigma-Aldrich, Buchs, Switzerland
Anti-FOXO1 (p322)	Rabbit	Abcam, Cambridge, UK

Table 7: secondary antibody

Antibody	Host organism	Producer
Anti-rabbit HRP-linked	Anti-rabbit	Cell signaling, Danvers, USA

2.5 Solutions

Table 8: Solutions

Product	Producer
20xNuPAGE SDS Running buffer	Invitrogen, Basel, Switzerland
20xNuPAGE Transfer buffer	Invitrogen, Basel, Switzerland
25xTAE buffer	Life Technologies, Oslo, Sweden
Chemiluminiscence detection reagents ECL	GEHealthcare, Amersham, Switzerland
Dimethylsulfon (DMSO)	Sigma-Aldrich, Buchs, Switzerland
DMEM	Sigma-Aldrich, Buchs, Switzerland
Dynabeads	Life Technologies, Oslo, Sweden
FBS	Invitrogen, Basel, Switzerland
GelRed	Biotium, Hayward, USA
Non-fat dry milk	Migros, Zurich, Switzerland
10xPhosphate buffered saline (PBS)	Sigma-Aldrich, Buchs, Switzerland
Super signal West Femto Maximum Sensitivity Substrate	Thermo scientific, Reinach, Switzerland
TaqMan Gene Expression Master MIx	Applied Biosystem, Zug, Switzerland
Trypsin/Ethylenediaminetetraacetic (EDTA)	Bioconcept, Allschwill, Switzerland

2.6 Chemicals and enzymes

Table 9: chemicals and enzymes

Product	Producer
4% Formalin	Carl Roth, Arlesheim, Switzerland
Agarose	Eurogentec, Seraing, Belgium
Ampicillin	Sigma-Aldrich, Buchs, Switzerland
Bacto-Agar	BD, Allschwill, Switzerland
Bacto-Tryptone	BD, Allschwill, Switzerland
$CaCl_2$	Sigma-Aldrich, Buchs, Switzerland
Chloramphenicol	Fluka, Buchs, Switzerland
CIP (Calf intestinal phosphatase)	Promega, Fitchburg, Madison, USA
Complete protease inhibitor	Roche, Reinach, Switzerland
Cycloheximide	Fluka, Buchs, Switzerland
DpnI	Thermo scientific, Reinach, Switzerland
DTT	Sigma-Aldrich, Buchs, Switzerland
EGTA	Sigma-Aldrich, Buchs, Switzerland
Ethanol	Kantonsapotheke Zurich, Switzerland
Glycerol	Sigma-Aldrich, Buchs, Switzerland
IPTG	Eurogentec, Seraing, Belgium
L-Glutamine	Bioconcept, Allschwill, Switzerland
Methanol	Hänseler AG, Herisau, Switerland
$MgCl_2$	Sigma-Aldrich, Buchs, Switzerland
Na_3VO_4	Sigma-Aldrich, Buchs, Switzerland
NaCl	Sigma-Aldrich, Buchs, Switzerland
Na-Deoxycholate	Sigma-Aldrich, Buchs, Switzerland
NaF	Sigma-Aldrich, Buchs, Switzerland
Natrium Pyrophosphat	Sigma-Aldrich, Buchs, Switzerland

NP 40	Fluka, Buchs, Switzerland
Penicillin	Invitrogen, Basel, Switzerland
PLK1 recombinant kinase	Invitorgen, Basel, Switerland
PMSF	Sigma-Aldrich, Buchs, Switzerland
Polybrene	Fluka, Buchs, Switzerland
Ponceau	Sigma-Aldrich, Buchs, Switzerland
RNase-Free DNase Set	Qiagen, Basel, Switzerland
SDS	Sigma-Aldrich, Buchs, Switzerland
Streptomycin	Invitrogen, Basel, Switzerland
Tetracycline	Fluka, Buchs, Switzerland
Tris-Cl (pH=7.5)	Sigma-Aldrich, Buchs, Switzerland
Triton X-100	Sigma-Aldrich, Buchs, Switzerland
Tween 20	Sigma-Aldrich, Buchs, Switzerland
Yeast extract	BD, Allschwill, Switzerland
XhoI	Thermo scientific, Reinach, Switzerland
β-Glycerolphosphat	Sigma-Aldrich, Buchs, Switzerland

2.7 Plasmids

Table 10: plasmids

Plasmid name	Gift from	Backbone Producer, product number
pMSCV-IRES-GFP	Dr. Elisa Zimmermann	Addgene, no. 33336
pMSCV-PAX3/FOXO1-IRES-GFP	Dr. Elisa Zimmermann	Addgene, no. 33336
pcDNA3-PAX3/FOXO1 (6xA, S201A, S205A, G48S, N269A)	Dr. Marco Wachtel	Invitrogen, V790-20
pCMV-NFlag-PAX3/FOXO1	Verena Thalhammer	Stratagene, #240229
pTXB1	Dr. Laura Lopez	New England Biolabs, N6707S

2.8 Software

Table 11: Software

Product	Producer
FlowJo	Tree Star Inc., Ashland, USA
SDS 2.2	Rasband, W.S., National Institutes of Health, Bethesda, Maryland, USA
ImageJ	Applied Biosystem, Zug, Switzerland
Prism 6 trial	www.graphpad.com
Clone manager	Scientific & Educational Software, Cary, USA

3 METHODS

3.1 Bacteria and Cloning

3.1.1 Transformation of competent bacteria

Transformation of competent Escherichia Coli (DH5α) is the method to amplify plasmid DNA through cellular replication. For each transformation, an aliquot of 50 µl competent bacteria was thawed on ice. Afterwards, 1µl of plasmid DNA recovered with Miniprep Kit or 2 µl of In-Fusion HD cloning Kit Reactions were added. The mixture then was incubated on ice for 12 minutes. Heat shock was performed in a water bath at 42°C for 2 minutes, followed by a 2 minutes incubation on ice. 400 µl of prewarmed SOC medium were added and the mixture was incubated for 1h at 37°C shaking at 200 rpm. Finally, 100 µl of the transformation mixture were plated on agar plates containing the appropriate antibiotic (e.g. 100 µg/ml Ampicillin). The plates were incubated at 37°C overnight.

3.1.2 Plasmid Miniprep

Single colonies were picked and used to inoculate 5ml of LB medium containing the appropriate antibiotic (e.g. 100 µg/ml Ampicillin). The inoculates were incubated overnight at 37°C. The next day, bacteria were pelleted by centrifugation at 4000 rpm for 10 minutes. The supernatant was discarded and the QIAprep Spin Miniprep Kit protocol was followed. DNA was eluted in 50 µl H_2O. Concentrations of plasmid DNA were determined by measuring OD260nm using the NanoDrop ND-1000 Spectrophotometer.

3.1.3 Site directed mutagenesis of PAX3/FOXO1

Mutagenesis was performed using QuikChange (Stratagene) recommendations. As a first step, mutagenic primers were designed using clone manager software. By using the PAX3/FOXO1 coding sequence, the codon coding for each amino acid to be mutated was determined. By changing nucleotides, codons coding for alanine (or aspartic acid) were generated. Complementary primers of 40-42 bp were designed with the desired mutations in the middle of the primers. The primers were generated by Microsynth. A list of all primers used for mutagenesis is shown below.

Table 12: primers used for site directed mutagenesis

Primer name	Primer sequence
P3F_S30A_F	5'-GTT CCC GCT GGA AGT GGC CAG TCC CCT CGG CCA GGG CCG CG-3'
P3F_S30A_R	5'-CGC GGC CCT GGC CGA GGG CAG TGG ACA CTT CCA GCG GGA AC-3'
P3F_T31A_F	5'-GTT CCC GCT GGA AGT GTC CGC TCC CCT CGG CCA GGG CCG CG-3'
P3F_T31A_R	5'-CGC GGC CCT GGC CGA GGG GAG CGG ACA CTT CCA GCG GGA AC-3'
P3F_T31D_F	5'-GTT CCC GCT GGA AGT GTC CGA TCC CCT CGG CCA GGG CCG CG-3'
P3F_T31D_R	5'-CGC GGC CCT GGC CGA GGG GAT CGG ACA CTT CCA GCG GGA AC-3'
P3F_S389/393A_F	5'-AAT GGC CTC GCA CCT CAG AAT GCA ATT CGT CAT AAT CTG TCC-3'
P3F_S389/393A_R	5'-AGA TTA TGA CGA ATT GCA TTC TGA GGT GCG AGG CCA TTG CC-3'
P3F_S399A_F	5'-ATT CAA TTC GTC ATA ATC TGG CCC TAC ACA GCA AGT TCA TTC G-3'
P3F_S399A_R	5'-CGA ATG AAC TTG CTG TGT AGG GCC AGA TTA TGA CGA ATT GAA T-3'
P3F_S399/402A_F	5'-TCA TAA TCT GGC CCT ACA CGC CAA GTT CAT TCG TGT GC-3'
P3F_S399/402A_R	5'-CGA ATG AAC TTG GCG TGT AGG GCC AGA TTA TGA CGA ATT G-3'
P3F_S503A_F	5'-ACT AGC TCA AAT GCT ACT ATT AGT GGG AGA CTC TCA CC-3'
P3F_S503A_R	5'-GGT GAG AGT CTC CCA CTA ATA GTA GCA GCA TTT GAG CTA GT-3'
P3F_510A_F	5'-TAC TAT TAG TGG GAG ACT CGC ACC CAT TAT GAC CGA ACA GG-3'
P3F_510A_R	5'-CCT GTT CGG TCA TAA TGG GTG CGA GTC TCC CAC TAA TAG TA-3'

In a second step, a PCR reaction mix was prepared as shown below.

Table 13: PCR reaction mix for site directed mutagenesis

Component	Amount
pMSCV-P3F-IRES-GFP plasmid DNA	0.5 µl (≈ 25 ng)
Forward primer (10 µM)	1.25 µl
Reverse primer (10 µM)	1.25 µl
Accu Prime Pfx DNA Polymerase	0.3 µl
10x Accu Prime reaction mix	2.5 µl
H_2O	19.2 µl

The cycling conditions for the PCR were as follows. For some reactions, cycle numbers and annealing temperature had to be modified.

94°C	2 min	
94°C	30 sec	16 cycles
55°C	1 min	
68°C	12 min	
68°C	7 min	
4°C	∞	

1.2 µl of DpnI enzyme was directly added to the reaction mix and incubated at 37°C for 3 hours to digest parental plasmid DNA. It was verified on an agarose gel that the PCR reaction was successful. Competent bacteria were transformed and the next day, colonies were picked for Minipreps. Sequencing was done by Microsynth.

3.1.4 Subcloning

Subcloning of PAX3/FOXO1 DNA sequences was performed following the In-Fusion HD cloning Kit protocol. As a first step, the target vector (pMSCV-IRES-GFP or pTXB1) had to be linearized by restriction enzyme digestion. In our case we always used XhoI. The digestion mix was incubated overnight at 37°C.

Table 14: Digestion reaction mix for subcloning

Coponent	Amount
Target vector plasmid DNA	2 µg (x µl)
XhoI	2 µl
NEB3 buffer (10x)	2 µl
H_2O	To total volume of 20 µl

Secondly, a PCR of PAX3/FOXO1 was made using primers with 15 bp 5' extensions complementary to the ends of the linearized vector. The primers were designed using clone manager software. A summary of all primers used for subcloning is shown below.

Table 15: Primers used for subcloning

Primer name	Primer sequence
pMSCV_P3Fumkl_F	5'-GAA TTC AGA TCT CGA ATG ACC ACG CTG GCC GGC-3'
pMSCV_P3Fumkl_R	5'-ATT GAT CCC GCT CGA TCA GCC TGA CAC CCA GCT-3'
pTXB1_P3Fumkl_F	5'-CCG CGA ATT CCT CGA ATG ACC ACG CTG GCC GGC-3'
pTXB1_P3Fumkl_R	5'-AGG AAG AGC CCT CGA TAA GCC TGA CAC CCA GCT-3'

The PCR was conducted according to the suggested conditions mentioned in the Phusion High-Fidelity DNA Polymerase Product Information sheet.

It was verified on an agarose gel that the vector was linearized and the target DNA was amplified. The bands were excised from the gel and DNA was extracted using the QIAquick Gel Extraction Kit. DNA concentrations were determined using the NanoDrop ND-1000 Spectrophotometer. The In-Fusion reaction was set up and

conducted as described in the In-Fusion HD Cloning Kit protocol. Competent bacteria were transformed with 2 μl of the reaction mix. The next day, colonies were picked for Minipreps. Sequencing was performed by Microsynth.

3.2 Cell culture

3.2.1 Thawing, Splitting and Freezing of cell lines

aRMS cell lines, mMSCs and Phoenix ampho cells were cultured in complete medium. C2C12 cells were cultured in complete medium with 20% FBS to prevent differentiation. 293 GPG cells were cultured in complete medium with 1 μg/ml tetracycline, except for periods of virus production. Primary hMSCs were cultured in mesenchymal stem cell medium. All cells were incubated at 37°C and 5% CO_2.

1ml aliquots of frozen cell lines were thawed in a 37°C water bath and transferred in a falcon tube with 9ml culture medium. Then the cells were centrifuged for 5 minutes at 1200 rpm. The supernatant was removed and the pellet was resuspended in the correct volume of complete medium required for the size of corresponding culture dishes.

Cell lines were split when they reached approximately 80% confluency. The medium was removed from the cells followed by a washing step with 1xPBS. Cells were incubated for 3-5 minutes with Trypsin/EDTA at 37°C. After resuspending the cells in complete medium, the desired fraction was transferred in a new cell culture dish and complete medium was added to the final volume required.

For long-term storage, cells were frozen in freezing medium consisting of complete medium with 10% DMSO. Cells were trypsinized and after addition of medium centrifuged for 1200 rpm 5 minutes. The pellet was resuspended in freezing medium and aliquots of 1 ml were transferred into cryotubes. For short-term storage, cryotubes were put in -80°C. For longer storage periods, cryotubes were transferred into the liquid nitrogen tank.

3.2.2 siRNA Knockdowns

All transient siRNA mediated knockdown experiments in aRMS cell lines were performed following the instructions of the INTERFERin Easy protocol. For this, cells were transfected with PLK1 specific siRNA (s449) or scrambled siRNA as a control using INTERFERin. All experiments were performed in 6-well format using 200’000 cells. Cells were collected 48 hours or 72 hours after transfection for further analysis.

Table 16: silencer select siRNAs for knockdown experiments

Gene name	Silencer Select siRNA ID
Scrambled # 2 (negative control)	4390846
PLK1	s449

3.2.3 Transient transfections

In my experiments I used two different protocols for transient transfections of cells.

For transfections with Jet-Prime, cells were seeded the day before transfection (Table 17). 1.5 ml Eppendorf tubes were prepared with the appropriate JetPrime buffer volume and according amounts of plasmid DNA was added. The tubes were vortexed and briefly centrifuged. Then JetPrime reagent was added and the tubes were again vortexed and centrifuged (Table 17). The reaction mix was then incubated at room temperature for 10 minutes to allow formation of DNA precipitate. Medium on the cells was changed and the reaction mix was directly added dropwise to the fresh medium. The next day, medium was changed again.

Table 17: conditions for Jet-Prime transfections

Culture Vessel	Number of cells seeded	Volume of JetPrime buffer (μl)	Amount of DNA (μg)	Volume of JetPrime reagent (μl)	Volume of growth medium (ml)
6-well	200'000	200	1	2	2
10 cm	2.5 Mio	500	10	20	10

For transfections with calcium phosphate, 6.5 Mio HEK293T cells were plated in a 15 cm plate the day before transfection. 24 hours later, medium was changed. 50 μg of plasmid DNA were added to 0.5 ml mixing solution. To this mixture, 0.5 ml of 0.5 M $CaCl_2$ was added. Then, 1 ml of 2xHeBS was added dropwise while vortexing. After incubation for 15 minutes at room temperature, the solution was added dropwise to the plate. The next day, medium was changed.

3.2.4 Retroviral transductions

Packaging cell lines allow production of infectious viral particles. In my experiments I used two different packaging cell lines for the production of retrovirus.

The 293 GPG packaging cell line, based on HEK293T cells, is considered to produce high titers of amphotropic retrovirus. 293 GPG cells are stable transfected with packaging plasmids, containing the Gag and Pol genes from MoMLV (Moloney Murine Leukemia Virus) and the VSV-G gene from vesicular stomatitis virus. Gag encodes for the viral matrix-, capsid- and nucleocapsid proteins. Pol encodes for the viral enzymes protease, reverse transcriptase and integrase. The VSV-G gene encodes the envelope glycoprotein, which interacts with host cell receptors and is responsible for the broad range of tropism of the virus. Because the VSV-G coat protein is toxic to 293 GPG cells, its expression is repressed during cell growth via a TET repressor. This is why cells were kept in DMEM containing 1 μg/ml tetracycline, except for periods of virus production.

The Phoenix ampho packaging cell line has also been engineered based on HEK293T cells. It contains the same Gag and Pol genes from MoMLV as 293 GPG cells. In contrast to the 293 GPG cells, this cell line contains an amphotropic envelope gene from MoMLV instead of the VSV-G glycoprotein. This cell line produces viral particles able to infect most dividing cell types. The Phoenix ampho cell line can be cultured in complete medium without any additives.

On day 0, packaging cells were plated. Seeding was performed with 2.5 Mio cells per 10 cm dish in DMEM. 293 GPG cells were plated in DMEM without Tetracyclin. 24h later, the medium was changed and the packaging cells were transfected with retroviral plasmid containing PAX3/FOXO1 (wild type or mutants) (Fig. 12), using the Jet-Prime Protocol.

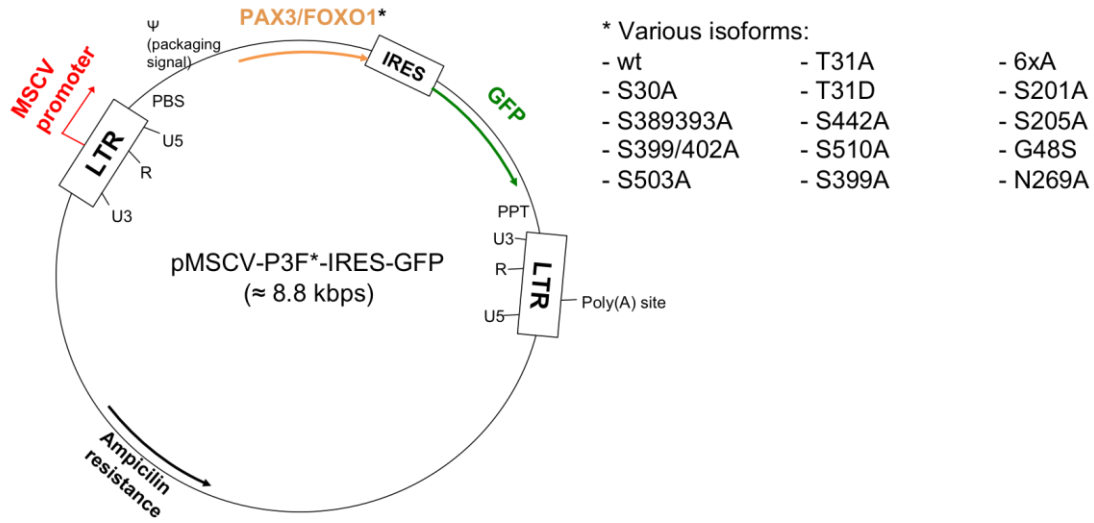

Figure 12: plasmid constructs used for retrovirus production

Another 24h later, the medium was changed again. Then cells were kept in culture to allow the production of viral particles. 72h post transfection, the virus supernatant was collected in a 50 ml Falcon tube and centrifuged for 4min at 1200 rpm to get rid of cellular components. After that, virus supernatant was filtered using a 0.45 nm cellulose acetate membrane filter tip. If virus supernatant was not directly used to infect cells, aliquots of 2-5 ml were frozen and stored at -80°C for later use.

24h before infection, 150'000 RD cells were plated per well of a 6-well plate in DMEM. Same amounts of cells were plated for mMSC, HS5, HEK293T and Rh4 cell lines. Primary hMSCs were plated in a density of 80'000 cells per well. The day of infection, medium was removed from target cells and replaced with virus supernatant. Polybrene was added to a final concentration of 10 μg/ml. Plates were securely closed with parafilm and centrifuged for 1h at 32°C and 800 g. Alternatively, infection was conducted by incubating the cells with virus supernatant overnight either once or twice. Then, virus supernatant was removed from target cells. Washing with 1 ml 1xPBS per well was performed twice before adding 2ml of fresh

medium to each well. Analysis of samples was performed after 48 – 192h post infection. The procedure of retrovirus production and target cell infection is summarized in Fig. 13.

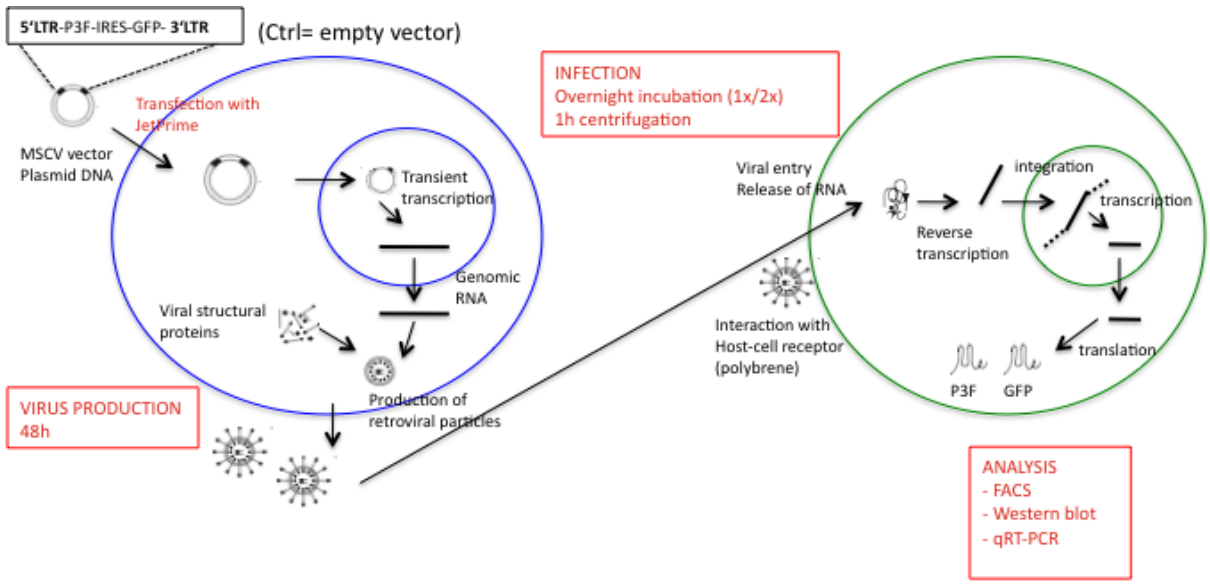

Figure 13: Representation of workflow for the retroviral PAX3/FOXO1 activity read out system
Packaging cell lines are represented in blue and target cells are represented in green

3.2.5 Cycloheximide treatments

Cycloheximide (CHX) is a compound interfering with the translocation step in protein synthesis and therefore inhibits translation. CHX treatment is a probate tool to investigate the stability of proteins.

200'000 cells were seeded the day before transfection in a well of a 6-well plate. 24 hours later, the cells were transfected with 1 μg plasmid DNA using the JetPrime protocol. The cells were incubated overnight (12-17h). Stock solutions of CHX (diluted in DMSO) were diluted in DMEM to reach the desired concentration of 35 μM. As a control, a solution with the same volume of DMSO was prepared. After the medium was removed from the cells, it was replaced with drug solution or DMSO solution. Protein was isolated and analyzed by Western blot at the indicated time points after treatment.

3.3 Quantification of gene expression level

3.3.1 RNA isolation

For RNA extraction, the RNeasy Mini Kit protocol was applied. As an optional step, DNase incubation for 15 minutes was performed to prevent genomic DNA contamination. RNA was eluted in 30 µl RNase-free H_2O and concentrations were determined by measuring OD260nm with the NanoDrop ND-1000 Spectrophotometer.

3.3.2 cDNA synthesis

For reverse transcription of RNA into complementary DNA, a high capacity reverse transcription kit was used. After RNA concentrations were determined, 1 µg RNA of all samples was diluted in water to a volume of 26.4 µl in a PCR tube. To this dilution, 13.6 µl of RT master mix (Table 18) was added.

Table 18: RT master mix for cDNA synthesis

Component	Amount
10xRT Buffer	4 µl
dNTPs	1.6 µl
10x random Primers	4 µl
Reverse Transcriptase	2 µl
RNase Inhibitor	2 µl

The resulting 40 µl reaction mix was put in a T3000 Thermocycler and reverse transcription was performed as follows:

10 min 25°C (annealing), 2h 37°C (reverse transcription), 5 sec 85°C (denaturation)

3.3.3 qRT-PCR

This method is designed to allow quantification of the increase of amplified templates per cycle of a PCR reaction. For this, template specific oligonucleotide probes containing a 5'-reporter fluorophore and a 3'-quencher are used. During synthesis of new amplicons, the 3'-exonuclease activity of the Taq-Polymerase degrades the probe. Because energy transfer from the fluorophore to the quencher can no longer take place, fluorescence can be detected. Measurements of fluorescence take place at the end of every elongation step during the entire PCR reaction. Proportional to the amplified template, also the fluorescence increases with each cycle. The cycle number at which the fluorescence exceeds a certain threshold, called CT value, is recorded.

For each qRT-PCR reaction, a mix containing 5 µl TaqMan Gene expression Master Mix and 0.5 µl gene specific TaqMan assay (Table 19) was prepared.

This mix was transferred to a well of a 384-well plate and 4.5 µl cDNA dilution (0.7 µl cDNA and 3.8 µl H_2O) was added. For each sample, reactions were performed in triplicates. The plates were closed with a clear adhesive cover, briefly centrifuged and put in the 7900HT Fast Real-Time PCR machine.

Analysis of the data was conducted with SDS2.2 software using the ΔΔCT method. Like this, the relative expression levels of the measured genes could be determined. In all experiments the housekeeping gene Glyceraldehyde 3-phosphate dehydrogenase (GAPDH) was used for normalization.

ΔΔCT method:

ΔCT values for all samples were determined by calculating the difference between CT values of the target gene and the CT value of GAPDH.

- ΔCT (sample)= CT (target gene) – CT (GAPDH)

ΔΔCT values were determined by calculating the difference between ΔCT values of the samples and the reference sample.

- ΔΔCT (sample)= ΔCT (sample) - ΔCT (reference sample)

The normalized level of gene expression for each sample was calculated using the formula:

- Gene expression level= $2^{-\Delta\Delta CT}$

Table 19: TaqMan gene expression assays for qRT-PCR

Gene name	TaqMan assay number	Producer
PAX3/FOXO1	Hs03024825_ft	Applied Biosystem, Zug, Switzerland
PAX3	Hs00240950_m1	Applied Biosystem, Zug, Switzerland
FGFR4	Hs01106908_m1	Applied Biosystem, Zug, Switzerland
AP2beta	Hs00231468_m1	Applied Biosystem, Zug, Switzerland
CDH3	Hs00354998_m1	Applied Biosystem, Zug, Switzerland
MYL1	Hs00984899_m1	Applied Biosystem, Zug, Switzerland
PIPOX	Hs04188866_m1	Applied Biosystem, Zug, Switzerland
MYCN	Hs02330075_m1	Applied Biosystem, Zug, Switzerland
MYOD	Hs02330075_g1	Applied Biosystem, Zug, Switzerland
DUSP4	Hs01027785_m1	Applied Biosystem, Zug, Switzerland
TNNC2	Hs00268519_m1	Applied Biosystem, Zug, Switzerland
MET	Hs01565584_m1	Applied Biosystem, Zug, Switzerland
PRKAR2B	Hs00176966_m1	Applied Biosystem, Zug, Switzerland
POU4F1	Hs00366711_m1	Applied Biosystem, Zug, Switzerland
CB1	Hs01038522_s1	Applied Biosystem, Zug, Switzerland
GAPDH	Hs02758991_g1	Applied Biosystem, Zug, Switzerland

3.4 Determination of Protein levels

3.4.1 Protein isolation

After washing with 1ml PBS, cells were lysed with 35-100 µl of cold RIPA buffer per 6-well depending on the confluency of the cells. Then the plates were scraped with a cell scraper and the lysate was collected in a 1.5 ml Eppendorf tube. Incubation was performed for 10 minutes on ice. Afterwards cell lysates were treated with 4 cycles of 40 seconds of sonification in a water bath followed by 1 minute incubation on ice after each cycle. Alternatively, cell lysates were pressed through a 25G needle several times. Finally, cell lysates were centrifuged at 4°C for 10 minutes at 10'000 rpm. The supernatant was collected and protein concentration was determined using the Pierce BCA Protein Assay Kit.

3.4.2 Western Blot

Protein lysates were mixed with 4xRotiLoad (or 4xLDS with 1 M DTT, 4:1) in appropriate amounts. This mixture was incubated at 70°C for 3-5 minutes. After cooling of the samples, equal amounts of protein were loaded on a NuPage 4-12% Bis-Tris Gel. Gel electrophoresis was performed in 1xNuPAGE SDS running buffer first at 80 V and later at 150 V until separation was completed. For blotting onto nitrocellulose membranes, the blotting sandwich was put in a blotting module and run in 1xNuPAGE transfer buffer at 33 V for 2 hours. To prevent heating, cold water with ice was filled around the chamber. Then the membrane was stained in Ponceau solution to check for blotting efficiency and shortly destained in H_2O. To prevent non-specific binding of antibodies, the membrane was blocked in 5% non-fat dry milk in 1xTBST solution (1xTBS and 0.1% Tween) for 30 minutes on a shaker. The membrane was incubated with primary antibody against the protein of interest, which was diluted in 1xTBST containing either 5% BSA (for phospho antibodies) or 5% non-fat dry milk. Incubation of the membrane in primary antibody was conducted overnight at 4°C. The next day, the membrane was washed 3 times for 10 minutes in 1xTBST. This was followed by incubation for 1 hour at room temperature in secondary antibody directed against the species-specific part of the primary antibody. The secondary antibody was diluted in 1xTBST 5% non-fat dry milk. Afterwards, the membrane was again washed 3 times for 10 minutes in 1x TBST. The membranes were incubated for 1 minute in 6 ml ECL chemoluminescence detection reagents mixture (A and B, 1:1). Chemoluminescence signal was detected with the LAS-3000 imaging system.

3.5 Flow cytometry

3.5.1 Estimating infection efficiency

After washing with 1xPBS, cells were detached from culture plates using trypsin. After addition of complete medium, the cells were transferred to a 15 ml falcon tube and centrifuged for 5 minutes at 1'200 rpm. The supernatant was aspirated. 200 µl of 4% Formalin solution were added and incubation was performed on ice for 10 minutes. 1 ml of 1xPBS was added to the cells followed by another round of centrifugation. Again the supernatant was removed. The cell pellet was resuspended in 500 µl 1xPBS. After pressing them through the filter caps of the FACS tubes, they were ready for analysis by FACS.

First, side scatter and forward scatter of untreated cells were measured and a gate wherein dead cells and doublets were excluded was applied. For this cell population, side scatter and GFP signal were measured. Like this, the threshold for GFP positive cells could be determined. A second gate above this threshold, which did not contain any cells, was applied.

Subsequently, samples of cells infected with retrovirus were measured using these settings. The shift in GFP signal to higher intensities allowed determination of the percentage of GFP positive cells within the whole cell population. The data were analyzed using FlowJo Software.

3.5.2 Cell cycle analysis

PI (propidium iodide) is a fluorescent vital dye, which intercalates into double stranded nucleic acids. Because PI binds in proportion to the amount of DNA present in cells, it can be used to determine in which part of the cell cycle cells are.

After detachment from culture plates and centrifugation of the cells as previously mentioned, the pellet was resuspended in 50 µl of 1xPBS. While votexing, 1 ml of 70% ethanol was added dropwise. Then the cells were stored at -20°C for one hour. After centrifugation at 4°C for 5 minutes at 1200 rpm, the supernatant was removed. The cells were washed once with 1xPBS. After another step of centrifugation and removal of supernatant, the pellet was resuspended in 500 µl PI solution. The cell suspension was pressed through the cap of FACS tubes. Cell cycle distribution was measured by FACS and analyzed with FlowJo software.

3.6 In vitro kinase Assay

All the steps mentioned below are described for one 15 cm plate. In order to have enough protein for subsequent mass spectrometrical analysis, everything was conducted simultaneously for 3 plates.

3.6.1 Purification of PAX3/FOXO1 from HEK293T cells

HEK293T cells were transfected with pCMV-NFlag-PAX3/FOXO1 plasmid DNA using the calcium phosphate technique. 40 hours post transfection, medium was removed and cells were washed with 10 ml 1xPBS. Cells were lysed with 2 ml lysis buffer and the lysate was collected. The lysate was pressed through a 25G needle several times. After 10 minutes incubation on ice, the lysate was centrifuged at 4°C for 10 minutes at 10'000 rpm. The supernatant was collected. A mixture of 75 µl Dynabeads, 0.4 ml PBS/0.02% Tween and 8 µl (8 µg) anti-Flag antibody was prepared in a 1.5 ml Eppendorf tube and incubated for 10 minutes at rotation. Afterwards, the tube was put in a Dyna-Mag magnetic concentrator rack and supernatant was removed. After washing with 2 ml PBS/0.02% Tween, the beads were resuspended in 1ml lysis buffer and distributed into low binding tubes. Again, the supernatant was removed. 2 ml supernatant of lysate after centrifugation were added and incubated at 4°C for 1 hour at rotation. After washing once with 2 ml lysis buffer and three times with 2 ml wash buffer, the beads were transferred to a new 1.5 ml Eppendorf tube.

3.6.2 CIP treatment

100 µl of CIP 1x reaction buffer and 4 µl (80 units) CIP enzyme were added to the beads and incubated for 1 hour at 37°C while shaking. 1 µl of CIP enzyme was added again followed by another 30 minutes of incubation. Afterwards, the tube was put in a Dyna-Mag magnetic concentrator rack and supernatant was removed. The beads were washed twice with lysis buffer and twice with wash buffer. Then the supernatant was removed.

3.6.3 In vitro phosphorylation

The dynabeads of 3 plates were combined (yielding approximately 2.5 µg PAX3/FOXO1 protein, estimated in previous experiments by Verena Thalhammer) and 20 µl of the following reaction mix was added.

Table 20: reaction mix for in vitro phosphorylation

Component	Amount
5x kinase buffer	8 µl
ATP 10mM	0.8 µl
PLK1	1.22 µl (500 ng)
H2O	29.98 µl

The reaction mix was then incubated at 30°C for 30 minutes while shaking. 13.5 µl of 4x LDS+DTT was added and incubated for 5 minutes at 70°C to elute the phosphorylated protein. The supernatant was collected. Proteins were separated by gel electrophoresis. Subsequent in gel digestion with Trypsin and Chymotrypsin, mass spectrometry (Velos), and data analysis (mascot software) was performed by Dr. Laura Lopez.

The working procedure of the in vitro kinase assay is summarized in Fig. 14.

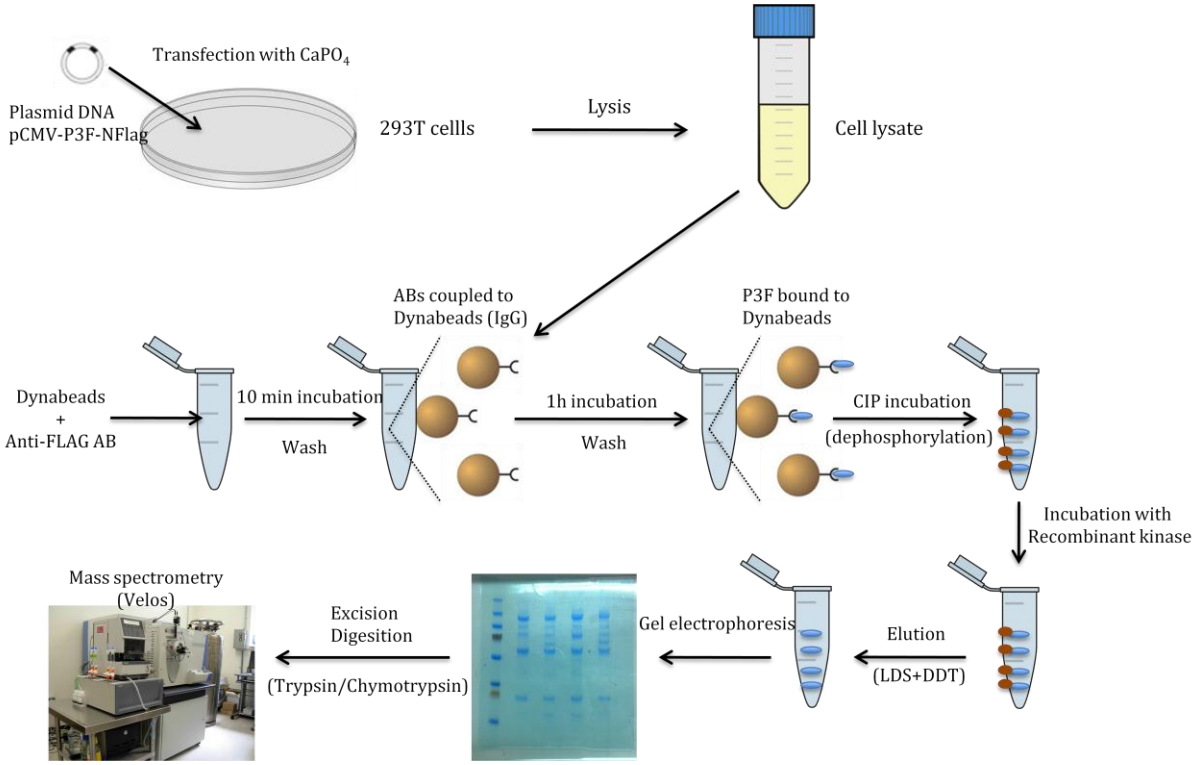

Figure 14: Work flow chart for purification of PAX3/FOXO1-NFlag from HEK293T cells and subsequent in vitro kinase assay

3.6.4 Purification of PAX3/FOXO1 from bacteria

BL21-CodonPlus (DE3)-RIL E.coli are bacteria containing a plasmid encoding for special t-RNAs that carries a chloramphenicol resistance gene, which allows expression of eukaryotic proteins containing rare codons.

PAX3/FOXO1 wt was subcloned from the pMSCV-P3F-IRES-GFP plasmid into pTXB1 expression vector, in which it is C-terminally fused to an intein/chitin-binding domain, using the In-Fusion HD cloning protocol. This allows purification of full-length protein by affinity chromatography (Fig. 15). The vector is inducible by IPTG and carries an ampicillin resistance gene.

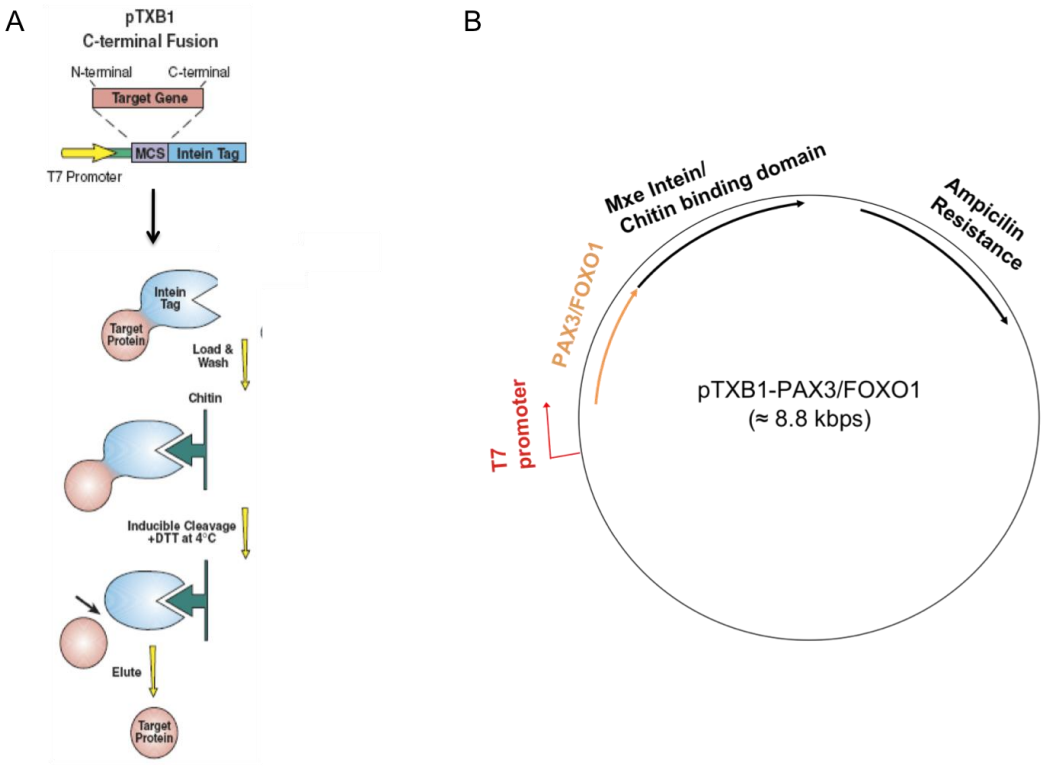

Figure 15: Purification of PAX3/FOXO1 from bacteria
A) Schematic representation of affinity chromatography procedure **B)** Plasmid construct for expression in bacteria and subsequent isolation on a chitin beads column

Bacteria were transformed by electroporation (kind help of Stefano Ferrari) and plated on LB agar plates containing 150 μg/ml ampicillin and 25 μg/ml chloramphenicol. The next day, colonies were picked to inoculate a 10 ml culture of LB medium with 150 μg/ml ampicillin and 25 μg/ml chloramphenicol. This inoculum was incubated for 6 hours at 37°C. With these 10 ml, a 1 L culture was inoculated. Bacterial growth was monitored by measuring OD600nm every 30 minutes. When the culture reached OD600nm=0.3, IPTG was added to a final concentration of 0.2 mM and the incubator was put to 18°C. The culture was let to grow overnight.

The following day, bacteria were pelleted by centrifugation at 4000rpm for 15 minutes at 4°C. After washing with 150 ml of 1xPBS and another round of centrifugation, the pellets were resuspended in 25 ml of pre-chilled (4°C) CH buffer with PMSF (0.1 mM) and complete protease inhibitor and put on ice. The bacterial suspension was sonicated at maximum power for 30 seconds followed by a 1 minute incubation time on ice. This cycle was repeated 4 times. Again PMSF was added. The sonicated bacteria were centrifuged at 18000 rpm for 45 minutes at 4°C. The supernatant was collected and again PMSF was added.

All further steps were performed in a cold room at 4°C. The column, containing 2 ml of chitin-beads suspension, was equilibrated by passing 10 ml of CH buffer by gravity. The 25 ml of collected supernatant were loaded onto the column and let to flow slowly. Then the column was washed with 30 ml CH buffer with PMSF. The

column was closed and 2ml of CH buffer with 30 mM DTT were poured into it. The beads were resuspended and incubated overnight.

The next day, the column was opened again and 2 fractions of 1 ml were recovered. After adding another 10 ml of CH buffer with 30 mM DTT, 10 more fractions of 1 ml were recovered. 10 μl of the first two fractions, of the supernatant after centrifugation, and of the flow through after loading to the column were used for analysis by Westen blot.

4 RESULTS

4.1 Validation of PLK1 knockdown experiments

To examine whether PLK1 is able to regulate the transcriptional activity of PAX3/FOXO1, silencing of PLK1 was performed in different aRMS cell lines. For this purpose, siRNA technique was applied. It was already shown that knockdown of PLK1 with s1341 siRNA led to a decrease of expression of PAX3/FOXO1 target genes in different aRMS cell lines. Previous experiments with 8 nM of s1341 showed efficient knockdown (around 80% reduction of PLK1 mRNA expression) without inducing a cell cycle arrest or degradation of PAX3/FOXO1. Increased siRNA concentrations (25 nM) led to a G2/M arrest and degradation of PAX3/FOXO1 protein. These findings suggested a direct effect of PLK1 phosphorylation on PAX3/FOXO1 transcriptional activity. Here, we wanted to validate this finding using a second siRNA. Different aRMS cells were incubated with scrambled siRNA as a control and with the second PLK1 specific siRNA (s449). I evaluated several conditions in a range of 2-8 nM (Table 1) to compare their knockdown efficiencies. Further I determined the effect of PLK1 silencing on PAX3/FOXO1 target gene expression. This was done by qRT-PCR (Taqman). mRNA expression levels were compared to scrambled siRNA treatment.

4.1.1 PLK1 knockdown in RMS13 cells induces reduction in PAX3/FOXO1 target gene expression

Table 1: Summary of tested PLK1 knockdown conditions with reduction of PLK1 mRNA expression shown in brackets

Rh3	Rh4		RMS13		RMS	
48h	48h	72h	48h	72h	48h	72h
5 nM (70%)	5 nM (77%) 4 nM (63%) 2 nM (53%)	5 nM (63%)	5 nM (66%) 8 nM (78%)	5 nM (63%)	5 nM (71%) 8 nM (n.d.)	5 nM (30%)

n.d.: not determined (high toxicity)

In general, Knockdown efficiencies were the highest in RMS13 cells using 8nM siRNA for 48 hours (around 80% reduction of PLK1 mRNA expression) (Table 1). In other cell lines, high toxicity was observed compared to RMS13 cells (judged by eye under light microscope). Relatively efficient knockdown of PLK1 in the other cell lines with different concentrations (despite 2 nM) of siRNA for 48hours was observed (around 60-70% reduction of PLK1 mRNA expression). Knockdowns were less efficient if cells were incubated for 72 hours (Table 1). Using 8 nM of siRNA for 48 hours in RMS 13 cells, PAX3/FOXO1 target gene expression was downregulated. This finding could also be reproduced using the same conditions. FGFR4 expression

was reduced by approximately 10%. AP2beta expression was downregulated by roughly 26%, CDH3 by 22% (high variability) and PIPOX by 25%. The differentiation marker MYL1 was upregulated by 181% upon PLK1 knockdown (Fig. 1), demonstrating the relief from the block of differentiation normally found in aRMS cells. However, no effect on PAX3/FOXO1 target gene expression was found in other cell lines. Also incubation for 72 hours in these cells did not change this fact. Minor downregulation of few PAX3/FOXO1 target genes in RMS and Rh4 cells using 5nM or 4nM for 48 hours respectively could not be reproduced (data not shown). A possible explanation why I was not able to detect an effect on PAX3/FOXO1 target genes in other cells could be that other PLK isoforms are compensating for PLK1 knockdown. Indeed, experiments of Verena Thalhammer showed that double knockdown of PLK1 and PLK2 or PLK4, could enhance the effect on PAX3/FOXO1 target gene donwregulation (data not shown).

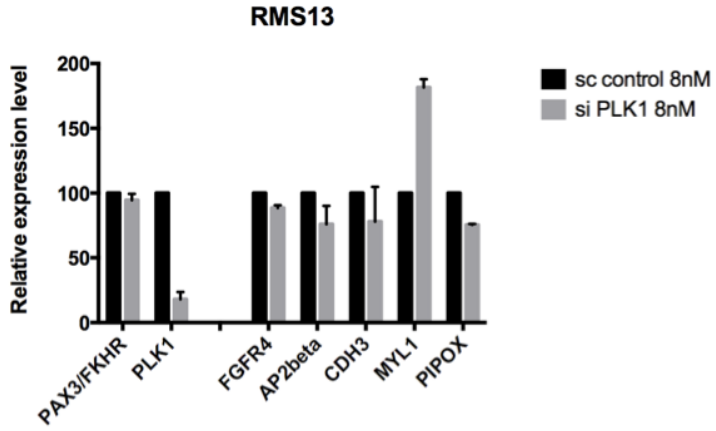

Figure 1: PLK1 knockdown reduces PAX3/FOXO1 target gene expression in RMS13 cells
TaqMan mRNA expression analysis of PAX3/FOXO1, PLK1 and PAX3/FOXO1 target genes after knockdown of PLK1 relative to scrambled siRNA treatment for 48 hours; FGFR4: Fibroblast growth factor receptor 4, AP2beta: activating enhancer binding protein 2 beta, CDH3: P-cadherin, MYL1: myosin light chain 1, PIPOX: pipecolic acid oxidase; biological replicates of two independent experiments. Error bars represent standard deviations

4.1.2 PLK1 knockdown in RMS13 cells induces degradation of PAX3/FOXO1 and G2/M arrest

Because we were able to detect PAX3/FOXO1 target gene downregulation in RMS13 cells only, we used this cell line for further experiments. To investigate if PLK1 knockdown has an effect on protein levels of PAX3/FOXO1 itself, we performed Western blot analysis with protein samples isolated 48 hours after treatment with 8 nM siRNA. To evaluate if PLK1 knockdown induces a cell cycle arrest, PI staining of cells was performed followed by FACS analysis after 8 nM siRNA treatment for 48 hours.

Interestingly, we found a strong degradation of PAX3/FOXO1 protein (Fig. 2A) and cell cycle arrest (Fig. 2B) in RMS13 cells (80% of cells in G2) after PLK1 knockdown

with 8 nM s449 (data provided by Verena Thalhammer). This effect was already observed previously with 25 nM of s1341.

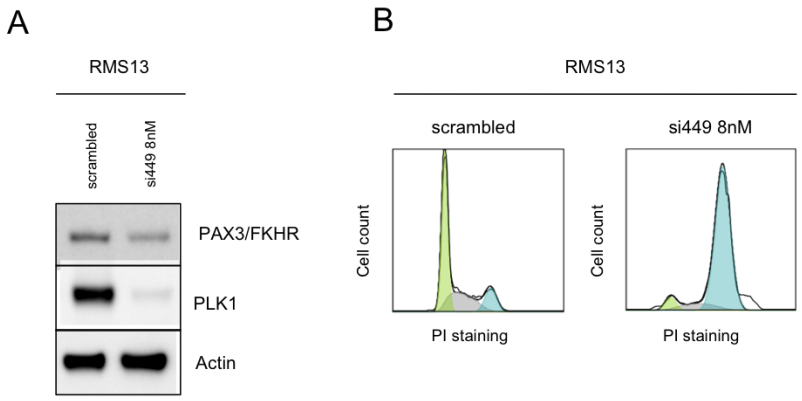

Figure 2: Effects of PLK1 silencing in RMS13 cells
A) Western blot analysis showing PAX3/FOXO1 and PLK1 protein levels after PLK1 knockdown in RMS13 cells with actin as loading control **B)** Cell cycle distribution after PLK1 knockdown in RMS13 cells measured by PI staining followed by FACS

To summarize, we were able to confirm that upon silencing of PLK1 in RMS13 cells, PAX3/FOXO1 target genes are downregulated. In other words, we could reproduce the findings of previous experiments with s1341 using another siRNA. This suggests that PLK1 is indeed able to influence the transcriptional activity of PAX3/FOXO1. Further, we observed that PLK1 knockdown causes a cell cycle arrest and reduces cell viability in aRMS cells. Because of the degradation of PAX3/FOXO1 protein after PLK1 knockdown, we suggest that PLK1 might have a stabilizing effect on PAX3/FOXO1.

4.2 Identification of phosphorylation sites in PAX3/FOXO1 by in vitro kinase assay and mass spectrometry

To investigate if PLK1 is able to directly phosphorylate PAX3/FOXO1 we performed an in vitro kinase assay with subsequent mass spectrometrical analysis. Using this approach we wanted to identify possible PLK1 phosphorylation sites within PAX3/FOXO1.

For this we transfected HEK293T cells with pCMV plasmid vector containing N-terminally Flag tagged PAX3/FOXO1 using the calcium phosphate technique. PAX3/FOXO1 was then purified by affinity chromatography. Afterwards, we dephosphorylated PAX3/FOXO1 with calf intestinal phosphatase (CIP) and incubated PAX3/FOXO1 with recombinant PLK1. Because previous experiments with 2500 or 2000 ng of PLK1 suggested that unspecific phosphorylation might have occurred, we now used only 500 ng of recombinant kinase instead. After gel electrophoresis, PAX3/FOXO1 was digested in gel with Trypsin or Chymotrypsin. The samples were analyzed by mass spectrometry using the Velos Mass Spectrometer. In-gel digestion, mass spectrometry and data analysis (mascot software) was performed by Dr. Laura Lopez.

4.2.1 PLK1 phosphorylates PAX3/FOXO1 at several sites in vitro

We were able to identify four different peptides within PAX3/FOXO1, which are potentially phosphorylated by PLK1 in vitro. Each peptide was only identified once in three different runs using the same conditions (500 ng PLK1). However, three of these peptides were previously found phosphorylated with 2500 or 2000 ng of PLK1 used in the kinase assay. Only runs where peptides were not found phosphorylated in CIP treated samples were considered. Interestingly, one peptide (T497-R508) was often not dephosphorylated by CIP treatment but when it was, it was always found phosphorylated (Table 2). To determine which sites within these peptides are most probably phosphorylated we used two criteria. The firs one were prediction values gathered by software analysis. Secondly, we checked the peptides for PLK1 consensus sequences [78, 79]. A site for witch both of those criteria were fulfilled was S503. Mass spectrometry data for this peptide are shown in Figure 3. Coverage of the protein was around 80% when combining the Trypsin and Chymotrypsin digested samples (Fig. 4A). In total we considered six potential PLK1 phosphorylation sites. The sites with the corresponding position in the amino acid sequence of PAX3/FOXO1 were S30, S389, S393, S399, S402 and S503 (Fig. 4A). S393, S399, S402 and S503 lie within the FOXO1 part of the fusion protein (Fig. 4B).

Table 2: Phospho-peptides within PAX3/FOXO1 identified after in vitro phosphorylation by PLK1

	assay 1 (2500 ng)		assay 2 (2000 ng)		assay 3 (500 ng)		assay 4 (500 ng)		assay 5 (500 ng)	
Peptide sequence	pep_score	pep_expect	pep_score	pep_expect	pep_score	pep_expect	pep_score	pep_expect	pep_score	pep_expect
SGFPLEVSTPLGQGR	in CIP sample		48	0.00078	not found		not found		17.85	0.021
HGFSSYTDSFVPPSGPSNPMNPTIGNGLSPQNSIR	not found		not found		not found		27.24	0.0028	not found	
HNLSLHSK	54.64	0.00011	49.81	0.00033	34.53	0.011	not found		not found	
TSSNASTISGR	in CIP sample		67.34	7.10E-06	in CIP sample		in CIP sample		27.19	0.0028

pep-score: value for goodness of protein sequence match
pep_expect: probability that mass change compared to reference is a result of coincidence

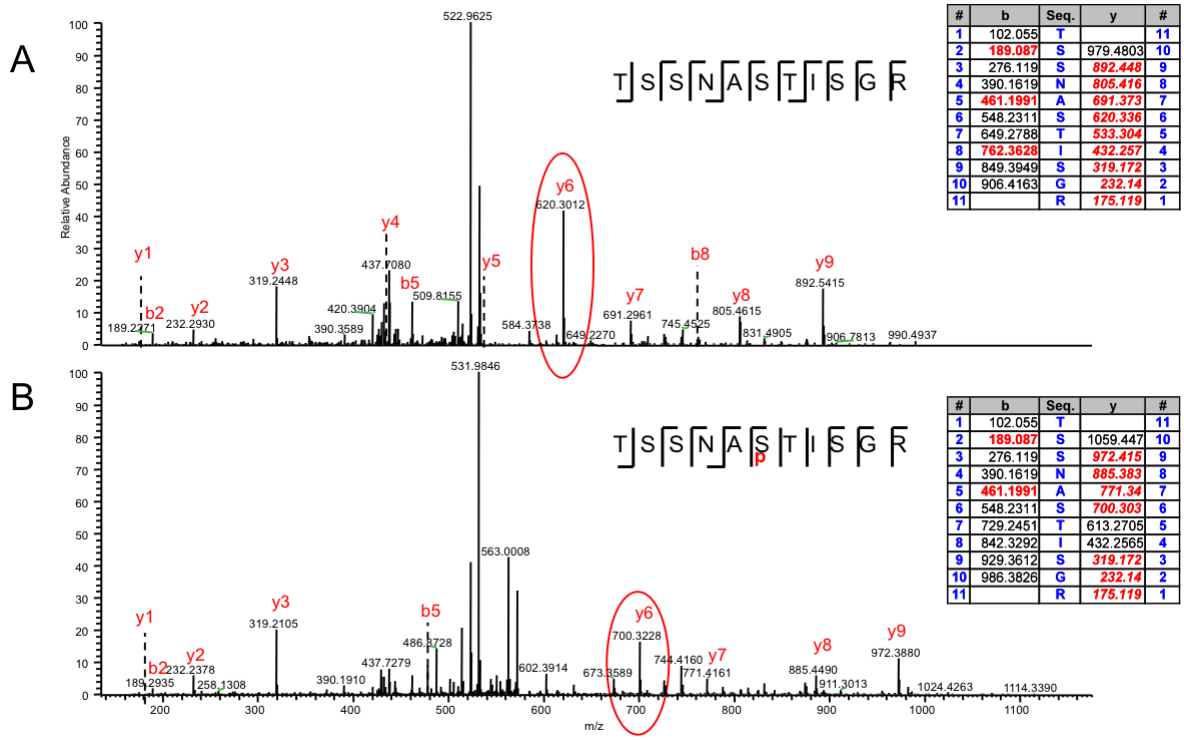

Figure 3: Representative MS spectra of the peptide containing S503
Flag-Pax3FOXO1 was overexpressed in HEK293T cells, immunoprecipitated using anti Flag antibody, dephosphorylated in vitro by CIP treatment and digested with trypsin for MS analysis. **A)** Dephosphorylated peptide showing the ion at 620 m/z representative of unmodified S503. **B)** Peptide after PLK1 in vitro kinase assay showing the shift of the ion to 700 m/z indicating phosphorylation of S503, however, phosphorylation of T504 instead, cannot be discarded by the MS result.

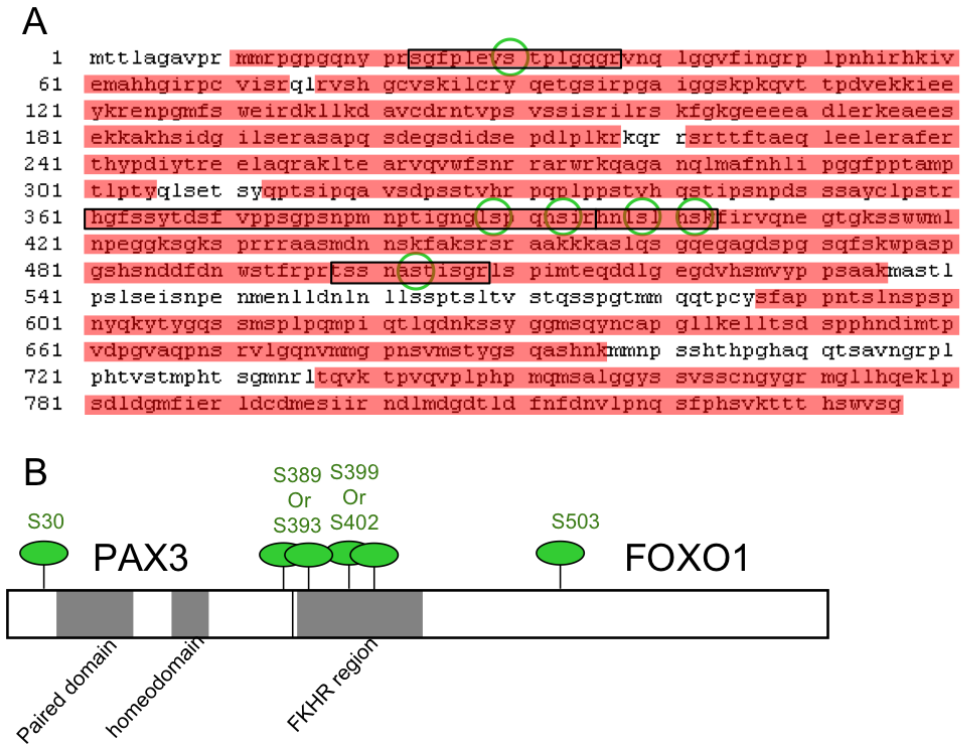

Figure 4: Identification of potential PLK1 phosphorylation sites within PAX3/FOXO1
A) Aminoacid sequence of PAX3/FOXO1 with identified phosho-peptides (black bars) and potential phosphorylation sites (green circles) by mass spectrometry after in vitro phosphorylation by PLK1. Covered sequences are shown in red **B)** Schematic representation of PAX3/FOXO1 with potential PLK1 phosphosites depicted in green

Because there is also a phospho-antibody available against pS322 in FOXO1 (corresponding to pS503 in PAX3/FOXO1), we also tested by Western blot if this site is phosphorylated after in vitro phosphorylation by PLK1. S322 is described in the literature as a site for CK1 phosphorylation, which mediates nuclear export of FOXO1 [60]. For this we analyzed samples of PAX3/FOXO1 after the in vitro phosphorylation with PLK1 or CK1 and a sample of PAX3/FOXO1 after CIP treatment as a control and performed Western blot analysis. This experiment demonstrated that PLK1 as well as CK1 is able to phosphorylate PAX3/FOXO1 in vitro (Fig. 5). This phosphorylation was not detected in the CIP treated sample. This result confirmed our findings from the mass spectrometrical analysis, demonstrating that PLK1 can phosphorylate PAX3/FOXO1 at S503.

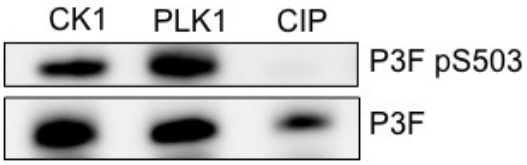

Figure 5: PLK1 phosphorylates PAX3/FOXO1 at S503 in vitro
Western blot of PAX3/FOXO1 after in vitro phosphorylation by CK1 or PLK1 and after dephosphorylation by CIP as a control; P3F pS503: Anti-FOXO1 (p322), P3F: Anti-FOXO1

4.2.2 Purification of PAX3/FOXO1 from bacteria

Because dephosphorylation of purified protein was not 100% successful, we decided to express PAX3/FOXO1 in bacteria, since they lack most of the eukaryotic posttranslational machinery and therefore PAX3/FOXO1 will not be phosphorylated. For this, we transformed BL21-CodonPlus (DE3)-RIL E.coli with PAX3/FOXO1, fused to an intein/chitin-binding domain (for plasmid construct see material and methods) and tried to recover the protein by affinity chromatography. To detect if PAX3/FOXO1 protein was expressed and also properly purified, we performed Western blot analysis. We loaded 10μl of the first two recovered fractions after elution from the chitin beads column. Additionally, 10μl of a control sample after lyisis of the bacteria and 10μl of a control sample of the flow through after loading the column were loaded.

As it turned out, no protein was eluted from the column (Fig. 6). However, the bacterial lysate contained high amount of protein, demonstrating that induction of expression by IPTG worked. The problem was that the flow through after loading of the column also showed high amount of protein, indicating that the binding to the chitin beads was compromised. The whole intein/chitin-binding domain has an approximate size of 30kDa. However, no shift correlating with this size was observed. In general, PAX3/FOXO1 was running at the level of the wild type protein (≈100 kDa) on this blot (Fig. 6).

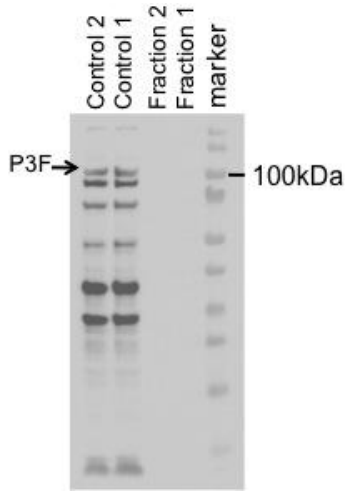

Figure 6: Unsuccessful purification of PAX3/FOXO1 from BL21-CodonPlus (DE3)-RIL E.coli
Western blot with samples of the two first fractions after elution from the chitin beads column (Fractions 1 and 2) and the two control samples; Control1: bacterial lysate after centrifugation, Control 2: flow through after loading of the column

Detailed sequence analysis revealed that an insertion of two base pairs at the beginning of the intein tag resulted in frame shift. As a consequence of this, a stop-codon was generated shortly after the beginning of the tag, which explains why PAX3/FOXO1 did not bind to the chitin column and also why we were not able to see a shift in size compared to wild type PAX3/FOXO1 protein on the blot.

4.3 Retroviral transduction of RD cells is a suitable tool for testing PAX3/FOXO1 activity

I wanted to investigate if any of the identified phosphosites of PAX3/FOXO1 indeed have an influence on the transcriptional activity of PAX3/FOXO1. Since I aimed to test a bigger subset of PAX3/FOXO1 target genes, a novel read-out system was needed. Because transient transfection of target cells (Rh4, Rh4 with AP2beta luciferase reporter and HEK293T) with PAX3/FOXO1 did not have any effect on target gene expression levels in previous experiments, we decided to use a retroviral system instead. I transduced different target cells including human and mouse mesenchymal stem cells (MSCs), primary human MSCs and RD, an embryonal rhabdomyosarcoma cell line not expressing PAX3/FOXO1. HS5 is a human cell line derived from bone marrow tissue and is routinely used for co-culture with hematopoietic progenitor cells. This cell line was used as a first model to infect human mesenchymal stem cells. The decision to use mesenchymal stem cells was based on the fact that they might be the cells of origin for RMS and therefore are thought to provide an ideal cellular background in this context. Previous publications showed that retroviral transduction of mMSC and RD cells with PAX3/FOXO1 is possible and transduction of PAX3/FOXO1 induces gradual target gene expression in those cell lines [80, 81].

4.3.1 RD cells can be efficiently transduced with PAX3/FOXO1

First of all I optimized transduction efficiencies since this is a prerequisite for inducing PAX3/FOXO1 target gene expression, which is important for a system in which PAX3/FOXO1 activity will be tested. I was provided with the pMSCV-PAX3/FOXO1-IRES-GFP retroviral plasmid by Elisa Zimmermann. This vector allows production of retroviral particles containing PAX3/FOXO1 when transfected in an appropriate packaging cell line. An advantage of this plasmid is that it encodes for GFP and therefore allows monitoring how many cells are infected by FACS. I used two different packaging cell lines, which have different envelope proteins and therefore different tropisms. Also I tried different infection protocols. Cells were either infected by just incubating target cells with virus supernatant overnight (once or twice) or by one hour centrifugation of target cells with virus supernatant (Table 3). As a control I infected target cells with virus produced with empty retroviral vector (GFP). Infection efficiencies were measured 96 hours after infection of target cells by FACS. The data were then analyzed with FlowJo software (example see Fig. 7).

Table 3: Overview of tested infection conditions showing percentages of GFP positive cells 96 hours post transduction

	Overnight incubation		1h centrifugation
	1x	2x	1x
Phoenix ampho	**mMSC:** GFP = 14.6% P3F wt= 11.3% (Clone1)	**mMSC:** GFP = 13% P3F wt= 9.7% (Clone1)	**mMSC:** GFP = 44.7% P3F wt= 40.3%
	mMSC: GFP = 14.6% P3F wt= 12.6% (Clone 2)	**mMSC:** GFP = 13% P3F wt= 11.4% (Clone 2)	**HS5:** GFP = 8.49% P3F wt= 5.8%
293 GPG	**mMSC:** GFP = 25.7% P3F wt= 9.13%		**mMSC:** GFP = 87% P3F wt= 72.3%
			HS5: GFP = 69.4% P3F wt=47.4%
			RD: GFP = 92.4% P3F wt= 71.3%
			Primary hMSC: GFP = 23.9% P3F wt= 7.4%
			Rh4: GFP = 66.5% P3F wt = 36.6%
			293 T (n.d.)

GFP: transduction with empty vector
P3F wt: transduction with PAX3/FOXO1 wild type
n.d. : not determined

Evaluation of percentages of GFP positive cells transduced with empty vector led to the following conclusions. In general, transduction was more efficient when virus was produced with 293 GPG cells (Table 3). Additionally, infection was better when I infected target cells by one hour centrifugation compared to overnight incubation. Also two subsequent overnight incubations with virus supernatant did not improve infection efficiencies (Table 3). Interestingly, virus produced with phoenix ampho packaging cells was more infectious on mouse cell lines than on human cell lines. One hour centrifugation with virus produced in phoenix ampho cells led to an infection rate in mMSC cells of 44.7%, whereas only 8.5% of HS5 cells were infected (Table 3). On the other hand, virus produced with 293 GPG packaging cells was highly infectious for mMSCs (87% GFP positive) and HS5 (69.4% GFP positive). Additionally, virus produced in 293 GPG cells was much more infectious in general (Table 3). This is why I decided to infect RD, primary hMSC, Rh4 and HEK293T cells by one hour centrifugation with virus produced in 293 GPG packaging cells. Primary hMSCs were much more difficult to infect than all other cell lines (Table 3). I was able to reach the highest infection rates in RD cells, where over 90% of cells were GFP positive (Table 3).

These data show that virus produced in different packaging cell lines have different tropisms due to their envelope proteins. For my purpose, I could reach higher infection efficiencies when virus was produced with 293 GPG cells and infection was

performed by one hour centrifugation. Therefore, all further infections were performed with virus produced in 293 GPG cells by centrifugation for one hour.

I could observe that the GFP positive cells transduced with empty vector showed higher fluorescence intensities than GFP positive cells infected with PAX3/FOXO1 expressing virus (Fig. 7A/B). The reason for this is that the translation of the second gene in the cassette is significantly lower than that of the first one [82]. Since PAX3/FOXO1 is the first gene in the vector before the IRES element, downstream GFP expression will be lower.

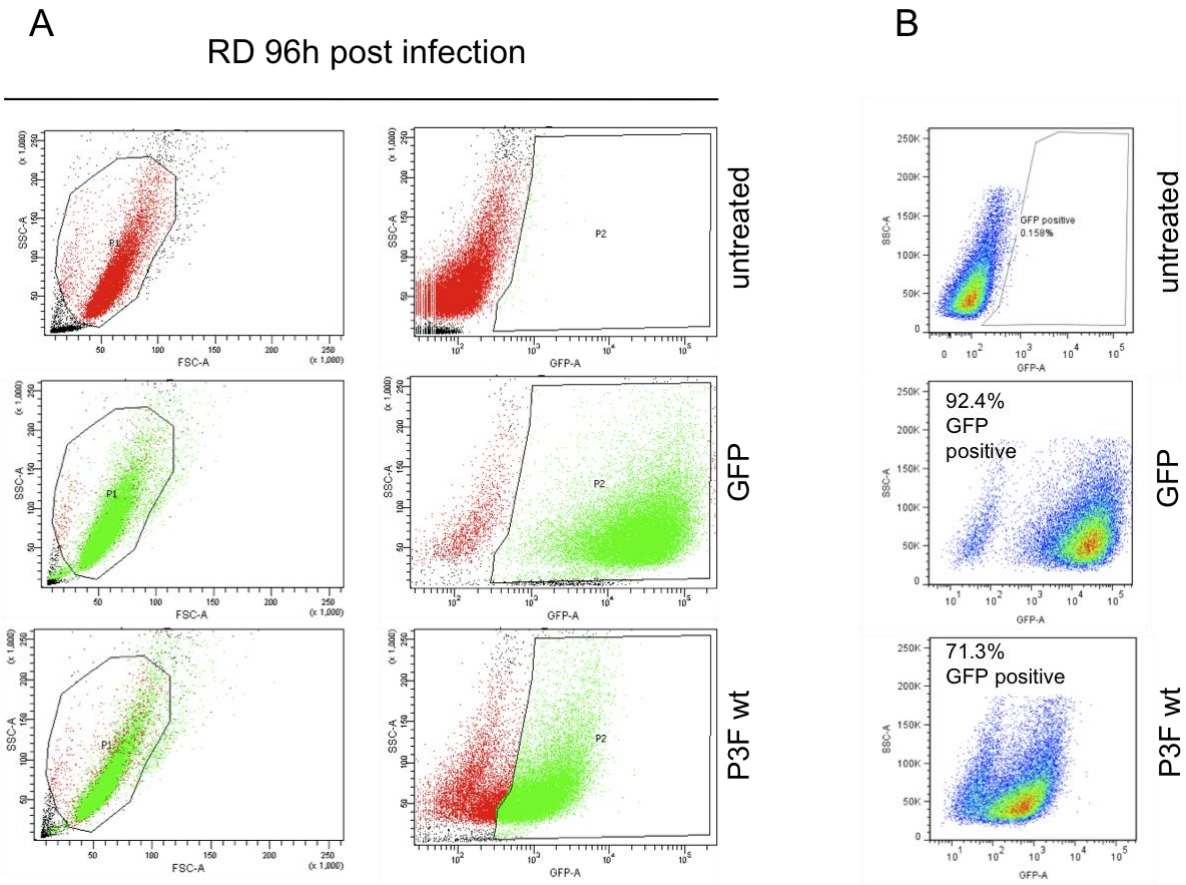

Figure 7: Infection of RD cells with viruses produced in 293 GPG packaging cells by one hour centrifugation yields high transduction efficiencies.
FACS analysis performed 96h post infection; **A)** FACS output data: untreated cells were used for gating (top row), GFP: empty vector control retrovirus infected cells (middle row), P3F wt: PAX3/FOXO1 wild type retrovirus infected cells, black: total of counted cells, red: P1= viable single cells, green: P2= GFP positive cells **B)** Same dataset analyzed with FlowJo software: after refinement of gating, only P1 subpopulations were analyzed

4.3.2 Transduction with PAX3/FOXO1 induces target gene expression in RD cells as well as in other cell lines

To identify target genes of PAX3/FOXO1, which are upregulated upon transduction with P3F wt, I performed qRT-PCR analysis 96 hours post transduction. Expression of target genes were compared to empty vector transduced cells (GFP). As target genes, I investigated all genes previously identified from knockdown studies, as well

as some additional target genes reported to be upregulated in RD cells upon transduction with PAX3/FOXO1 [80].

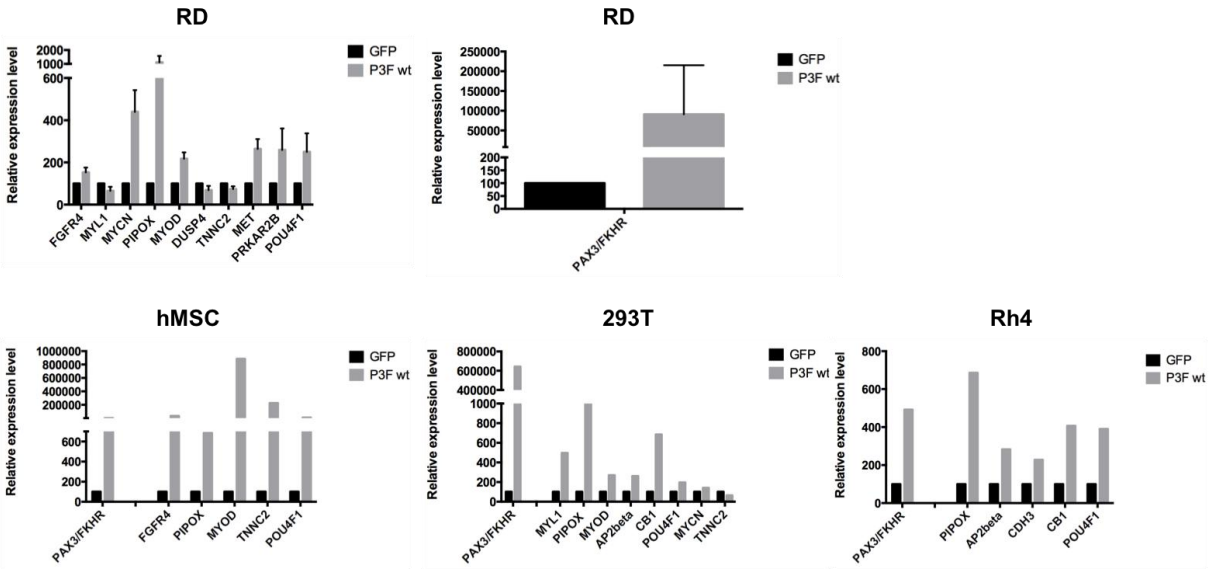

Figure 8: Transduction with PAX3/FOXO1 induces target gene expression in different cell lines
TaqMan mRNA expression analysis of PAX3/FOXO1 and different target genes in various cell lines measured 96h after transduction with PAX3/FOXO1 retrovirus. Relative mRNA expression levels compared to empty vector retrovirus infected cells; FGFR4: fibroblast growth factor receptor 4, MYL1: myosin light chain 1, MYCN: N-MYC proto oncogene protein, PIPOX: pipecolic acid oxidase, MYOD: myoblast determination protein 1, DUSP4: dual specific phosphatase 4, TNNC2: troponin C type 2, MET: hepatocyte growth factor receptor, PRKAR2B: cAMP-dependent protein kinase type II-beta, POU4F1: POU class 4 homeobox 1, AP2beta: activating enhancer binding protein 2 beta, CB1: cannabinoid receptor 1, CDH3: cadherin 3. Error bars represent standard deviations of three independent biological replicates

Two types of target cells, which showed PAX3/FOXO1 target gene induction, were RD and primary hMSCs. RD cells showed minor upregulation of FGFR4 expression (153%), intermediate upregulation of MYOD (217%), MET (264%), PRKAR2B (259%) and POU4F (250%) expression. Minor downregulation was observed for MYL1 (65%), DUSP4 (69%) and TNNC2 (74%) expression (Fig. 8). This was expected since MYL1 and TNNC2 are differentiation markers and PAX3/FOXO1 is known to inhibit differentiation. DUSP4 was already described to be downregulated upon transduction of RD cells with PAX3/FOXO1 [80]. Strong upregulation of MYCN (440%) and PIPOX (1115%) expression was detected (Fig. 8). All target genes were already expressed in the empty vector retrovirus infected control samples (GFP). PAX3/FOXO1 expression in GFP samples were at assay background levels (detected in all experiments: ct≈36). Expression of the fusion protein was increased 900 fold compared to control samples (Fig. 8). The finding of target gene induction in hMSCs was rather surprising because only 7.4% of cells were infected. Consequently, expression of the fusion protein was less strong than in RD cells (only 20 fold increase compared to control). Nevertheless, strong upregulation (over 600% compared to control) of FGFR4, PIPOX, MYOD, TNNC2 and POU4F expression was detected (Fig. 8). All of these target genes except FGFR4 were not expressed in the empty vector transduced control samples (GFP). These two cell lines were therefore

considered to serve as possible systems for testing the activity of PAX3/FOXO1 phosphomutants. Because primary hMSCs did grow very slowly and were difficult to infect, I focused on RD for all subsequent experiments. Additionally, I found target gene induction in HEK293T and Rh4 cell lines (Fig. 8). Although in these cell lines the most well characterized PAX3/FOXO1 target genes were upregulated upon infection with the fusion protein, they were not suitable for the testing of phosphomutants, because of high endogenous PAX3/FOXO1 expression in Rh4 and the lack of potentially important cellular background for PAX3/FOXO1 transcriptional activity in HEK293T.

Taken together, I was able to induce PAX3/FOXO1 target gene expression by transduction with PAX3/FOXO1 wild type in RD cells in a reproducible manner. The percentage of upregulation of target genes in this cell line was suggested to provide a big enough window for the testing of phosphomutants. In addition, RD cells also express high amounts of PLK1, which is important as we are interested in PLK1 dependent phosphorylation of PAX3/FOXO1 and its effect on transcriptional activity.

4.3.3 Differences in activity between PAX3/FOXO1 wild type and PAX3/FOXO1 phosphomutants are time point dependent

To test whether I am able to detect differences in transcriptional activities between wild type PAX3/FOXO1 and the phosphomutant isoforms, I established a positive control, which is known to have less transcriptional activiy compared to PAX3/FOXO1 wild type. This phosphomutant control is the previously described mutant with six serines transformed into alanine (S187A, S193A, S197A, S201A, S205A, S209A), which lie between the homeodomain and the paired domain of PAX3 and is reported to have decreased DNA binding ability (P3F 6xA) [46]. To be able to produce virus with this mutant, I had to subclone it from the pcDNA3 vector into my pMSCV-IRES-GFP retroviral vector.

To investigate if the differences in target gene expression between wild type PAX3/FOXO1 and the phosphomutant isoforms are time dependent and which time point should be used for testing phosphomutants, I performed a time course experiment. For this I transduced RD cells with PAX3/FOXO1 wild type, PAX3/FOXO1 6xA and empty vector virus (GFP) as a control. Analysis of gene expression was performed by qRT-PCR after 48, 96, 144 and 192 hours. I checked all upreglated target genes that I was able to identify upon PAX3/FOXO1 wild type transduction (FGFR4, MYCN, PIPOX, MYOD, PRKAR2B, MET and POU4F1) and only MYL1 as a downregulated target gene.

It is important to mention that the mRNA expression levels of PAX3/FOXO1 itself were not exactly the same for P3F wt and P3F 6xA at 96 (30% less P3F 6xA) and 144 (19% less P3F 6xA) hours post transduction (Fig. 9A). Apart from MET and

MYL1, all target genes showed lower expression upon transduction with P3F 6xA (at least after 96 hours). The differences of FGFR4 expression were minor (Fig. 9B). For MYCN, PIPOX, MYOD and PRKAR2B the expression levels peaked after 96 hours post infection. At this time point, also the differences between induced target gene expression of P3F wt and P3F 6xA were most pronounced. POU4F1 expression instead was highest after 48 hours and progressively decreased afterwards but still with less expression after transduction with P3F 6xA (Fig. 9B). The differences of target gene expressions did exceed the differences between P3F wt and P3F 6xA expression (strongest in MYCN and PIPOX). Additionally, differences in target gene expression could also be detected for time points with equal PAX3/FOXO1 expression (Fig. 9A/B).

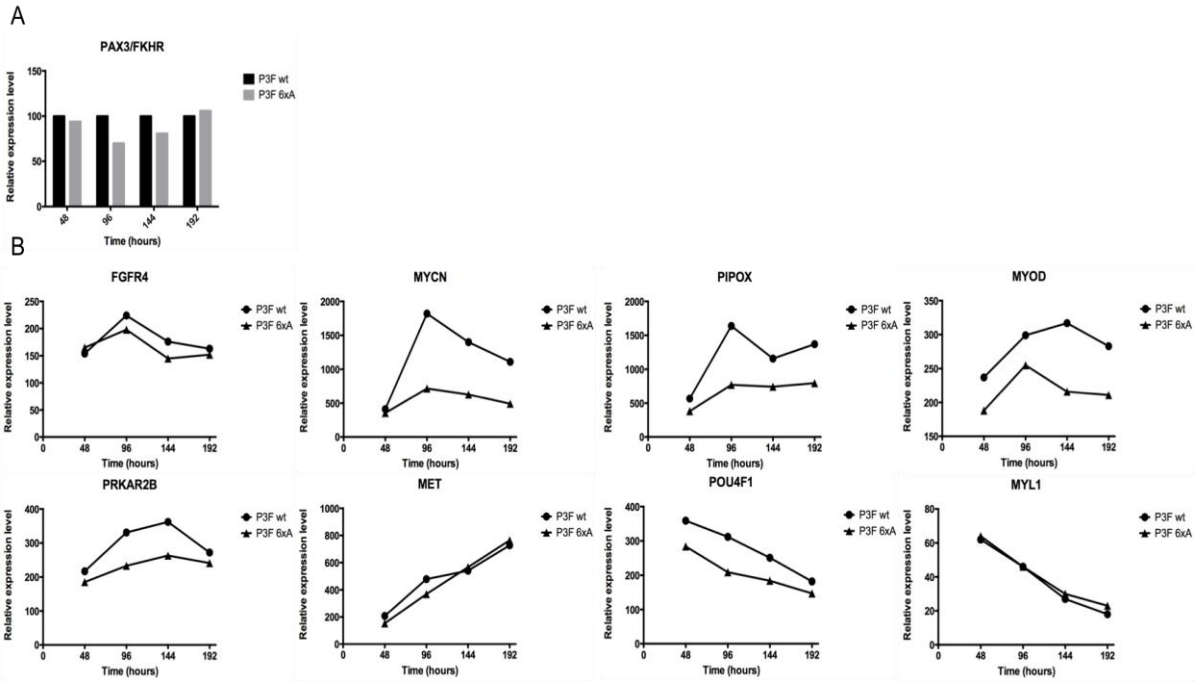

Figure 9: Timecourse experiment of RD cells transduced with PAX3/FOXO1 wild type and PAX3/FOXO1 6xA respectively
A) TaqMan mRNA expression analysis of PAX3/FOXO1 6xA relative to PAX3/FOXO1 wild type in transduced cells **B)** TaqMan mRNA expression levels of PAX3/FOXO1 wild type and PAX3/FOXO1 6xA induced target genes relative to empty vector control; FGFR4: fibroblast growth factor receptor 4, MYL1: myosin light chain 1, MYCN: N-MYC proto oncogene protein, PIPOX: pipecolic acid oxidase, MYOD: myoblast determination protein 1, DUSP4: dual specific phosphatase 4, TNNC2: troponin C type 2, MET: hepatocyte growth factor receptor, PRKAR2B: cAMP-dependent protein kinase type II-beta, POU4F1: POU class 4 homeobox 1

This time course experiment showed that differences between the activities of P3F wt and P3F 6xA after transduction are time dependent. The biggest difference in transcriptional activity was observed between 96 and 144 hours post transduction. On this basis, I decided to use 120 hours as the time point for the testing of all phosphomutants with MYCN, PIPOX, MYOD, PRKAR2B and POU4F1 as read-out target genes. FGFR4, MET and MYL 1 were neglected in subsequent experiments.

4.3.4 Positive controls show less activity than PAX3/FOXO1 wild type upon transduction of RD cells 120 hours after infection

To confirm that differences between PAX3/FOXO1 wild type and positive controls can be detected in the same setting in which I wanted to test my phosphomutants, I infected RD cells with P3F wt, P3F 6xA, P3F G48S, P3F N269A and empty vector virus (GFP) as a control. The latter two mutants are DNA binding deficient mutants with muatated sites within the homeodomain (G48S) and the paired domain (N269A) of PAX3 [83]. Also these mutants were generated by subcloning from the pcDNA3 vector into pMSCV-IRES-GFP retroviral vector.

I analyzed target gene expression 120 hours after transduction by qRT-PCR and performed Western blot to quantify protein levels. Infection efficiencies were measured at the same time point in parallel by FACS.

On mRNA level, the two DNA binding mutants were much higher expressed than P3F wt. P3F 6xA was approximately 10% less expressed than P3F wt (Fig. 10A). I found that PIPOX and MYOD expression was not increased by either infection with P3F G48S or P3F N269A virus compared to empty vector virus infected cells (Fig. 10A). This suggests that binding of PAX3/FOXO1 to enhancer or promoter regions of these genes occurs through both the homeodomain and the paired domain of PAX3. On the other hand, expression levels of NMYC did not increase upon infection with P3F G48S virus compared to infection with empty vector virus, whereas P3F N269A infected cells showed increased expression of NMYC compared to empty vector infected cells (Fig. 10A). This suggests that binding of PAX3/FOXO1 to transcriptional regulatory elements of NMYC mainly involves the homeodomain. The same was true for PRKAR2B. The opposite effect was observed for POU4F1 expression (Fig.10A), since binding of PAX3/FOXO1 to regulatory DNA sequences seems to be mediated mostly through the paired domain of PAX3. Most importantly, for every target gene at least one DNA binding mutant did not increase expression compared to empty vector control. An outlier in this context is PRKAR2B, expression of which was induced by both P3F G48S and P3F N269A. The latter even induced stronger expression than P3F wt (Fig. 10A). This fact leaves room for arguing that PRKAR2B might not be a direct target of PAX3/FOXO1. Finally, cells transduced with P3F 6xA virus displayed a reduced target gene expression profile compared to P3F wt infected cells. This reduction of target gene expression ranged from 20-40% between the target genes (Fig. 10A). I saw that infection efficiencies were very similar for P3F wt and P3F G48S, whereas P3F N269A virus infected roughly 10% more cells. P3F 6xA virus did infect approximately 10% less cells than did P3F wt virus (Fig. 10B). Interestingly, P3F 6xA was also expressed 10% less on mRNA level compared to P3F wt. Protein levels of P3F G48S and P3F N269A were much higher (2 fold more for P3F G48S and over 3 fold more for P3F N269A) than that of P3F wt

(Fig. 10C). This is probably because cells tend to tolerate higher amounts of inactive protein. Protein levels of P3F 6xA were slightly lower than P3F wt protein levels (around 25% less) (Fig. 10C). Because on mRNA level expression of both was approximately the same, an additional effect on protein stability besides the already described effect on DNA binding was taken into consideration. Preliminary data also suggest that this mutant might have reduced stability (Fig. 16A). However I cannot exclude that the effect on protein level is due to unequal infection rates.

A

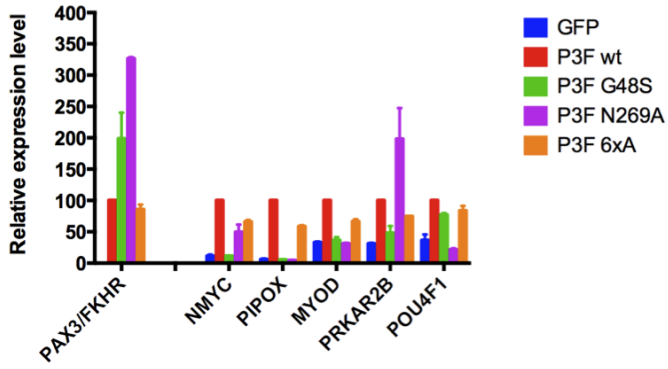

B

		GFP positive
Virus	P3F wt	63%
	P3F 6xA	52%
	P3F G48S	59.2%
	P3F N269A	73.9%

C

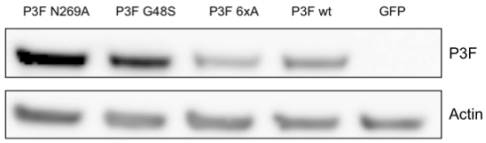

Figure 10: Transduction of RD cells with positive control PAX3/FOXO1 isoforms results in decreased target gene expression compared to PAX3/FOXO1 wild type
A) TaqMan mRNA expression analysis of PAX3/FOXO1 and PAX3/FOXO1 target genes in RD cells 120h after transduction with either PAX3/FOXO1 wild type or PAX3/FOXO1 6xA, expression levels relative to PAX3FOXO1 wild type. Biological replicates of 2 experiments conducted with same virus supernatants. Error bars represent standard deviations **B)** FACS analysis was used to assess percentages of GFP positive cells for each transduction procedure 120h after infection **C)** Western blot analysis showing PAX3/FOXO1 protein levels 120h after transduction

Alltogether, these findings suggest that with this retroviral approach, I am technically able to see differences in PAX3/FOXO1 target gene expression between wild type PAX3/FOXO1 and PAX3/FOXO1 phosphomutants with an effect on transcriptional activity.

4.4 Testing the activity of PAX3/FOXO1 phosphomutants by transduction of RD cells

Phosphomutants of the sites identified by mass spectrometry after in vitro phosphorylation with PLK1 were generated by site directed mutagenesis (Table 4). Additionally to these mutants, I generated phosphomutants of other sites. One of these sites was T31, which was found to be phosphorylated in vitro by CDK1 and is

located within a polobox-binding motif potentially priming for PLK1 binding. The T31A and T31D phosphomutants were generated by site directed mutagenesis (Table 4). Two single mutants with sites of the P3F 6xA mutant were also tested (S201A and S205A). These mutants were subcloned from the pcDNA3 vector into pMSCV-IRES-GFP retroviral vector (Table 4). Also S399 was tested as a single mutant. Another site, which was predicted to be phosphorylated by PLK1 was S442. Also these mutants were generated by site directed mutagenesis (Table 4).

Table 4: Overview of generated PAX3/FOXO1 mutants

PLK1 sites (MS)	PLK1 predicted	Potential PLK1 binding site	Known phospho sites	DNA binding mutants
S30A	S442A	T31A	S201A	G48S *
S389/393A	S510A **	T31D	S205A	N269A *
S399/402A			6xA *	
S503A				
S399A				

* : positive controls for measuring transcriptional activity (see sections 4.3.3 and 4.3.4)
** : only used for testing stability (see section 4.6.1)

In general, alanine mutants can no longer be phosphorylated. Should phosphorylation of one of those sites have an influence on the transcriptional activity of PAX3/FOXO1, reduced activity of the alanine mutants is expected. In other words, PAX3/FOXO1 alanine phosphomutants should not induce target genes as strong as PAX3/FOXO1 wild type. In contrast, aspartic acid phosphomutants mimic phosphorylation at this site and should rescue the decrease in activity of the alanine mutants.

To investigate if any of these mutations affect transcriptional activity of the fusion protein, I transduced RD cells with the phosphomutant isoforms of P3F, P3F wt and empty vector retrovirus (GFP) as controls. 120 hours after infection I measured target gene expression by qRT-PCR. Infection efficiency was also measured 120 hours post transduction by FACS as well as Western blot analysis to quantify protein levels. Protein levels were quantified by densitometry using ImageJ software.

4.4.1 Phosphomutants of PLK1 sites do not display reduced activity but S503A might be less stable

On mRNA level, expression of PAX3/FOXO1 was higher for all phosphomutants compared to P3F wt (Fig. 11A). For P3F S399/402A, expression could not be detected with breakpoint specific PAX3/FOXO1 gene expression assay and had to be measured using a PAX3 gene expression assay (Fig. 11A). Probably, binding of the TaqMan probe or of the primers to the target sequence was affected by the mutations. Target gene expression was not reduced by any of the phosphomutants tested compared to wild type PAX3/FOXO1 in this setting. Interestingly, quite the contrary seemed to be the case. Target genes were a little higher expressed in

phosphomutant P3F transduced cells than in P3F transduced cells (Fig. 11A). This might be caused by the fact that higher amounts of infectious viral particles were used, resulting in higher infection efficiencies, since I did not titrate the viral stocks. Indeed, infection efficiencies were not the same for the different viruses. Compared to P3F wt, all phosphomutant viruses were more infectious. The only exception was P3F S30A virus, which infected almost same amounts of cells as did P3F wt virus. For the other phosphomutants, infection efficiencies were 15-20% higher compared to P3F wt virus (Fig. 11B). Protein levels of P3F S389/399A and P3F S399/402A were much higher than that of P3F wt (Fig. 11C), as could be expected from the higher infection rates. P3F S30A protein amounts were comparable to those of P3F wt (Fig. 11C), probably also because infection efficiencies were similar. Surprisingly, protein levels of P3F S503A were also in the range of P3F wt although infection was much more efficient with P3F S503A and also mRNA expression levels were much higher compared to P3F wt (Fig. 11A/B/C). One possible reason for this observation could be that P3F S503A protein is less stable than P3F wt.

A

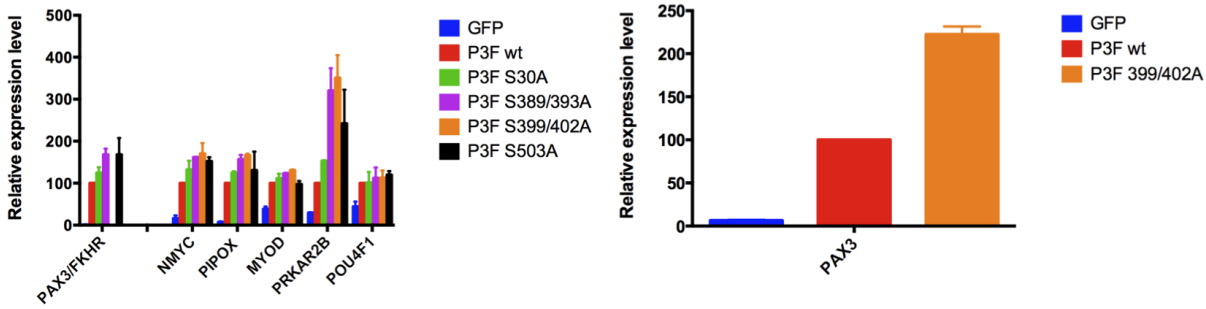

B

		GFP positive
Virus	P3F wt	44.6%, 50.4%
	P3F S30A	47.8% 57.1%
	P3F S389/393A	66.9% 69%
	P3F S399/402A	63.5% 65.1%
	P3F S503A	60.3% 62.5%

C

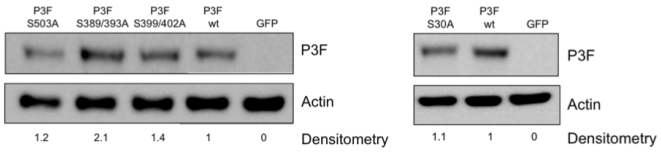

Figure 11: Testing the transcriptional activity of PAX3/FOXO1 phosphomutants (sites identified with mass spectrometry after in vitro phosphorylation by PLK1) by retroviral transduction of RD cells
A) TaqMan mRNA expression analysis of PAX3/FOXO1 and PAX3/FOXO1 target genes in RD cells 120h after transduction with either PAX3/FOXO1 wild type or PAX3/FOXO1 phosphomutants, expression levels relative to PAX3FOXO1 wild type. Biological replicates of two independtent experiments. Error bars represent standard deviations **B)** FACS analysis was used to assess percentages of GFP positive cells for each transduction procedure 120h after infection **C)** Western blot analysis showing PAX3/FOXO1 protein levels 120h after transduction, densitometrical analysis performed with ImageJ software showing protein levels relative to PAX3/FOXO1 wild type

4.4.2 Additional phosphomutants also do not display reduced activity

All additional phosphomutants were also more expressed on mRNA level than was P3F wt (Fig. 12A). Also here no phosphomutant with reduced transcriptional activity compared to wild type PAX3/FOXO1 could be identified. All phosphomutants induced higher target gene expression than did P3F wt (Fig. 12A). With the exception of P3F S399A, all phosphomutant viruses were more infectious than P3F wt virus (Fig. 12B). Interestingly, also this phosphomutant was higher expressed than P3F wt like all other phosphomutants. On protein level, all phosphomutants showed higher expression than did P3F wt (Fig. 12C). Again, as it was mentioned previously, differences in target gene expression between P3F wt and the P3F phosphomutants are likely due to differences in infection efficiencies.

A

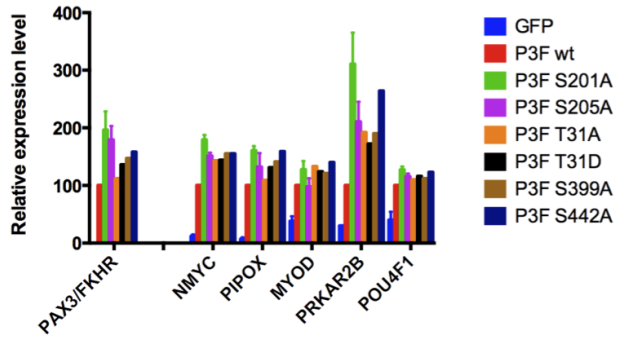

B

		GFP positive
Virus	P3F wt	50.1% 40%
	P3F S201A	61.9%
	P3F S205A	67%
	P3F T31A	47.4%
	P3F T31D	54.4%
	P3F S399A	38.4%
	P3F S442A	52.8%

C

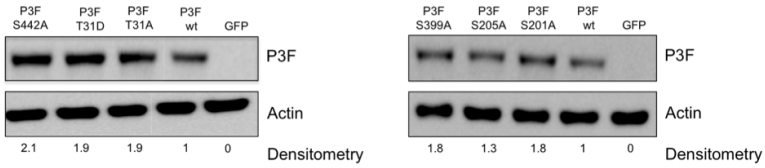

Figure 12: Testing the transcriptional activity of additional PAX3/FOXO1 phosphomutants
A) TaqMan mRNA expression analysis of PAX3/FOXO1 and PAX3/FOXO1 target genes in RD cells 120h after transduction with either PAX3/FOXO1 wild type or PAX3/FOXO1 phosphomutants, expression levels relative to PAX3FOXO1 wild type. **B)** FACS analysis was used to assess percentages of GFP positive cells for each transduction procedure 120h after infection **C)** Western blot analysis showing PAX3/FOXO1 protein levels 120h after transduction, densitometrical analysis performed with ImageJ software showing protein levels relative to PAX3/FOXO1 wild type

Taken together, I was not able to identify a PAX3/FOXO1 phosphomutant with reduced transcriptional activity. As a remark I would like to mention that this activity read-out system for testing of PAX3/FOXO1 phosphomutants remains to be improved (see discussion). As time was a limiting factor for my work in the laboratory, I regret that I have not been able to make these refinements. However, some results might indicate that P3F S503A has decreased protein stability and therefore might be less active.

4.5 Cycloheximide treatment of transfected RD cells is an instrument to measure PAX3/FOXO1 stability

We found that phosphorylation by PLK1 might stabilize PAX3/FOXO1 (see section 4.1.2) and my experiments gave additional hints that some phosphomutants (especially P3F S503A) might be less stable (see section 4.4.1). For this reason we wanted to directly investigate if any P3F phospomutant of potential PLK1 sites is less stable than P3F wt. Towards this end, we treated cells with cycloheximide (CHX) and monitored protein levels after treatment.

4.5.1 PAX3/FOXO1 is degraded in RD cells after cycloheximide treatment

First, I investigated whether I can detect degradation of P3F wt upon CHX treatment. I used RD cells for these experiments since they also were my choice for testing the activity before. This decision was based on the same arguments mentioned previously. Additionally, I chose C2C12 cells, which is a mouse myoblast cell line, because it was already published that PAX3/FOXO1 is degraded in C2C12 cells treated with 5 μM CHX [84]. Since I did not want to express high amounts of protein, I only transfected cells overnight with 1 μg of pMSCV-PAX3/FOXO1-IRES-GFP plasmid DNA using the JetPrime protocol in order to be able to see degradation after short periods of CHX exposure. I treated cells with 10 μg/ml CHX (35 μM) or DMSO for 3, 6 and 24 hours. Protein was isolated at the indicated time points and analyzed by Western blot. Quantification of protein levels was performed with ImageJ software, corrected for loading using GAPDH and normalized to the 0h time point. As a control for efficiency of CHX treatment Cyclin B1 protein levels were monitored, which is known to be rapidly degraded. This is because Cyclin B1 protein levels cannot be replenished after anaphase under efficient CHX treatment.

As far as toxicity is concerned, RD cells were more resistant to the treatment, whereas C2C12 cells did not seem to tolerate such high doses of CHX equally well (judged by eye under light microscope). A first observation was that RD cells expressed lower amounts of protein compared to C2C12 cells for all time points (Fig. 13A). Probably these cells are more efficiently transfected or have a higher synthesis rate in general. Importantly, CHX treatment seemed to be more efficient in RD cells, as Cyclin B1 protein levels decreased faster (Fig. 13A/B). As a consequence, protein levels of PAX3/FOXO1 were decreased more in RD (around 50%) than in C2C12 cells (around 15%) after 6 hours of CHX treatment (Fig 13A/B). Exposure of cells to CHX for 24h was already too long, at least for C2C12 cells, because principally all cells died already. I selected the 6 hours treatment with 10 μg/ml CHX in RD cells for further experiments, because I was able to detect sufficient degradation of PAX3/FOXO1 at this time point and concentration.

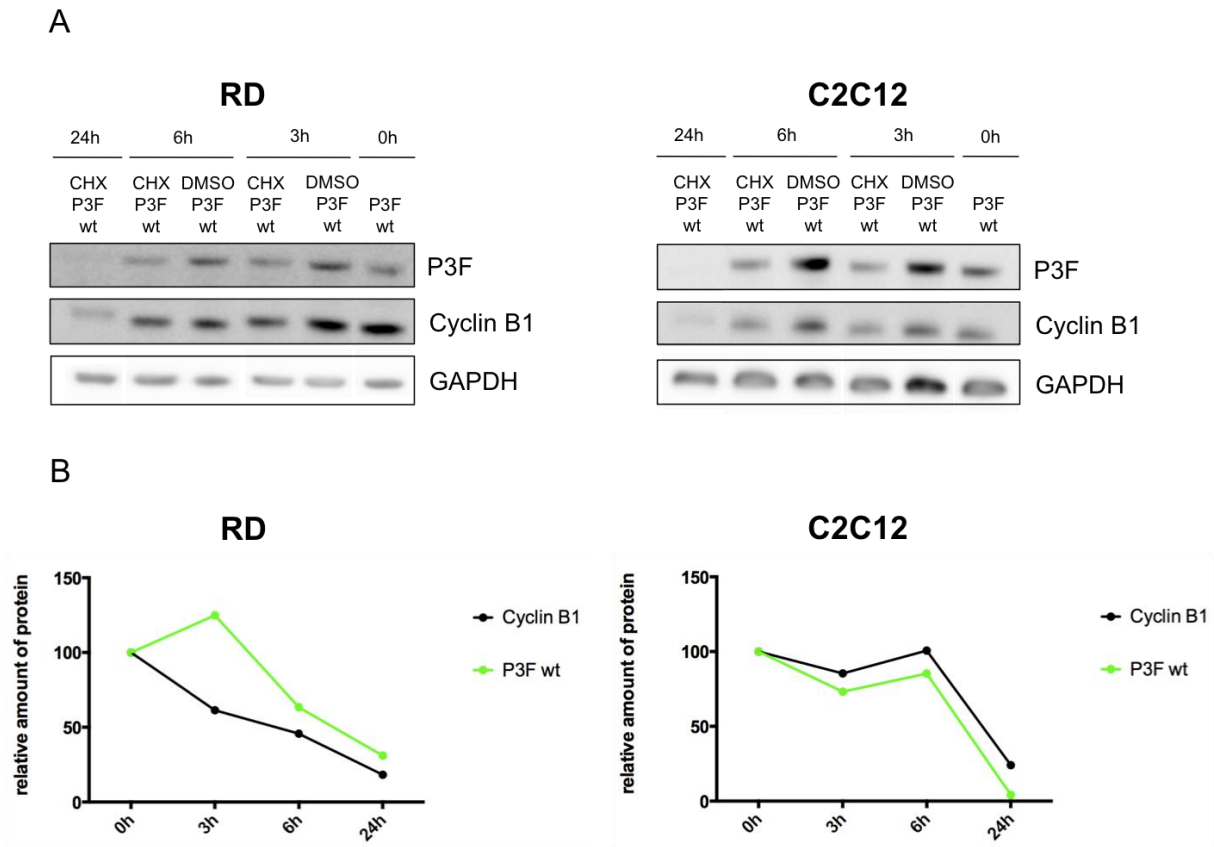

Figure 13: PAX3/FOXO1 gets degraded after cycloheximide treatment
A) Western blots showing PAX3/FOXO1 wild type protein levels after overnight transfection (0h) and 3h, 6h, 24h cycloheximide treatment (10μg/ml) in RD and C2C12 cells. Cyclin B1 protein levels are shown for each time point too as an indicator of effective cycloheximide treatment. GAPDH is shown as loading control **B)** Relative quantification of PAX3/FOXO1 and Cyclin B1 protein levels was performed with ImageJ software. Protein levels are relative to the 0h time point

4.5.2 PAX3/FOXO1 wild type is less expressed in RD cells compared to PAX3/FOXO1 phosphomutants

All sites found by mass spectrometry to be phosphorylated by PLK1 in vitro were tested to see if they have an influence on PAX3/FOXO1 protein stability. For this, RD cells were transfected again with 1μg of plasmid DNA overnight and then treated with 10 μg/ml CHX or DMSO for 6 hours. Protein was isolated and analyzed by Western blot at 0h and 6h. Densitometrical quantification was performed with ImageJ software. I corrected for loading and measured the 6h time points relative to the 0h time points. Then these values were normalized with P3F wt protein levels for each mutant. Relative amounts of residual protein of P3F wt served as a reference value (100%). Relative amounts of residual protein of the phosphomutants were compared to this reference.

Samples were distributed on two gels. I included the same samples of P3F wt on both gels. I observed huge variations for P3F wt protein levels after 6h CHX treatment relative to 0h. On the first blot (Fig. 14A left panel), P3F wt protein levels were reduced to about 68%, whereas on the second blot (Fig. 14A right panel) amount of protein was only reduced by 12%. It was reasoned that this is because of

difficulties to accurately quantify low protein levels. It was again seen that P3F wt was less expressed than all phosphomutants with the exception of P3F S30A (Fig. 14A). This was also an observation that I made in my infection experiments. However, in this setting I transfected exactly the same amount of plasmid DNA. This suggests that P3F wt is expressed less than P3F phosphomutants in RD cells. CHX treatment caused successful degradation of all proteins (Fig. 14A). The extent of Cyclin B1 degradation however was not consistent throughout all samples (Fig. 14A). On the first blot, where P3F S30A and P3F S389/393A were included, neither of the mutants were less stable than P3F wt (Fig. 14B left panel). On the second blot, both P3F S399/402A and P3F S503A were apparently less stable than P3F wt (Fig. 14B right panel). However, exact quantification of P3F wt was not possible, since too little P3F wt protein was loaded. Therefore I could not be completely sure that the effects I saw were real.

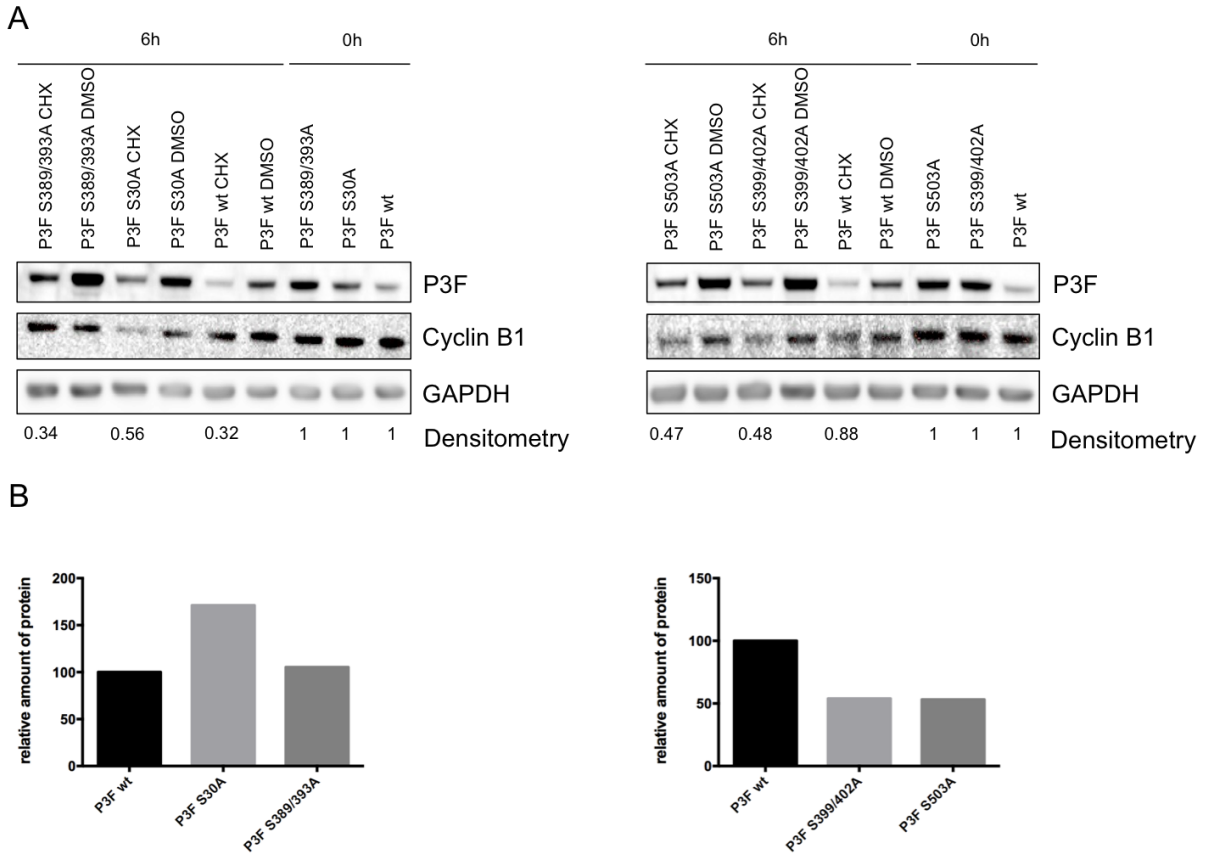

Figure 14: Testing the stability of PAX3/FOXO1 phosphomutants of sites identified by mass spectrometry after in vitro phosphorylation with PLK1

A) Western blots showing PAX3/FOXO1 wild type and PAX3/FOXO1 phosphomutants protein levels after overnight transfection (0h) and 6h cycloheximide treatment (10μg/ml) in RD cells. Cyclin B1 protein levels are shown for each time point too as an indicator of effective cycloheximide treatment. GAPDH is shown as loading control. Densitometrical analysis performed with ImageJ software showing relative protein levels compared to the 0h time point **B)** Amounts of residual protein after cycloheximide treatment relative to PAX3/FOXO1 wild type residual protein levels

4.6 Validating the stability of PAX3/FOXO1 phosphomutants by CHX treatment of transfected RD cells

Because of the findings described above, I decided to repeat the experiment with the same conditions but loading higher volumes of P3F wt and P3F S30A samples in order to have similar amounts of protein to compare. Additionally I wanted to load all samples on a single gel. Therefore I excluded all DMSO samples. The two time points for the samples were loaded next to each other for further clarification.

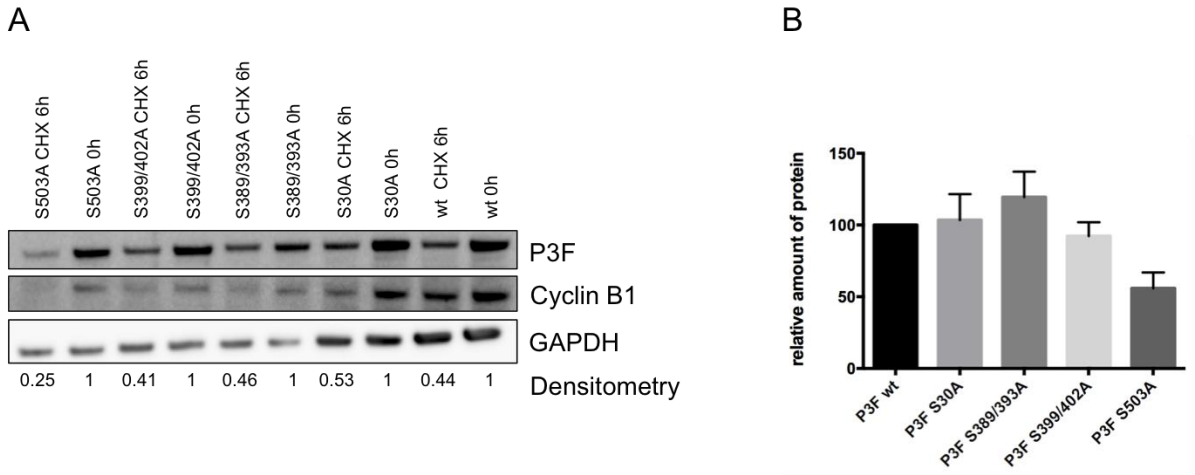

Figure 15: Testing the stability of PAX3/FOXO1 phosphomutants of sites identified by mass spectrometry after in vitro phosphorylation with PLK1
A) Western blot showing PAX3/FOXO1 wild type and PAX3/FOXO1 phosphomutants protein levels after overnight transfection (0h) and 6h cycloheximide treatment (10μg/ml) in RD cells. Cyclin B1 protein levels are shown for each time point too as an indicator of effective cycloheximide treatment. GAPDH is shown as loading control. Densitometrical analysis performed with ImageJ software showing relative protein levels compared to the 0h time point **B)** Amounts of residual protein after cycloheximide treatment relative to PAX3/FOXO1 wild type residual protein levels; technical replicates with same samples of one experiment. Error bars represent standard deviations

In contrast to previous experiments, by adjusting the sample volumes, I was able to see similar amounts of P3F wt and P3F phosphomutants for the 0h time points (Fig. 15A). This made it less difficult to accurately quantify how much protein was degraded after 6 hours of CHX treatment. Also degradation of Cyclin B1 was more consistent throughout all samples, suggesting equal effectiveness of CHX treatment (Fig. 15A). I determined that P3F wt levels were reduced by 56% after treatment. P3F S389/393A and P3F S399/402A protein amounts were reduced by almost exactly the same percentage. P3F S30A was not degraded as strongly (47% reduction of protein level). However, the only phosphomutant with significantly stronger reduction of protein levels after 6 hours of CHX treatment was P3F S503A, which was degraded by 75% (Fig. 15A). This suggests that this mutant indeed might be less stable than P3F wt. To confirm that this result did not depend on loading or blotting procedures, I loaded the same samples with higher volumes a second time. Again P3F S503A was the only mutant with a higher level of degradation than P3F wt (Fig. 15B). In general, values of protein levels after quantification with ImageJ

software were differing only for P3F S30A and P3F S389/393A by about 10%. All the other values were nearly identical with the previous values. Taken together, these results indicated that the P3F S503A phosphomutant might be less stable than P3F wt. Hence phosphorylation of P3F by PLK1 could influence protein stability through the cell cycle.

4.6.1 PAX3/FOXO1 6xA might display reduced stability but needs further investigation

A site within PAX3/FOXO1, which was predicted to be phosphorylated by PLK1 in silico, is S510. Interestingly, literature research revealed that PLK1 phosphorylates MYC at a site that shows high sequence homology to S510 in PAX3/FOXO1. By this phosphorylation event, ubiquitinylation and degradation of MYC is reduced and therefore gets stabilized [56, 57]. Because of this I wanted to test the P3F S510A phosphomutant in regard to protein stability. The mutant was generated by site directed mutagenesis as described before. A second mutant I wanted to test was P3F 6xA, because I saw that protein levels differed compared to P3F wt after retroviral transduction of RD cells despite equal expression on mRNA level (see section 4.3.4). The same protocol as before was used (see sections 4.4 - 4.6). However, the data presented below are preliminary, since I only repeated the experiment once.

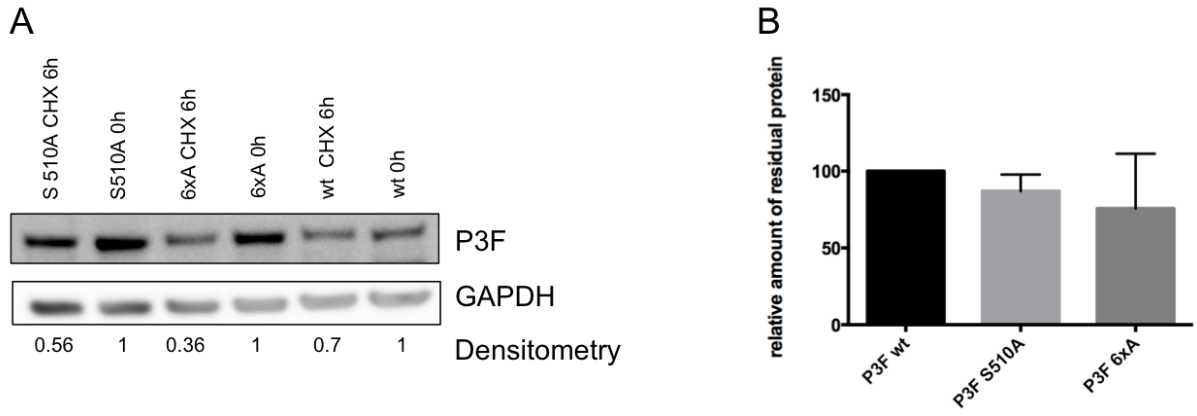

Figure 16: PAX3/FOXO1 S510A and 6xA display no differences in stability compared to PAX3/FOXO1 wild type (Preliminary data)
RD cells were transfected with PAX3/FOXO1 wild type and PAX3/FOXO1 phosphomutants and treated with 10μg/ml cycloheximide for 6h **A)** Western blot showing relative amounts of residual PAX3/FOXO1 wilt type and PAX3/FOXO1 S510A and 6xA proteins. Protein levels are relative to PAX3/FOXO1 wild type **B)** Western blot showing relative amounts of residual PAX3/FOXO1 wilt type and PAX3/FOXO1 S510Aand 6xA proteins. Protein levels are relative to PAX3/FOXO1 wild type. Biological replicates of two independent experiments. Error bars represent standard deviations

In a first experiment, P3F 6xA was almost twice as strongly degraded as P3F wt (Fig. 16A). However, this was not reproducible in a second experiment, where P3F 6xA was again almost equally degraded as P3F wt (101%). For P3F S510A, I could determine that the protein was degraded to almost the same level as P3F wt in two independent experiments (80% and 94%) (Fig. 16 A/B). So far I can conclude that

probably P3F S510A is not less stable than P3F wt. As far as P3F 6xA is concerned, further experiments have to be done to allow definite conclusions.

4.6.2 PAX3/FOXO1 S503A displays decreased protein stability compared to PAX3/FOXO1 wild type

Finally, biological triplicates were generated using the same protocol as mentioned above (see sections 4.4 - 4.6). I was able to reproduce that P3F S503A protein levels were more decreased than those of P3F wt after 6h treatment with 10 μg/ml CHX. Hence, I could demonstrate that P3F S503A has a significantly lower stability compared to P3F wt (Fig. 17A). On average, protein levels of P3F S503 were 47% stronger reduced than those of P3F wt. All other P3F phosphomutants of sites identified to be phosphorylated in vitro by PLK1 showed no significant difference in protein stability after 6h treatment with 10 μg/ml CHX (Fig. 17B).

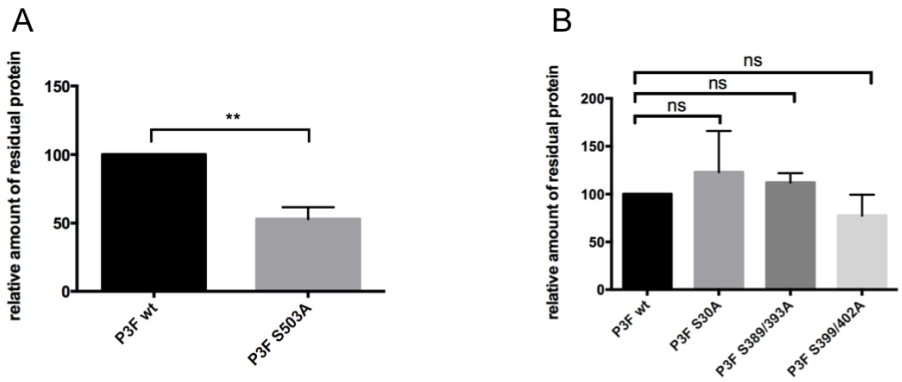

Figure 17: The PAX3/FOXO1 S503A phosphomutant displays lower stability upon cycloheximide treatment in RD cells
Biological replicates of three independent experiments; RD cells were transfected with PAX3/FOXO1 wild type and PAX3/FOXO1 phosphomutants and treated with 10μg/ml cycloheximide for 6h **A)** Western blot showing relative amounts of residual PAX3/FOXO1 wilt type and PAX3/FOXO1 S503A proteins. Protein levels are relative to PAX3/FOXO1 wild type. p=0.0052 (unpaired t-test) **B)** Western blot showing relative amounts of residual PAX3/FOXO1 wilt type and PAX3/FOXO1 S30A, S389/393A and S399/402A proteins. Protein levels are relative to PAX3/FOXO1 wild type. No significant differences were detected (unpaired t-test)

In conclusion, I could identify a novel site of phosphorylation at S503 in PAX3/FOXO1. In addition, further experiments suggest that this phosphorylation event contributes to PAX3/FOXO1 stabilization and thereby enhances its transcriptional activity. Since PLK1 is specifically active during the G2/M phase of the cell cycle, stabilization of PAX3/FOXO1 might contribute to cell cycle progression.

5 DISCUSSION

Oncogenic fusion proteins, like the PAX3/FOXO1 chimeric transcription factor in aRMS, represent an attractive therapeutic target, because their expression is limited to tumor cells. Most importantly, it is suggested that also the tumorigenic driving force in aRMS is PAX3/FOXO1 itself. Because aRMS is clinically more aggressive than eRMS, and the PAX3/FOXO1 fusion status confers the worst prognosis, novel therapies targeting PAX3/FOXO1 are needed. The fact that metastasizing aRMS tumors become resistant to conventional chemotherapy and radiotherapy and are almost always fatal is another reason to investigate new possibilities for therapy. Since it is not possible to inhibit transcription factors directly by small molecules, other strategies to indirectly inhibit PAX3/FOXO1 are urgently needed. Interfering with posttranslational modifications of PAX3/FOXO1, which play a role in regulating its transcriptional activity, may therefore be a useful strategy. Phosphorylation is known to regulate the activity of most transcription factors in the human genome by several mechanisms. These mechanisms include changes in subcellular localization, protein stability, DNA binding ability or protein-protein interactions. Indeed it was shown that also PAX3/FOXO1 transcriptional activity is regulated by phosphorylation events [46, 61-63]. This indicates that interfering with upstream regulating kinases is a promising approach for new molecular therapies. In order to find kinases able to regulate PAX3/FOXO1 activity, a RNAi screen of the human kinome and a screen with a kinase inhibitor library was performed in aRMS cells with an AP2beta luciferase reporter construct. PLK1 was one of the top hits and was further shown to interact with PAX3/FOXO1, to regulate its transcriptional activity and also its stability. An independent study identified PLK1 through a siRNA library screen against human kinases to reduce growth and increase apoptosis in RMS cell lines but not normal muscle cells [66]. These findings suggest that PLK1 might be a promising novel therapeutic target in aRMS.

After validating that PLK1 indeed regulates the transcriptional activity of PAX3/FOXO1, the aim of this thesis was to identify potential PLK1 phosphorylation sites within PAX3/FOXO1. Further I investigated if phosphorylation at any of the identified sites influences transcriptional activity of PAX3/FOXO1. Moreover, I wanted to know if any of the phosphorylation sites has an influence on PAX3/FOXO1 protein stability.

5.1 Downregulation of PLK1 decreases transcriptional activity of PAX3/FOXO1 by induction of degradation

In previous experiments, downregulation of PAX3/FOXO1 target gene expression was observed after knockdown of PLK1 in aRMS cell lines. Under mild knockdown conditions, no degradation of PAX3/FOXO1 nor cell cycle arrest was observed. However, if treated with higher concentrations of siRNA both degradation of PAX3/FOXO1 and cell cycle arrest were induced. Also other studies indicate that a common effect of PLK1 knockdown is cell cycle arrest [66, 72, 73]. This is not surprising considering the roles of PLK1 in mitotic progression. We validated the reduction of target gene expression in RMS13 cells using a second siRNA. Again, we induced degradation of PAX3/FOXO1 protein after siRNA treatment. Also, a strong G2/M arrest was observed. These findings were made with lower siRNA concentrations compared to experiments with the first siRNA. Because s449 siRNA is a second generation product, it is supposed to be more potent.

Together these results indicate that PLK1 is able to regulate the transcriptional activity of PAX3/FOXO1. Most probably, this effect is mediated by direct phosphorylation of PAX3/FOXO1 by PLK1 because both were shown to interact with each other. We therefore suggest a mechanism by which PAX3/FOXO1 is stabilized upon phosphorylation by PLK1. However, degradation could additionally be indirectly caused by cell cycle arrest. Later experiments of Verena Thalhammer showed degradation of PAX3/FOXO1 upon treatment of cells with vincristine or colchicine, which also induce mitotic arrest. Besides influencing the stability of PAX3/FOXO1, other effects of PLK1 mediated phosphorylation are likely because target gene expression was also reduced without degradation of the protein, as observed in knockdown experiments with s1341. Since we did never observe the same in experiments with s449 siRNA, also an off target effect of the first siRNA cannot be excluded.

5.2 PLK1 phosphorylates PAX3/FOXO1 in vitro

To better understand the underlying molecular mechanisms, by which PLK1 regulates the activity of PAX3/FOXO1, it is crucial to characterize the sites of phosphorylation within PAX3/FOXO1 for PLK1. To investigate this, we phosphorylated PAX3/FOXO1 in vitro and detected the phosphorylation sites using mass spectrometry.

We found several different peptides to be phosphorylated by PLK1 in vitro. Because of technical obstacles, it was not possible to define the exact site of phosphorylation within single peptides. However, we investigated six potential PLK1 phosphorylation sites, which might have an influence on PAX3/FOXO1 activity. We further had some

problems including incomplete dephosphorylation after CIP treatment. Unfortunately, we were so far not able to purify PAX3/FOXO1 from bacteria, which probably would have been an advantage in this regard. Also some sequences of PAX3/FOXO1 were not covered. To cover sequences previously uncovered, I suggest digestion of samples with additional endoproteinases in future experiments. Therefore, we think that there could be more potential PLK1 phosphorylation sites in PAX3/FOXO1. It is also not completely sure that the identified sites within PAX3/FOXO1 are also phosphorylated by PLK1 in vivo. The reason for this is that sometimes in vitro phosphorylation can be unspecific. Besides the identification of phosphorylation by mass spectrometry, we were also able to identify in vitro phosphorylation of S503 with a phosphospecific antibody by Western blot analysis, since phosphorylation at this site in FOXO1 (S322) is already described. Together these findings indicate that S503 is a phosphorylation site in PAX3/FOXO1 for PLK1. Using the same antibody to demonstrate in vivo phosphorylation at this site will be an important step in future experiments. In previous experiments, the peptide containing S503 was found phosphorylated by mass spectrometry if PAX3/FOXO1 was purified from RMS13 cells.

5.3 Phosphorylation of PAX3/FOXO1 at S503 by PLK1 has a stabilizing effect

Studies in differentiating mouse myoblasts revealed that PAX3/FOXO1 is more stable than PAX3 and persists throughout myogenic differentiation, which may lead to the inability to terminally differentiate. It was reasoned that this is caused by posttranslational stabilization of PAX3/FOXO1 [85]. Phosphorylation can increase the stability of proteins by several mechanisms. One of which is the inhibition of E3 ubiquitin ligase substrate recognition [86]. Such an effect was already described for MYC, which is stabilized by PLK1 mediated phosphorylation [56, 57]. A recently published study also found that treatment of aRMS cells with thapsigargin, which activates AKT, inhibits PAX3/FOXO1 activity by phosphorylation. Thapsigargin inhibited the binding of PAX3/FOXO1 to target genes and promoted its proteasomal degradation [63]. Together this shows that phosphorylation by PLK1 can have a stabilizing effect and that phosphorylation of PAX3/FOXO1 can influence its stability.

Site directed mutagenesis of sites that are potentially phosphorylated by kinases is a useful strategy to determine the functional effect of phosphorylation at this site on the protein. With this in mind, I transformed the sites identified to be phosphorylated in vitro by PLK1 into alanine. These sites can therefore no longer be phosphorylated. Because we assumed that PLK1 mediated phosphorylation also stabilizes PAX3/FOXO1, as knockdown experiments suggested, I investigated the stability of phospomutants of sites identified after in vitro phosphorylation by PLK1. I did this by

transfecting RD cells with P3F wt or P3F phosphomutants followed by cycloheximide treatment for 6 hours.

I was able to identify one phosphomutant with reduced stability compared to P3F wt. This mutant was PAX3/FOXO1 S503A. This result indicates that phosphorylation of PAX3/FOXO1 at S503 by PLK1 stabilizes the protein. This leads me to the assumption that PAX3/FOXO1 can act more efficiently as a transcriptional regulator due to this stabilization event. This induces enhanced expression of PAX3/FOXO1 target genes with high tumorigenic capacity and finally contributes to malignant transformation. Thus, intervening with PLK1 function using small molecule inhibitors is an excellent strategy, also because PLK1 is overexpressed in RMS tumors (Fig. 18).

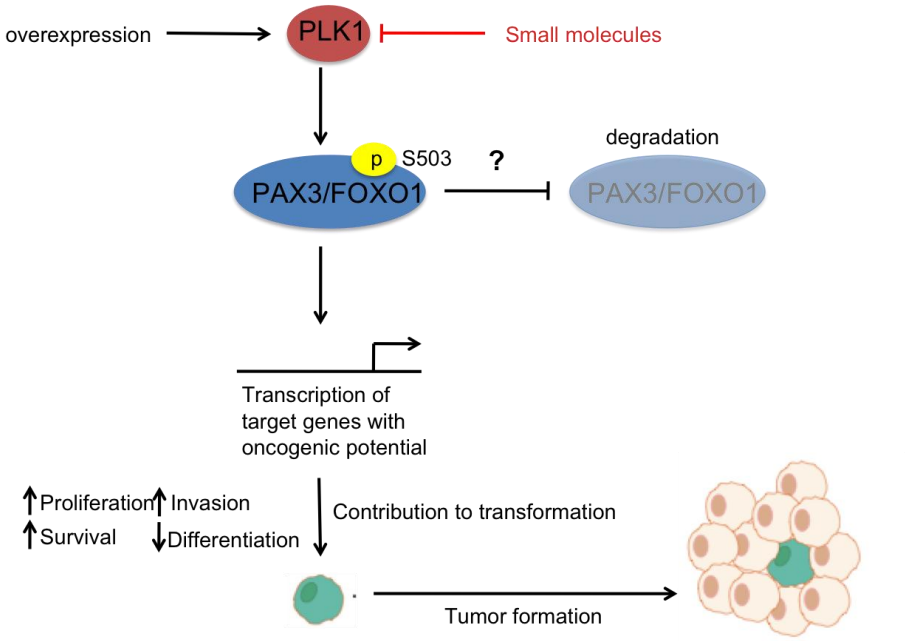

Figure 18: Working hypothesis for the regulation of PAX3/FOXO1 by PLK1 mediated phosporylation at S503 in aRMS cells

This working hypothesis provides a molecular mechanism for the deeper understanding of how PLK1 regulates PAX3/FOXO1 and reinforces the establishment of PLK1 as a novel therapeutic target in aRMS. However, further experiments have to be performed for validation.

A first important experiment would be to mutate S503 into aspartic acid. This mutation should mimic phosphorylation and therefore lead to a rescue of PAX3/FOXO1 degradation in CHX experiments. The same could also be tested in pulse-chase experiments with higher accuracy. A particular advantage of pulse chase experiments over CHX treatements is that it provides minimal distortion of normal cell physiology. To prove that S503A can no longer be phosphorylated by PLK1, an in vitro phosporylation with PLK1 with this mutant should be performed. No band on Western blot should be detected with anti-FOXO1 (pS322) antibody. A

particularly important experiment would be to treat aRMS cells with PLK1 inhibitors and check with anti-FOXO1 (p322) antibody if phosphorylation of endogenous PAX3/FOXO1 at this site still occurs.

If my findings can be validated by these means, further investigations in order to reveal the mechanistic background of how PAX3/FOXO1 stabilization is achieved should be made.

A possibility would be that the phosphorylation event on S503A of PAX3/FOXO1 by PLK1 interferes with binding to an E3 ligase, which ubiquitinates it and targets it for proteasomal degradation. This assuption is partly supported by previous experiments in which a rescue of degradation of P3F wt was observed after PLK1 inhibition and treatment with proteasomal inhibitor (bortezomib) in aRMS cells. If a rescue can be found in experiments where P3F S503A transfected cells are treated with CHX and proteasomal inhibitor, it would strengthen this hypothesis. In order to find which E3 ligase might be associated, co-immunoprecipitation experiments could be performed. E3 ligases, which pull down with P3F S503A but not P3F S503D would be interesting candidates. Alternatively, a siRNA screening against E3 ligases is another possible approach. Knockdown of associated E3 ligases should lead to a rescue in degradation of P3F S503A. However, association with E3 ligases is not the only mean by which phosphorylation can affect protein stability. Theoretically, phosphorylation can affect the structure of a protein and directly alter its thermodynamic stability.

5.4 PLK1 is a promising therapeutic target especially for aRMS

Consistent with its role in promoting proliferation, chromosome instability and aneuploidy, PLK1 overexpression has been observed in many cancers and in some tumor types even correlates with worse prognosis [72, 75]. By immunohistochemical stainings of tissue micro arrays, PLK1 overexpression also was found to confer poorer prognosis in aRMS [65]. Numerous studies with siRNA or small molecule mediated PLK1 inhibition indicated that cancer cells undergo mitotic arrest, proliferation inhibition and apoptosis [72, 73, 87-89]. Importantly, PLK1 inhibition was shown to preferentially kill cancer cells compared with normal cells [66, 88], which provides a potential therapeutic window. In vivo studies with BI2536 PLK1 inhibitor additionally showed reduced tumor growth and even regression [65, 90] All these findings indicate that PLK1 is a promising cancer target and several clinical trials with PLK1 inhibitors have been made [77]. However, genetic evidence of PLK1 being an oncogene is not very strong [75].

In contrast to studies in other cancer types, my work provides evidence for a cancer specific mechanism by which PLK1 inhibition mediates an antitumorigenic effect.

One could argue that PLK1 overexpression is just a feature of fast proliferating cancer cells and does not contribute to tumorigenesis. However, my work suggests that PLK1 exerts a direct tumor supporting effect in aRMS by stabilizing PAX3/FOXO1 via phosphorylation, which might contribute to cell cycle progression. Because aRMS cells depend on the constitutive expression of PAX3/FOXO1, apoptosis upon PLK1 inhibitor treatment might be induced by degradation of PAX3/FOXO1.

My results, if they can be validated, strongly suggest that PLK1 is a suitable therapeutic target especially in aRMS, because of its potency to stabilize PAX3/FOXO1 by direct phosphorylation. This argues for increased inclusion of aRMS patients in clinical trials with PLK1 inhibitors. Especially aRMS patients with PLK1 overexpression could benefit from such treatment. Of course there are difficulties to recrute enough patients since aRMS is a very rare disease. Additionally children are difficult to include for clinical trials. Because PLK1 is additionally involved in stabilization of the MYC oncogene, which is currently undruggable, MYC overexpressing tumors could also benefit from PLK1 inhibitors. Since MYC plays an important role in promotion of many human cancers, PLK1 inhibitors might be applicable to a broad range of cancers other than aRMS.

5.5 Retroviral transduction of RD and hMSC cells as a potential tool for testing PAX3/FOXO1 phosphomutants

To test phosphomutants in regard of transcriptional activity, I needed to develop a new read-out system. Delivery of genetic material using retroviruses is a commonly used method to stably express genes of interest in target cells. Previous experiments of Verena Thalhammer indicated that stable expression of PAX3/FOXO1 is necessary to induce target gene expression. It was shown that upon transduction of RD cells with PAX3/FOXO1, an expression profile was induced that resembled the expression signature of aRMS cell lines [80]. Another study showed that mMSC cells transduced with PAX3/FOXO1 and SV40-LT induced tumors in mice, which expressed aRMS specific genes [81].

Regarding these findings, I tried to induce PAX3/FOXO1 target gene expression by retroviral transduction of different cell lines. The purpose was to find a cell line in which I could test the activity of PAX3/FOXO1 phosphomutants compared to PAX3/FOXO1 wild type. I was able to show that transduction of RD cells with PAX3/FOXO1 induces target gene expression. But no target gene expression was induced in mMSC cells. A possible explanation for this might be that cooperating secondary mutations and/or correct in vivo cellular background are needed in addition. Also other cell lines showed PAX3/FOXO1 target gene expression after transduction but were less suitable for the testing of PAX3/FOXO1 phosphomutants.

Primary hMSCs for example were difficult to infect. Additionally, this cell line grows very slowly in culture. However, the infection efficiency might improve if virus supernatant would be concentrated before infecting the cells. Additionally, the effect on PAX3/FOXO1 target genes was quite strong and also genes that were previously not expressed could be induced. This is why this cell line is still an alternative to try for testing of phosphomutants. Anyway, the best system for this purpose would be to knock down endogenous PAX3/FOXO1 in aRMS cell lines with shRNA directed against the 3'UTR and subsequently transduce these cells with PAX3/FOXO1 phosphomutants. This is currently being established in our laboratory.

I was able to show that in principal, testing of transcriptional activity of PAX3/FOXO1 phosphomutants is possible using retroviral transduction of RD cells. This assumption is based on the fact that transduction with positive controls (DNA binding mutants and the 6xA phosphomutant of PAX3/FOXO1) led to a weaker induction of target genes compared to transduction with PAX3/FOXO1 wild type. However, I could not identify a PAX3/FOXO1 mutant of sites phosphorylated by PLK1 in vitro with reduced transcriptional activity. In my experiments, target gene expression was stronger in cells transduced with PAX3/FOXO1 phosphomutants compared to PAX3/FOXO1 wild type. Most probably, this is because I did not titrate virus supernatants and transduction was more efficient with PAX3/FOXO1 phosphomutants compared to PAX3/FOXO1 wild type. This indicates that for the correct testing of PAX3/FOXO1 phosphomutants in this setting, it is crucial to have same infection efficiencies compared to PAX3/FOXO1 wild type, in order to be able to accurately compare transcriptional activities. Therefore I strongly suggest calculating viral titers of all viral stocks and transduce cells with same amounts of viral particles, to improve the retroviral system for testing the activity of PAX3/FOXO1 phosphomutants.

Determination of viral titer using flow cytometry allows calculating the number of actual viable transducing viral particles present in the viral stock. Since my retroviral plasmid codes for the GFP reporter gene, this would be the method of choice. Other techniques like qRT-PCR assay simply determine how many particles are present but do not consider how many of those particles are viable and also capable of infection. I suggest to directly titrate viruses on cells that will have to be infected later. In my case these would be RD or also primary hMSC cells. Virus can be produced in the same way as successfully done previously. Additionally, I would concentrate virus supernatant for later infection of primary hMSC cells. Because the VSV-G glycoprotein of virus produced with 293 GPG cells adds physical stability to retroviral particles, they are suitable for concentration by high-speed ultracentrifugation. Afterwards, serial dilutions of virus stock should be made. The goal of this is to reach transduction in the range of 1-20% GFP positive cells. Above this range, chances

that GFP positive cells were infected more than once is very likely. This would lead to an underestimation of viral titer [91]. Infection of target cells with dilutions of viral stock can be performed as described. 72 hours post infection, the percentage of GFP positive cells for each infection condition can be estimated by FACS as described. In the condition resulting in 1-20% GFP positive cells, the titer of transducing units per ml (TU/ml) can be calculated by dividing the number of transduced cells, assuming a doubling 24 hours after plating, by the volume of viral stock used. This should be done for viral stocks of PAX3/FOXO1 wild type virus and PAX3/FOXO1 phosphomutants viruses. MOI (multiplicity of infection) is the ratio of transducing units present per cell. Using a specific MOI allows prediction of how many particles will transduce one cell. Same MOIs should be used to transduce cells with PAX3/FOXO1 wild type and PAX3/FOXO1 phosphomutants. This ensures that the same percentage of cells get infected with same amounts of viral particles per cell. To determine the optimal MOI for this assay, I would use a range of MOIs in a first experiment.

The differences observed in transduction efficiencies between PAX3/FOXO1 wild type and PAX3/FOXO1 phosphomutants in my experiments indicate two things. First, more cells are transduced with PAX3/FOXO1 phosphomutants compared to PAX3/FOXO1 wild type. Second, they probably also contain more copies per cell than cells transduced with PAX3/FOXO1 wild type. Consequently, they are also higher expressed on mRNA level and also induce PAX3/FOXO1 target gene expression more strongly. Thus, even if a mutation might have an effect on PAX3/FOXO1 transcriptional activity, no difference can be observed, simply because more protein is present. Another problem is that, at least with RD cells, PAX3/FOXO1 wild type seems to be less expressed than PAX3/FOXO1 phosphomutants. If this is an effect only observed after short periods of transient transfection remains to be seen. Although I cannot predict if I can expect to see differences in target gene expression with titrated virus supernatants, it is an important step for evaluating the quality of the read-out system. If, using same MOIs for transduction of cells, target gene expression should be weaker in P3F 6xA (already observed), P3F 4xA and P3F 5xA (not investigated yet) transduced cells compared to P3F wt transduced cells, this would be a sign of good quality and high sensitivity. If so, I would also expect to see less target gene expression with the P3F S503A phosphomutant (considering the working hypothesis). However, an effect resulting from reduced stability of this mutant might get masked on target gene level because of constitutive expression of the mutant in this system. Consequently, compensation for degraded protein happens. A possible alternative could be to test target gene expression compared to P3F wt after exposure to CHX. Since other mechanisms than PAX3/FOXO1 protein stabilization are potentially induced by PLK1 mediated phosphorylation, other

phosphomutants might affect transcriptional activity. If single alanine mutants should not lead to a decrease of target gene expression, I would suggest mutating whole clusters of potential phosphorylation sites.

5.6 Synopsis

In conclusion, I was able to validate that downregulation of PLK1 leads to decreased transcriptional activity of PAX3/FOXO1 in aRMS cell lines. Additionally I identified sites within PAX3/FOXO1, which are potentially phosphorylated by PLK1 in vitro. My findings of cycloheximide treatments suggest that phosphorylation of PAX3/FOXO1 at S503 has a stabilizing function. These results provide a mechanism for the regulation of PAX3/FOXO1 through phosphorylation by PLK1. This reinforces the establishment of PLK1 as a novel target for the treatment of aRMS. Additionally, retroviral transduction of RD and also primary hMSC cells may be a useful tool for the identification of phosphosites with an influence on PAX3/FOXO1 transcriptional activity.

6 Acknowledgements

I would like to thank the people mentioned below for their contribution and support during my master thesis.

First of all I would like to thank Prof. Dr. Beat Schäfer for giving me the opportunity to conduct my masters thesis in the oncology research group on a very interesting and challenging topic.

I also thank Prof. Dr. Thierry Hennet for the external supervision of my master thesis.

Especially, I want to thank my supervisor Verena Thalhammer. Thank you very much for teaching me scientific skills, always answering all my questions patiently, and your support and encouragement at any time. Thank you for the very pleasant time that I had working on this project.

Further I would like to thank Dr. Laura Lopez for analyzing my samples by mass spectrometry. I am very grateful for your collaboration and helpfulness. You always had good advice for me, which I appreciated a lot. I also would like to thank Dr. Elisa Zimmermann for providing me with retroviral plasmids and teaching me how to work with viruses. Thanks to Dr. Marco Wachtel for the provided plasmids and your expertise in any regard.

Additionally, I would like to thank all members of the Experimental Infectious Diseases and Cancer research groups. You all deserve gratitude for the nice working atmosphere at August Forel Strasse. I had a great time in the lab.

Finally, I want to thank the most important persons in my life, my family and friends.

Special thanks go to my parents. You always supported me and believed in me in whatever circumstances. Without you my studies would not have been possible.

7 References

1. Jemal, A., et al., *Global cancer statistics.* CA Cancer J Clin, 2011. 61(2): p. 69-90.
2. Weinberg, R.A., *The Biology of Cancer*2007, New York, Abingdon: Garland Science.
3. Jemal, A., et al., *Cancer Statistics, 2010.* CA: A Cancer Journal for Clinicians, 2010. 60(5): p. 277-300.
4. Hanahan, D. and R.A. Weinberg, *Hallmarks of cancer: the next generation.* Cell, 2011. 144(5): p. 646-74.
5. www.cancer.org. *What are the differences between cancers in adults and children?* 2013.
6. Stratton, M.R., *Exploring the genomes of cancer cells: progress and promise.* Science, 2011. 331(6024): p. 1553-8.
7. Downing, J.R., et al., *The Pediatric Cancer Genome Project.* Nat Genet, 2012. 44(6): p. 619-22.
8. Stiller, C.A., *Epidemiology and genetics of childhood cancer.* Oncogene, 2004. 23(38): p. 6429-44.
9. Kaatsch, P., *Epidemiology of childhood cancer.* Cancer Treat Rev, 2010. 36(4): p. 277-85.
10. Davenport, K.P., F.C. Blanco, and A.D. Sandler, *Pediatric malignancies: neuroblastoma, Wilm's tumor, hepatoblastoma, rhabdomyosarcoma, and sacroccygeal teratoma.* Surg Clin North Am, 2012. 92(3): p. 745-67, x.
11. Olanich, *A call to ARMS: targeting the PAX3-FOXO1 gene in alveolar rhabdomyosarcoma.* Expert Opinion on Therapeutic Targets, 2013. 17(5): p. 607-623.
12. Marshall, A. and G. Grosveld, *Alveolar rhabdomyosarcoma - The molecular drivers of PAX3/7-FOXO1-induced tumorigenesis.* Skeletal Muscle, 2012. 2(1): p. 25.
13. Dasgupta, R. and D.A. Rodeberg, *Update on rhabdomyosarcoma.* Semin Pediatr Surg, 2012. 21(1): p. 68-78.
14. Ruymann, F.B., et al., *Congenital anomalies associated with rhabdomyosarcoma: an autopsy study of 115 cases. A report from the Intergroup Rhabdomyosarcoma Study Committee (representing the Children's Cancer Study Group, the Pediatric Oncology Group, the United Kingdom Children's Cancer Study Group, and the Pediatric Intergroup Statistical Center).* Med Pediatr Oncol, 1988. 16(1): p. 33-9.
15. Grufferman, S., et al., *Parents' use of cocaine and marijuana and increased risk of rhabdomyosarcoma in their children.* Cancer Causes Control, 1993. 4(3): p. 217-24.
16. Belyea, B., et al., *Embryonic signaling pathways and rhabdomyosarcoma: contributions to cancer development and opportunities for therapeutic targeting.* Sarcoma, 2012. 2012: p. 406239.
17. Charytonowicz, E., et al., *Alveolar rhabdomyosarcoma: is the cell of origin a mesenchymal stem cell?* Cancer Lett, 2009. 279(2): p. 126-36.
18. Parham, D.M. and D.A. Ellison, *Rhabdomyosarcomas in adults and children: an update.* Arch Pathol Lab Med, 2006. 130(10): p. 1454-65.
19. Sorensen, P.H., et al., *PAX3-FKHR and PAX7-FKHR gene fusions are prognostic indicators in alveolar rhabdomyosarcoma: a report from the children's oncology group.* J Clin Oncol, 2002. 20(11): p. 2672-9.
20. Williamson, D., et al., *Fusion Gene Negative Alveolar Rhabdomyosarcoma Is Clinically and Molecularly Indistinguishable From Embryonal Rhabdomyosarcoma.* Journal of Clinical Oncology, 2010. 28(13): p. 2151-2158.
21. Wachtel, M., et al., *Gene expression signatures identify rhabdomyosarcoma subtypes and detect a novel t(2;2)(q35;p23) translocation fusing PAX3 to NCOA1.* Cancer Res, 2004. 64(16): p. 5539-45.
22. Galindo, R.L., J.A. Allport, and E.N. Olson, *A Drosophila model of the rhabdomyosarcoma initiator PAX7-FKHR.* Proc Natl Acad Sci U S A, 2006. 103(36): p. 13439-44.
23. Ridgeway, A.G. and I.S. Skerjanc, *Pax3 Is Essential for Skeletal Myogenesis and the Expression of Six1 and Eya2.* Journal of Biological Chemistry, 2001. 276(22): p. 19033-19039.

24. Dietz, K.N., et al., *Identification of serines 201 and 209 as sites of Pax3 phosphorylation and the altered phosphorylation status of Pax3-FOXO1 during early myogenic differentiation.* The International Journal of Biochemistry & Cell Biology, 2011. 43(6): p. 936-945.
25. Epstein, J., *Pax3 and Vertebrate Development*, in *Developmental Biology Protocols*, R. Tuan and C. Lo, Editors. 2000, Humana Press. p. 459-470.
26. Dietz, K.N., P.J. Miller, and A.D. Hollenbach, *Phosphorylation of Serine 205 by the Protein Kinase CK2 Persists on Pax3-FOXO1, but Not Pax3, throughout Early Myogenic Differentiation.* Biochemistry, 2009. 48(49): p. 11786-11795.
27. http://ghr.nlm.nih.gov/gene/PAX3. *PAX3*. 2012.
28. Iyengar, A.S., et al., *Identification of CK2 as the kinase that phosphorylates Pax3 at Ser209 in early myogenic differentiation.* Biochemical and Biophysical Research Communications, 2012. 428(1): p. 24-30.
29. Eijkelenboom, A. and B.M.T. Burgering, *FOXOs: signalling integrators for homeostasis maintenance.* Nat Rev Mol Cell Biol, 2013. 14(2): p. 83-97.
30. Tzivion, G., M. Dobson, and G. Ramakrishnan, *FoxO transcription factors; Regulation by AKT and 14-3-3 proteins.* Biochimica et Biophysica Acta (BBA) - Molecular Cell Research, 2011. 1813(11): p. 1938-1945.
31. Xie, Q., J. Chen, and Z. Yuan, *Post-translational regulation of FOXO.* Acta Biochimica et Biophysica Sinica, 2012. 44(11): p. 897-901.
32. http://ghr.nlm.nih.gov/gene/FOXO1. *FOXO1*. 2013.
33. Fredericks, W.J., et al., *The PAX3-FKHR fusion protein created by the t(2;13) translocation in alveolar rhabdomyosarcomas is a more potent transcriptional activator than PAX3.* Molecular and Cellular Biology, 1995. 15(3): p. 1522-35.
34. Bennicelli, J.L., R.H. Edwards, and F.G. Barr, *Mechanism for transcriptional gain of function resulting from chromosomal translocation in alveolar rhabdomyosarcoma.* Proceedings of the National Academy of Sciences, 1996. 93(11): p. 5455-5459.
35. Sublett, J.E., I.S. Jeon, and D.N. Shapiro, *The alveolar rhabdomyosarcoma PAX3/FKHR fusion protein is a transcriptional activator.* Oncogene, 1995. 11(3): p. 545-52.
36. Barr, F.G., *Gene fusions involving PAX and FOX family members in alveolar rhabdomyosarcoma.* Oncogene, 2001. 20(40): p. 5736-46.
37. Cao, L., et al., *Genome-wide identification of PAX3-FKHR binding sites in rhabdomyosarcoma reveals candidate target genes important for development and cancer.* Cancer Res, 2010. 70(16): p. 6497-508.
38. Linardic, C.M., *PAX3/FOXO1 fusion gene in rhabdomyosarcoma.* Cancer Letters, 2008. 270(1): p. 10-18.
39. Keller, C., et al., *Alveolar rhabdomyosarcomas in conditional Pax3:Fkhr mice: cooperativity of Ink4a/ARF and Trp53 loss of function.* Genes Dev, 2004. 18(21): p. 2614-26.
40. Barr, F.G., et al., *Examination of Gene Fusion Status in Archival Samples of Alveolar Rhabdomyosarcoma Entered on the Intergroup Rhabdomyosarcoma Study-III Trial: A Report from the Children's Oncology Group.* The Journal of Molecular Diagnostics, 2006. 8(2): p. 202-208.
41. Huh, W.W. and S.X. Skapek, *Childhood rhabdomyosarcoma: new insight on biology and treatment.* Curr Oncol Rep, 2010. 12(6): p. 402-10.
42. Ognjanovic, S., et al., *Trends in childhood rhabdomyosarcoma incidence and survival in the United States, 1975-2005.* Cancer, 2009. 115(18): p. 4218-26.
43. Wachtel, M. and B.W. Schafer, *Targets for cancer therapy in childhood sarcomas.* Cancer Treat Rev, 2010. 36(4): p. 318-27.
44. Sawyers, C., *Targeted cancer therapy.* Nature, 2004. 432(7015): p. 294-297.
45. Weinstein, I.B. and A. Joe, *Oncogene Addiction.* Cancer Research, 2008. 68(9): p. 3077-3080.
46. Amstutz, R., et al., *Phosphorylation Regulates Transcriptional Activity of PAX3/FKHR and Reveals Novel Therapeutic Possibilities.* Cancer Research, 2008. 68(10): p. 3767-3776.
47. Savage, D.G. and K.H. Antman, *Imatinib mesylate--a new oral targeted therapy.* N Engl J Med, 2002. 346(9): p. 683-93.

48. Futreal, P.A., et al., *A census of human cancer genes.* Nature Reviews. Cancer, 2004. 4(3): p. 177-183.
49. Libermann, T.A. and L.F. Zerbini, *Targeting transcription factors for cancer gene therapy.* Curr Gene Ther, 2006. 6(1): p. 17-33.
50. Redell, M.S. and D.J. Tweardy, *Targeting transcription factors for cancer therapy.* Current pharmaceutical design, 2005. 11(22): p. 2873-2887.
51. Yeh, J.E., P.A. Toniolo, and D.A. Frank, *Targeting transcription factors: promising new strategies for cancer therapy.* Curr Opin Oncol, 2013. 25(6): p. 652-8.
52. Bernasconi, M., et al., *Induction of apoptosis in rhabdomyosarcoma cells through down-regulation of PAX proteins.* Proc Natl Acad Sci U S A, 1996. 93(23): p. 13164-9.
53. Ebauer, M., et al., *Comparative expression profiling identifies an in vivo target gene signature with TFAP2B as a mediator of the survival function of PAX3/FKHR.* Oncogene, 2007. 26(51): p. 7267-7281.
54. Kikuchi, K., et al., *Effects of PAX3-FKHR on malignant phenotypes in alveolar rhabdomyosarcoma.* Biochem Biophys Res Commun, 2008. 365(3): p. 568-74.
55. Gardner, K.H. and M. Montminy, *Can you hear me now? Regulating transcriptional activators by phosphorylation.* Sci STKE, 2005. 2005(301): p. pe44.
56. Cunningham, J.T. and D. Ruggero, *New Connections between Old Pathways: PDK1 Signaling Promotes Cellular Transformation through PLK1-Dependent MYC Stabilization.* Cancer Discovery, 2013. 3(10): p. 1099-1102.
57. Tan, J., et al., *PDK1 Signaling Toward PLK1,ÄìMYC Activation Confers Oncogenic Transformation, Tumor-Initiating Cell Activation, and Resistance to mTOR-Targeted Therapy.* Cancer Discovery, 2013. 3(10): p. 1156-1171.
58. Mayr, B. and M. Montminy, *Transcriptional regulation by the phosphorylation-dependent factor CREB.* Nat Rev Mol Cell Biol, 2001. 2(8): p. 599-609.
59. Huang, H. and D.J. Tindall, *Regulation of FOXO protein stability via ubiquitination and proteasome degradation.* Biochimica et Biophysica Acta (BBA) - Molecular Cell Research, 2011. 1813(11): p. 1961-1964.
60. Rena, G., et al., *Two novel phosphorylation sites on FKHR that are critical for its nuclear exclusion.* EMBO J, 2002. 21(9): p. 2263-2271.
61. Zeng, F.Y., et al., *Glycogen synthase kinase 3 regulates PAX3-FKHR-mediated cell proliferation in human alveolar rhabdomyosarcoma cells.* Biochem Biophys Res Commun, 2010. 391(1): p. 1049-55.
62. Jothi, M., et al., *AKT and PAX3-FKHR cooperation enforces myogenic differentiation blockade in alveolar rhabdomyosarcoma cell.* Cell Cycle, 2012. 11(5): p. 895-908.
63. Jothi, M., et al., *Small Molecule Inhibition of PAX3-FOXO1 through AKT Activation Suppresses Malignant Phenotypes of Alveolar Rhabdomyosarcoma.* Molecular Cancer Therapeutics, 2013. 12(12): p. 2663-2674.
64. Hecker, *Functional RNAi screen of the human kinome to identify activators of the oncogenic transcription factor PAX3/FKHR.* Manuscript 2008.
65. Thalhammer, *Validation of Polo-like kinase 1 as a novel therapeutic target in alveolar Rhabdomyosarcoma.* Unpublished, 2010.
66. Hu, K., et al., *Small interfering RNA library screen of human kinases and phosphatases identifies polo-like kinase 1 as a promising new target for the treatment of pediatric rhabdomyosarcomas.* Molecular Cancer Therapeutics, 2009. 8(11): p. 3024-3035.
67. Archambault, V. and D.M. Glover, *Polo-like kinases: conservation and divergence in their functions and regulation.* Nat Rev Mol Cell Biol, 2009. 10(4): p. 265-275.
68. Strebhardt, K. and A. Ullrich, *Targeting polo-like kinase 1 for cancer therapy.* Nat Rev Cancer, 2006. 6(4): p. 321-330.
69. Lee, H.-J., H.-I. Hwang, and Y.-J. Jang, *Mitotic DNA damage response: Polo-like Kinase-1 is dephosphorylated through ATM-Chk1 pathway.* Cell Cycle, 2010. 9(12): p. 2389-2398.
70. Smits, V.A.J., et al., *Polo-like kinase-1 is a target of the DNA damage checkpoint.* Nat Cell Biol, 2000. 2(9): p. 672-676.

71. Gleixner, K.V., et al., *Polo-like kinase 1 (Plk1) as a novel drug target in chronic myeloid leukemia: overriding imatinib resistance with the Plk1 inhibitor BI 2536.* Cancer Res, 2010. 70(4): p. 1513-23.
72. Gray, P.J., et al., *Identification of human polo-like kinase 1 as a potential therapeutic target in pancreatic cancer.* Molecular Cancer Therapeutics, 2004. 3(5): p. 641-646.
73. Harris, P.S., et al., *Polo-like kinase 1 (PLK1) inhibition suppresses cell growth and enhances radiation sensitivity in medulloblastoma cells.* BMC Cancer, 2012. 12(80): p. 1471-2407.
74. Triscott, J., et al., *Personalizing the treatment of pediatric medulloblastoma: Polo-like kinase PLK1 as a molecular target in high-risk children.* Cancer Research, 2013.
75. Degenhardt, Y. and T. Lampkin, *Targeting Polo-like Kinase in Cancer Therapy.* Clinical Cancer Research, 2010. 16(2): p. 384-389.
76. Strebhardt, K., *Multifaceted polo-like kinases: drug targets and antitargets for cancer therapy.* Nat Rev Drug Discov, 2010. 9(8): p. 643-660.
77. Schöffski, P., *Polo-Like Kinase (PLK) Inhibitors in Preclinical and Early Clinical Development in Oncology.* The Oncologist, 2009. 14(6): p. 559-570.
78. Kettenbach, A.N., et al., *Quantitative Phosphoproteomics Identifies Substrates and Functional Modules of Aurora and Polo-Like Kinase Activities in Mitotic Cells.* Sci. Signal., 2011. 4(179): p. rs5-.
79. Kettenbach, A.N., et al., *Rapid Determination of Multiple Linear Kinase Substrate Motifs by Mass Spectrometry.* Chemistry & Biology, 2012. 19(5): p. 608-618.
80. Davicioni, E., et al., *Identification of a PAX-FKHR Gene Expression Signature that Defines Molecular Classes and Determines the Prognosis of Alveolar Rhabdomyosarcomas.* Cancer Research, 2006. 66(14): p. 6936-6946.
81. Ren, Y.-X., et al., *Mouse Mesenchymal Stem Cells Expressing PAX-FKHR Form Alveolar Rhabdomyosarcomas by Cooperating with Secondary Mutations.* Cancer Research, 2008. 68(16): p. 6587-6597.
82. Mizuguchi, H., et al., *IRES-dependent second gene expression is significantly lower than cap-dependent first gene expression in a bicistronic vector.* Mol Ther, 2000. 1(4): p. 376-82.
83. Lam, P.Y.P., et al., *The Oncogenic Potential of the Pax3-FKHR Fusion Protein Requires the Pax3 Homeodomain Recognition Helix but Not the Pax3 Paired-Box DNA Binding Domain.* Molecular and Cellular Biology, 1999. 19(1): p. 594-601.
84. Boutet, S.C., et al., *Regulation of Pax3 by proteasomal degradation of monoubiquitinated protein in skeletal muscle progenitors.* Cell, 2007. 130(2): p. 349-62.
85. Miller, P.J. and A.D. Hollenbach, *The oncogenic fusion protein Pax3-FKHR has a greater post-translational stability relative to Pax3 during early myogenesis.* Biochim Biophys Acta, 2007. 10(8): p. 13.
86. Hunter, T., *The age of crosstalk: phosphorylation, ubiquitination, and beyond.* Mol Cell, 2007. 28(5): p. 730-8.
87. Gumireddy, K., et al., *ON01910, a non-ATP-competitive small molecule inhibitor of Plk1, is a potent anticancer agent.* Cancer cell, 2005. 7(3): p. 275-286.
88. Liu, X., M. Lei, and R.L. Erikson, *Normal Cells, but Not Cancer Cells, Survive Severe Plk1 Depletion.* Molecular and Cellular Biology, 2006. 26(6): p. 2093-2108.
89. Spänkuch-Schmitt, B., et al., *Downregulation of human polo-like kinase activity by antisense oligonucleotides induces growth inhibition in cancer cells.* Oncogene, 2002. 21(20): p. 3162-3171.
90. Steegmaier, M., et al., *BI 2536, a Potent and Selective Inhibitor of Polo-like Kinase 1, Inhibits Tumor Growth In Vivo.* Current biology, 2007. 17(4): p. 316-322.
91. Fehse, B., et al., *Pois(s)on - It's a Question of Dose[hellip].* Gene Ther, 2004. 11(11): p. 879-881.